Novel Tuned Rectangular Patch Antenna As a Load for Phase Power Combining

Thesis submitted in partial fulfillment of the requirement for the degree of

Doctor of Philosophy (Ph. D.)

in

Engineering

By

Santanu Kumar Behera

Department of Electronics and Telecommunication Engineering

Jadavpur University, Kolkata

Dedicated to my Parents

CERTIFICATE FROM THE SUPERVISORS

This is to certify that the thesis entitled "**Novel Tuned Rectangular Patch Antenna As a Load For Phase Power Combining"** submitted by Shri **Santanu Kumar Behera** who got his name registered on **1st March 2002** for the award of Ph.D. (Engg.) degree of Jadavpur University, is absolutely based upon his own work under the supervision/s of **Prof. D. R. Poddar** and **Dr. R. K. Mishra,** and that neither his thesis nor any part of it has been submitted for any degree / diploma or any other academic award anywhere before.

1. (**Dipak Ranjan Poddar**)
Professor
Dept. of Electronics & Tele. Engg.
Jadavpur University, Kolkata

2. (**Rabindra Kishore Mishra)**
Reader in Electronics
Sambalpur University
Jyoti Vihar, Burla (Orissa)

LIST OF PUBLICATIONS BY THE AUTHOR RELATED TO THE THESIS

Conference Publications:

1. S. K. Behera, D. R. Poddar and R. K. Mishra, "Novel Push-Pull Integrated Antenna for Wireless Front-End" **International Conference on Communications, Devices and Intelligent Systems (CODIS-2004),** pp. 217-219,8-10 January 2004.Jadavpur University, Kolkata.

2. S. K. Behera, R. K. Mishra and D. R. Poddar, "A Novel Design for Active antenna", 5th Indian Conference on **Microwave, Antenna, Propagation and Remote Sensing-In CMARS-2005.**

3. S. K. Behera, D. R. Poddar and R. K. Mishra, "Dual Active Integrated Antenna", **International Conference on Computer & Devices for Communication (CODEC-2006),** University of Calcutta.

Journal Publications:

1. S. K. Behera, D. R. Poddar and R. K. Mishra, "Balanced Amplifying Active Patch Antenna", IETE Journal of Research (Communicated).

2. S. K. Behera, D. R. Poddar and R. K. Mishra, "2.4 GHz Balanced Amplifying Active Antenna for Circular Polarization", Microwave and Optical Wave Letters (Communicated).

3. S. K. Behera, D. R. Poddar and R. K. Mishra, " Sequentially Fed Balanced Amplifying Antenna for Circular Polarization" IEEE Trans. on Antennas & Propagation (Communicated).

ACKNOWLEDGEMENTS

“No man can be a good teacher unless he has feelings of warm affection toward his pupils and a genuine desire to impart to them what he himself believes to be of value” - Bertrand Russell. With this virgin idea my adorable teachers Prof. D. R. Poddar and Dr. R. K. Mishra led me throughout the Ph.D. work.

My deep obeisance naturally ventilates to my revered teacher Prof. D. R. Poddar, the torchbearer of an untrodden path who shaped my mind in his two loving palms and fine-tuned the techniques of surfacing this work into limelight. I have a claim upon his gratitude of inspiring me to shoulder a herculean task, ignited the spirit within to unveil my potentiality within and helped me to discover myself.

The integrated and dynamic personality with novelty of thought in my teacher Dr. R. K. Mishra who revealed the secrets of a new world of “Active Integrated Antenna”. His innovative thoughts can never go unacknowledged and my sincere indebtedness towards his loving guidance, his parental love and nursing spirit. He opened me the door of a challenging pleasure scarcely available to a research scholar and my gratefulness is sufficiently less in proportion to his contributions.

I am most appreciative of Prof. C. K. Sarkar, Head of the Department of ETCE and Prof. Bhaskar Gupta for their helpful comments and suggestions in reading my thesis.

I would specially like to thank **A. W. R. Inc., USA** for providing me the Demo copy of Microwave Office 2000.

I would like to express my thanks to Mr. Sudhansu Kumar Dash and Mr. Khageswar Singh for their constructive suggestions for improving this thesis and catching those pesky grammatical errors.

I would also like to thank Mr. Debasis Mishra for his support for printing this thesis.

At the end of this long list of people who have helped me to complete this Work, comes the least noticed but most important forces in my life: my parents, my son and especially my better half, who have inspired me, supported me, and loved me through it all.

Dated: 28.02.2007 **(Santanu Kumar Behera)**

CONTENTS

TABLES AND FIGURES

LIST OF TABLES:

LIST OF FIGURES:

Chapter 1

Chapter 1 Introduction

Wireless communication systems have advanced significantly from the simple components. Guglielmo Marconi used to transmit radio signals across the Atlantic Ocean at the turn of the 20th century. Today, mobile and satellite communications permeate all aspects of our lives. The number of mobile and cellular phones has skyrocketed in recent years while satellite communication traffics including international telephone calls and DBS-TV (direct broadcast satellite television) has also increased substantially.

Commercial cellular and PCS mobile communications [1] currently occupy the 800 MHz-2 GHz spectral region. Military and commercial satellite communications [2] including voice, data, and DBS-TV operate at higher frequencies ranging from 4-30 GHz, and are moving up higher to 60 GHz and beyond in order to facilitate higher data rates and a wider range of services. While the initial technological achievements in both mobile and satellite communications were geared to provide reliable service with wide functionality, there is a current focus on lowering the cost of service while maintaining superior quality. One of the main approaches to reducing system and operating costs is the conservation of system power resources and minimization of power wasted as heat. Of the approximately 250W of power produced by the solar-cell arrays on a typical satellite, more than 125W is dissipated as heat due to inefficient operation of the transmitter power amplifiers [2].

1.1 Reducing Costs by Conserving Power

The power amplifiers (PAs) in a wireless transmitter amplify the signal to high power levels before delivering it to the antenna for transmission. The transmit power should be high enough that the signal received at the destination is clear and within the error-tolerances of the receiver. For example, the power amplifier in a communications satellite has an output power level on the order of 40 W. To deliver this amount of power to the antenna, the PA consumes on average about 75% of the total available power [2]. If the PA operates at about 30% efficiency [2], then 70% of 75% of the total power is converted to heat. In other words, 52.5% of the total system power is dissipated as heat in the power amplifier. During an eclipse, the satellite is powered by onboard batteries whose lifetime is limited by the unnecessary waste of power by conversion to heat. Battery lifetime is also of concern to the cellular phone user whose talk-time is cut short due to inefficient use of battery power. By using more efficient PAs in these transmitters, satellite solar-cell arrays may possibly be made smaller while batteries will last longer, lengthening the satellite lifetime as well. Cellular phone usage will be cheaper since batteries will last longer, while cellular base-stations can reduce costs by drawing less electricity.

The heat generated due to inefficient power usage in the power amplifiers not only wastes valuable solar-cell or battery power, but also causes thermal degradation of electronic devices and necessitates bulky heat-sinking measures to cool the transmitter. In addition to the cost-cutting benefits of increased power

amplifier efficiency, reduced heat dissipation eases the heat-sinking requirements of the system. This is very important in satellite communications where thermal waste management is a challenge due to the harsh environment of space where the temperature varies from approximately 4K to hundreds of Kelvin when exposed to direct sunlight. Less heat-sinking also means less size and weight of the system, which directly translates to further cost savings in the satellite launching process. Some of the approaches being taken to improve the power-efficiency of transmitters include the use of high-efficiency power amplifiers [3], the formulation of power-efficient modulation techniques [4], and real-time power control of the power amplifiers [5].

1.2 CHAPTER ORGANIZATION

This dissertation contains seven chapters. The chapter-1 gives an introduction to the work carried out during this research and the organization of the thesis. The Microstrip antenna is reviewed in Chapter-2, starting with its concepts, and progressing gradually to size reduction techniques passing through rectangular Microstrip antenna and bandwidth enhancement.

The third chapter describes the progress from passive to active integrated Microstrip antenna. It embodies the following topics: Integrated antenna, diode integrated active antenna, transistor integrated active antenna, classification of active integrated antenna like oscillator type, amplifier type, frequency conversion type and other types.

Chapter 4 deals with the emerging trend in amplifier type integrated active antenna and describes the design of the push pull amplifying antenna using diode amplifiers in the first stage in place of the power splitter. Chapter 5 describes compares the push-pull and balanced amplifiers, and then proceeds to use the balanced amplifier as the amplifying unit in the AIA. Chapter 6 applies this concept to circularly polarized antenna. The last chapter summarizes the investigations and then suggest scopes for future research work in this area.

1.3 CONCLUSION

Following the brief discussion on the future communication systems and outline of our effort in adding an incremental increase to the existing knowledge in the above paragraphs, we move on to a brief introductory review of rectangular microstrip antenna in the Chapter 2 that follows this chapter.

Chapter 2

Chapter 2 RECTANGULAR PATCH ANTENNA

2.1 INTRODUCTION

Microstrip antennas are one of the most widely used types of antennas in the microwave frequency range, and they are often used in the millimetre-wave frequency range as well [1, 2, 3]. (Below approximately 1 GHz, the size of a microstrip antenna is usually too large to be practical, and other types of antennas such as wire antennas dominate). Also called patch antennas, microstrip patch antennas consist of a metallic patch of metal that is on top of a grounded dielectric substrate of thickness h, with relative permittivity and permeability ε_r and μ_r as shown in Figure 2.1 (usually $\mu_r = 1$). The metallic patch may be of various shapes, with rectangular and circular being the most common, as shown in Figure 2.1.

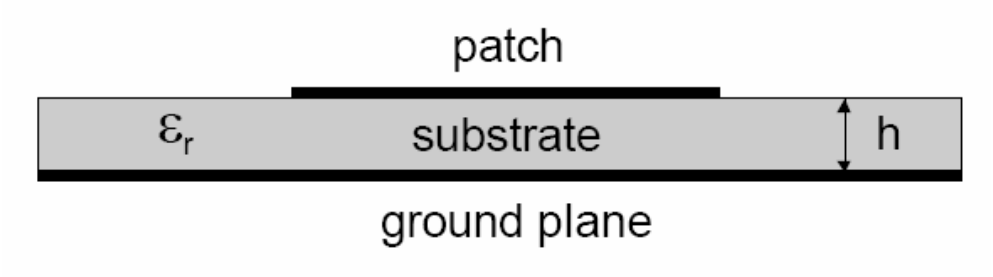

(a)Microstrip Patch Antenna

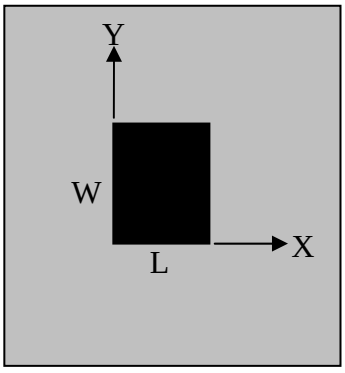

(b) Rectangular Patch Antenna

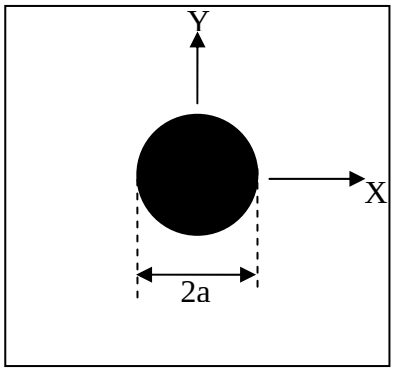

(C) Circular Patch Antenna

Fig. 2.1/ Rectangular & Circular Patch Antenna

Most of the discussion in this section will be limited to the rectangular patch, although the basic principles are the same for the circular patch. (Many of the CAD formulas presented will apply approximately for the circular patch if the circular patch is modelled as a square patch of the same area.) Various methods may be used to feed the patch, as discussed below.

One advantage of the microstrip antenna is that it is usually low profile, in the sense that the substrate is fairly thin. If the substrate is thin enough, the antenna actually becomes “conformal,” meaning that the substrate can be bent to conform to a curved surface (e.g., a cylindrical structure). A typical substrate thickness is about 0.02 λ_0. The metallic patch is usually fabricated by a photolithographic etching process or a mechanical milling process, making the construction relatively easy and inexpensive (the cost is mainly that of the substrate material). Other advantages include the fact that the microstrip antenna is usually lightweight (for thin substrates) and durable.

Disadvantages of the microstrip antenna include the fact that it is usually narrowband, with bandwidths of a few percent being typical. Some methods for enhancing bandwidth are discussed later, however. Also, the radiation efficiency of the patch antenna tends to be lower than some other types of antennas, with efficiencies between 70% and 90% being typical.

2.2 BASIC PRINCIPLES OF OPERATION

The metallic patch essentially creates a resonant cavity, where the patch is the top of the cavity, the ground plane is the bottom of the cavity, and the edges of the patch form the sides of the cavity. The edges of the patch act approximately as an open-circuit boundary condition. Hence, the patch acts approximately as a cavity with perfect electric conductor on the top and bottom surfaces, and a perfect “magnetic conductor” on the sides. This point of view is very useful in analyzing the patch antenna, as well as in understanding its behaviour. Inside the patch cavity the electric field is essentially z directed and independent of the z coordinate. Hence, the patch cavity modes are described by a double index (m, n). For the (m, n) cavity mode of the rectangular patch in Figure 1b, the electric field has the form

$$E_z(x,y) = A_{mn}\cos\left(\frac{m\pi x}{L}\right)\cos\left(\frac{n\pi y}{W}\right) \qquad (2.1)$$

Where L is the patch length and W is the patch width. The patch is usually operated in the (1, 0) mode, so that L is the resonant dimension, and the field is essentially constant in the y direction. The surface current on the bottom of the metal patch is then x directed, and is given by

$$J_{sx}(x) = A_{10}\left(\frac{\pi/L}{j\omega\mu_0\mu_r}\right) \qquad (2.2)$$

For this mode the patch may be regarded as a wide microstrip line of width W, having a resonant length L that is approximately one-half wavelength in the dielectric. The current is maximum at the centre of the patch, $x = L/2$, while the electric field is maximum at the two "radiating" edges, $x = 0$ and $x = L$. The width W is usually chosen to be larger than the length ($W = 1.5\ L$ is typical) to maximize the bandwidth, since the bandwidth is proportional to the width. (The width should be kept less than twice the length, however, to avoid excitation of the (0,2) mode.)

At first glance, it might appear that the microstrip antenna will not be an effective radiator when the substrate is electrically thin, since the patch current in (2) will be effectively shorted by the close proximity to the ground plane. If the modal amplitude A_{10} were constant, the strength of the radiated field would in fact be proportional to h. However, the Q of the cavity increases as h decreases (the radiation Q is inversely proportional to h). Hence, the amplitude A_{10} of the modal field at resonance is inversely proportional to h. Hence, the strength of the radiated field from a resonant patch is essentially independent of h, if losses are ignored. The resonant input resistance will likewise be nearly independent of h. This explains why a patch antenna can be an effective radiator even for very thin substrates, although the bandwidth will be small.

2.3 FEEDING TECHNIQUES

The Microstrip antenna may be fed in various ways. Perhaps the most common is the direct probe feed, shown in Figure 2.2a for a rectangular patch, where the centre conductor of a coaxial feed line penetrates the substrate to

make direct contact with the patch. For linear polarization, the patch is usually fed along the centreline, $y = W/2$. The feed point location at $x = x_f$ controls the resonant input resistance. The input resistance is highest when the patch is fed at the edge, and smallest (essentially zero) when the patch is fed at the centre ($x = L/2$). Another common feeding method, preferred for planar fabrication, is the direct-contact microstrip feed line, shown in Figure 2.2b. An inset notch is used to control the resonant input resistance at the contact point. The input impedance seen by the microstrip line is approximately the same as that seen by a probe at the contact point, provided the notch does not disturb the modal field significantly.

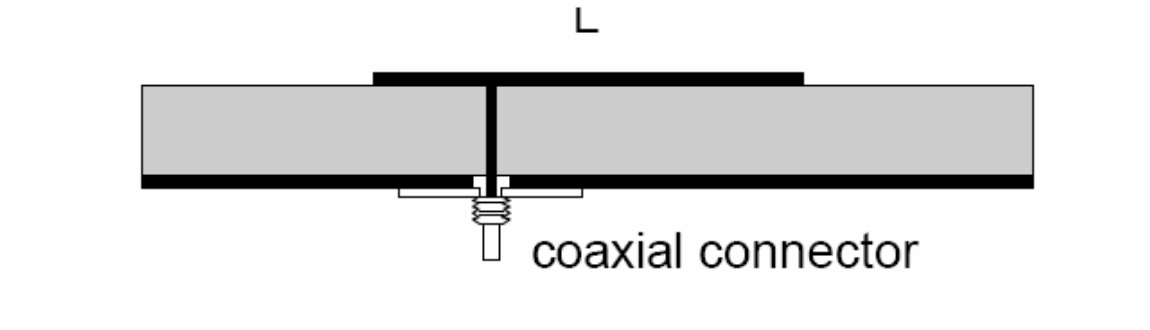

(a) Probe Feed

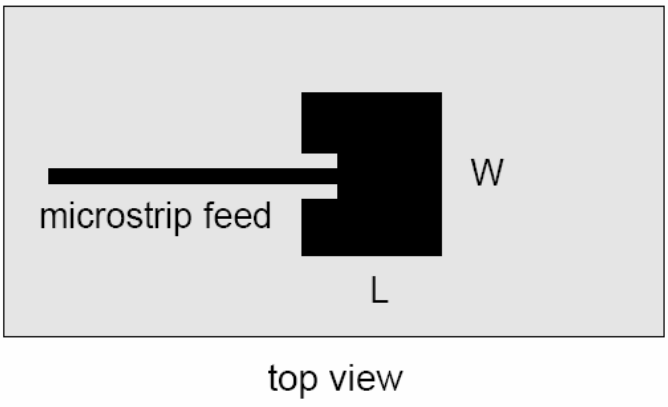

(b) Microstrip Feed

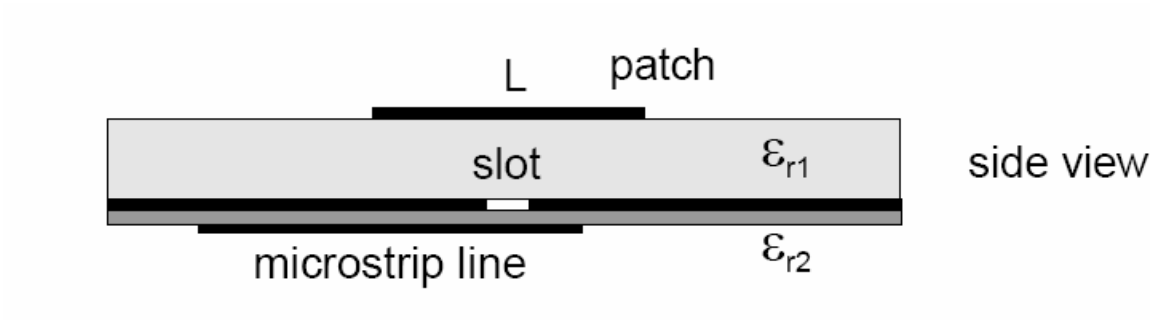

(C) Aperture Coupled Feed

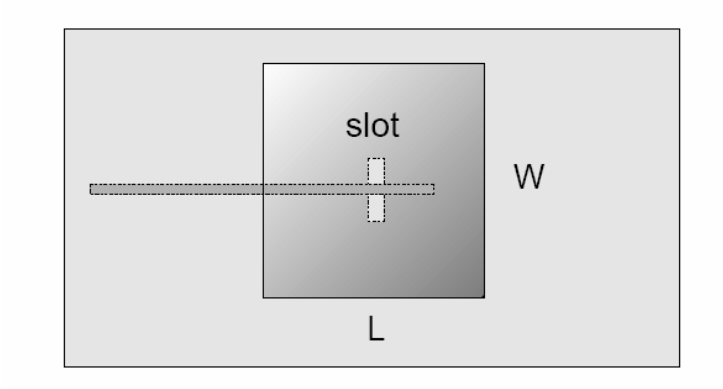

2.2 (abc) Top View

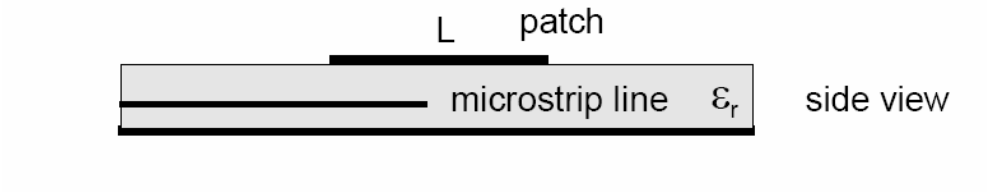

(d) Electromagnetic Coupling

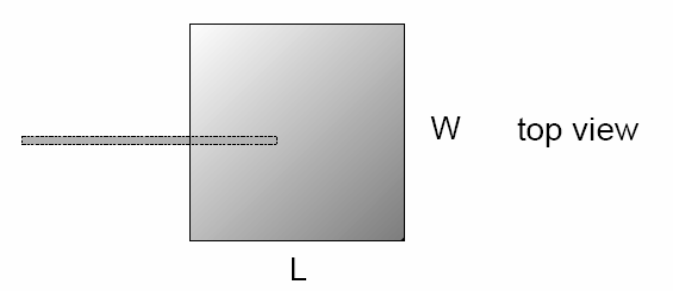

2.2(d)

Fig.2.2/ Feed Mechanism

An alternative type of feed is the aperture-coupled feed shown in Figure 2.2c. In this scheme, a microstrip line on a back substrate excites a slot in the

ground plane, which then excites the patch cavity. This scheme has the advantage of isolating the feeding network from the radiating patch element. It also overcomes the limitation on substrate thickness imposed by the feed inductance of a coaxial probe, so that thicker substrates and hence higher bandwidths can be obtained. Using this feeding technique together with a foam substrate, it is possible to achieve bandwidths greater than 25% [4].

Another alternative, which has some of the advantages of the aperture-coupled feed, is the “electromagnetically-coupled” or “proximity” feed, shown in Figure 2.2d. In this arrangement the microstrip line is on the same side of the ground plane as the patch, but does not make direct contact. The microstrip line feeds the patch via electromagnetic (largely capacitive) coupling. With this scheme it is possible to keep the feed line closer to the ground plane compared with the direct feed, in order to minimize feed line radiation. However, the fabrication is more difficult, requiring two substrate layers. Another variation of this technique is to have the microstrip line on the same layer as the patch, with a capacitive gap between the line and the patch edge. This allows for an input match to be achieved without the use of a notch.

2.4 RESONANCE FREQUENCY

The resonance frequency for the (1, 0) mode is given by

$$f_0 = \frac{c}{2L_e\sqrt{\varepsilon_r}} \qquad (2.3)$$

Where c is the speed of light in vacuum. To account for the fringing of the cavity fields at the edges of the patch, the length, the effective length L_e is chosen as

$$L_e = L + 2\Delta L \qquad (2.4)$$

The Hammerstad formula for the fringing extension is [1]

$$\frac{\Delta L}{h} = 0.412 \left(\frac{\left(\varepsilon_{eff} + 0.3\right)\left(\frac{W}{h} + 0.264\right)}{\left(\varepsilon_{eff} - 0.258\right)\left(\frac{W}{h} + 0.8\right)} \right) \tag{2.5}$$

Where

$$\varepsilon_{eff} = \frac{\varepsilon_r + 1}{2} + \frac{\varepsilon_r - 1}{2}\left(1 + \frac{12h}{W}\right)^{-1/2} \tag{2.6}$$

2.5 RADIATION PATTERNS

The radiation field of the microstrip antenna may be determined using either an “electric current model” or a “magnetic current model”. In the electric current model, the current in (2) is used directly to find the far-field radiation pattern. Figure 2.3a shows the electric current for the (1, 0) patch mode. If the substrate is neglected (replaced by air) for the calculation of the radiation pattern, the pattern may be found directly from image theory. If the substrate is accounted for, and is assumed infinite, the reciprocity method may be used to determine the far-field pattern [5].

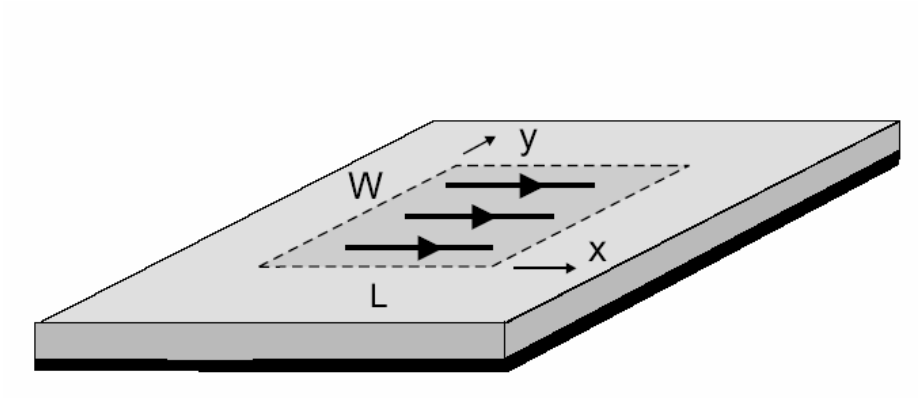

(a) Electric Current for (1,0) patch

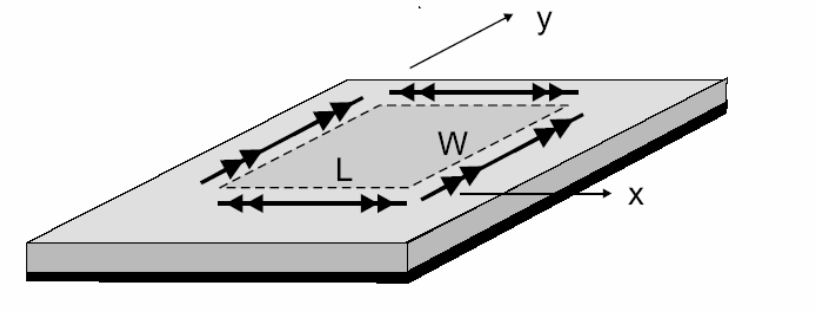

(b) Magnetic Current for (1,0) patch

Fig. 2.3 / Electric & Magnetic Current Distribution

In the magnetic current model, the equivalence principle is used to replace the patch by a magnetic surface current that flows on the perimeter of the patch. The magnetic surface current is given by

$$\vec{M}_s = -\hat{n} \times \vec{E} \qquad (2.7)$$

Where **E** is the electric field of the cavity mode at the edge of the patch and **n** is the outward pointing unit-normal vector at the patch boundary. Figure 3b shows the magnetic current for the (1, 0) patch mode. The far-field pattern may once again be determined by image theory or reciprocity, depending on whether the substrate is neglected or not [4]. The dominant part of the radiation field comes from the "radiating edges" at x = 0 and $x = L$. The two non-radiating edges do not affect the pattern in the principle planes (the E plane at ϕ = 0 and the H plane at $\phi = \pi/2$), and have a small effect for other planes.

It can be shown that the electric and magnetic current models yield exactly the same result for the far-field pattern, provided the pattern of each current is calculated in the presence of the substrate at the resonant frequency of the patch cavity mode [5]. If the substrate is neglected, the agreement is only approximate, with the largest difference being near the horizon.

According to the electric current model, accounting for the infinite substrate, the far-field pattern is given by [5]

$$E_i(r,\theta,\phi) = E_i^h(r,\theta,\phi)\left(\frac{\pi WL}{2}\right)\left(\frac{\sin\left(\frac{k_y W}{2}\right)}{\frac{k_y W}{2}}\right)\left(\frac{\cos\left(\frac{k_x L}{2}\right)}{\left(\frac{\pi}{2}\right)^2 - \left(\frac{k_x L}{2}\right)^2}\right) \qquad (2.8)$$

Where

$k_x = k_0 \sin\theta\cos\phi$ (2.9)

$k_y = k_0 \sin\theta\sin\phi$ (2.10)

and E_i^h is the far-field pattern of an infinitesimal (Hertzian) unit-amplitude x-directed electric dipole at the centre of the patch. This pattern is given by [5]

$$E_\theta^h(r,\theta,\phi) = E_0\cos\phi G(\theta) \qquad (2.11)$$

$$E_\phi^h(r,\theta,\phi) = -E_0\sin\phi F(\theta) \qquad (2.12)$$

Where

$$E_0 = \left(\frac{-j\omega\mu_0}{4\pi r}\right)e^{-jk_0 r} \qquad (2.13)$$

$$F(\theta) = \frac{2\tan(k_0 hN(\theta))}{\tan(k_0 hN(\theta)) - j\frac{N(\theta)}{\mu_r}\sec\theta} \qquad (2.14)$$

$$G(\theta) = \frac{2\tan(k_0 hN(\theta))\cos\theta}{\tan(k_0 hN(\theta)) - j\frac{\varepsilon_r}{N(\theta)}\cos\theta} \qquad (2.15)$$

and

$$N(\theta) = \sqrt{n_1^2 - \sin^2\theta} \qquad (2.16)$$

$$n_1^2 = \varepsilon_r\mu_r \qquad (2.17)$$

The radiation patterns (E- and H-plane) for a rectangular patch antenna on an infinite substrate of permittivity ε_r = 2.2 and thickness h/λ_0 = 0.02 are shown in Figure 2.4. The patch is resonant with $W/L = 1.5$. Note that the E-plane pattern is broader than the H-plane pattern. The directivity is approximately 6 dB.

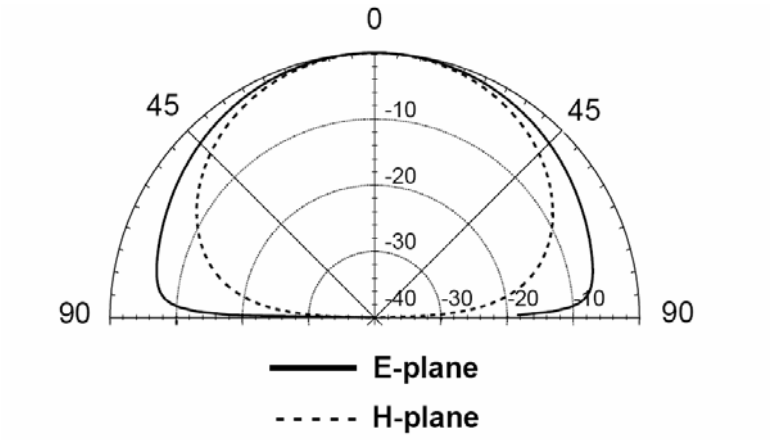

Fig. 2.4 / Radiation Pattern (E & H plane)

2.6 RADIATION EFFICIENCY

The radiation efficiency of the patch antenna is affected not only by conductor and dielectric losses, but also by surface-wave excitation - since the dominant TM_0 mode of the grounded substrate will be excited by the patch. As the substrate thickness decreases, the effect of the conductor and dielectric losses becomes more severe, limiting the efficiency. On the other hand, as the substrate thickness increases, the surface-wave power increases, thus limiting the efficiency. Surface-wave excitation is undesirable for other reasons as well, since surface waves contribute to mutual coupling between elements in an array, and also cause undesirable edge diffraction at the edges of the ground plane or substrate, which often contributes to distortions in the pattern and to back radiation. For an air (or foam) substrate there is no surface-wave excitation. In

this case, higher efficiency is obtained by making the substrate thicker, to minimize conductor and dielectric losses (making the substrate too thick may lead to difficulty in matching, however, as discussed above). For a substrate with a moderate relative permittivity such as ε_r = 2.2, the efficiency will be maximum when the substrate thickness is approximately λ_0 = 0.02. The radiation efficiency is defined as

$$e_r = \frac{P_{sp}}{P_{Total}} = \frac{P_{sp}}{P_c + P_d + + P_{sw} + P_{sp}} \tag{2.18}$$

Where P_{sp} is the power radiated into space, and the total input power P_{total} is given as the sum of P_c - the power dissipated by conductor loss, P_d - the power dissipated by dielectric loss, and P_{sw} - the surface-wave power. The efficiency may also be expressed in terms of the corresponding Q factors as

$$e_r = \left(\frac{Q_{sp}}{Q_{Total}} \right)^{-1} \tag{2.19}$$

where

$$\frac{1}{Q_{Total}} = \frac{1}{Q_c} + \frac{1}{Q_d} + \frac{1}{Q_{sw}} + \frac{1}{Q_{sp}} \tag{2.20}$$

The dielectric and conductor Q factors are given by

$$Q_d = \frac{1}{\tan \delta_d} \tag{2.21}$$

$$Q_c = \frac{1}{2} \eta_0 \mu_r \left(\frac{k_0 h}{R_s} \right) \tag{2.22}$$

Where $\tan\delta_d$ is the loss tangent of the substrate and R_s is the surface resistance of the patch and ground plane metal at radian frequency $\omega = 2\pi f$, given by

$$R_s = \left(\frac{\omega \mu_0}{2\sigma} \right)^{1/2} \tag{2.23}$$

where σ is the conductivity of the metal.

The space-wave Q factor is given approximately as [6]

$$Q_{sp} = \frac{3}{16} \left(\frac{\varepsilon_r}{p c_1} \right) \left(\frac{L}{W} \right) \left(\frac{1}{h/\lambda_0} \right) \tag{2.24}$$

Where

$$c_1 = 1 - \frac{1}{n_1^2} + \frac{2/5}{n_1^4} \tag{2.25}$$

and

$$\begin{aligned} p = 1 &+ \frac{a_2}{10} (k_0 W)^2 + \left(a_2^2 + 2a_4 \right) \left(\frac{3}{560} \right) (k_0 W)^4 + c_2 \left(\frac{1}{5} \right) (k_0 L)^2 \\ &+ a_2 c_2 \left(\frac{1}{70} \right) (k_0 W)^2 (k_0 L)^2 \end{aligned} \tag{2.26}$$

with $a_2 = -0.16605$, $a_4 = 0.00761$, and $c_2 = -0.0914153$.

The surface-wave Q factor is related to the space-wave Q factor as

$$Q_{sw} = Q_{sp} \left(\frac{e_r^{sw}}{1 - e_r^{sw}} \right) \tag{2.27}$$

where e_r^{sw} is the radiation efficiency accounting only for surface-wave loss. This efficiency may be accurately approximated by using the radiation efficiency of an infinitesimal dipole on the substrate layer [6], giving

$$e_r^{sw} = \frac{1}{1 + (k_0 h) \left(\frac{3}{4} \right) (\pi \mu_r) \left(\frac{1}{c_1} \right) \left(1 - \frac{1}{n_1^3} \right)^3} \tag{2.28}$$

A plot of radiation efficiency for a resonant rectangular patch antenna with W / L = 1.5 on a substrate of relative permittivity ε_r = 2.2 or ε_r = 10.8 is shown in Figure 2.5. The conductivity of the copper patch and ground plane is assumed to be $\sigma = 3.0\times10^7$ [S/m] and the dielectric loss tangent is taken as $\tan\delta_d$ = 0.001. The resonance frequency is 5.0 GHz. (The result is plotted versus normalized (electrical) thickness of the substrate, which does not involve frequency.

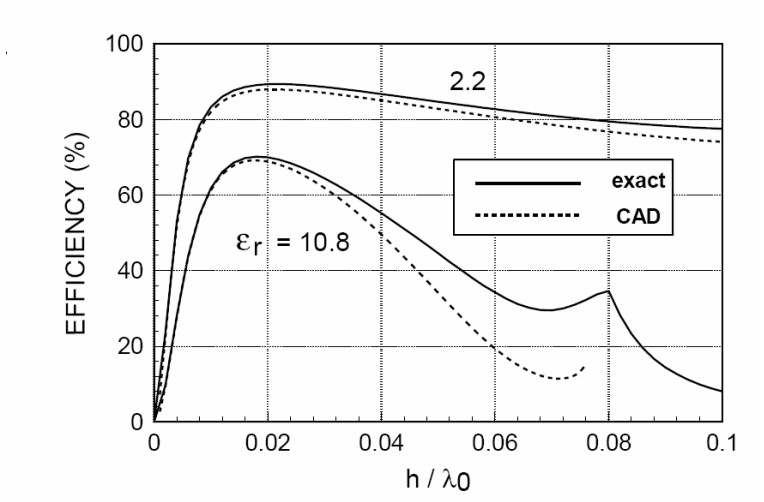

Fig.2.5 / Radiation Efficiency for a rectangular patch Antenna

However, a specified frequency is necessary to determine conductor loss.) For $h / \lambda_0 < 0.02$, the conductor and dielectric losses dominate, while for $h / \lambda_0 < 0.02$, the surface-wave losses dominate. (If there were no conductor or dielectric losses, the efficiency would approach 100% as the substrate thickness approaches zero.)

2.7 BANDWIDTH

The bandwidth increases as the substrate thickness increases (the bandwidth is directly proportional to h if conductor, dielectric, and surface-wave losses are ignored). However, increasing the substrate thickness lowers the Q of the cavity, which increases spurious radiation from the feed, as well as from

higher-order modes in the patch cavity. Also, the patch typically becomes difficult to match as the substrate thickness increases beyond a certain point (typically about 0.05 λ_0). This is especially true when feeding with a coaxial probe, since a thicker substrate results in a larger probe inductance appearing in series with the patch impedance. However, in recent years considerable effort has been spent to improve the bandwidth of the microstrip antenna, in part by using alternative feeding schemes. The aperture-coupled feed of Figure 2.2c is one scheme that overcomes the problem of probe inductance, at the cost of increased complexity[7].

Lowering the substrate permittivity also increases the bandwidth of the patch antenna. However, this has the disadvantage of making the patch larger. Also, because the Q of the patch cavity is lowered, there will usually be increased radiation from higher-order modes, degrading the polarization purity of the radiation.

By using a combination of aperture-coupled feeding and a low-permittivity foam substrate, bandwidths exceeding 25% have been obtained. The use of stacked patches (a parasitic patch located above the primary driven patch) can also be used to increase bandwidth even further, by increasing the effective height of the structure and by creating a double-tuned resonance effect [8].

A CAD formula for the bandwidth (defined by SWR < 2.0) is

$$BW = \frac{1}{\sqrt{2}}\left[\tan\delta_d + \left(\frac{R_s}{\pi\eta_0\mu_r}\right)\left(\frac{1}{h/\lambda_0}\right) + \left(\frac{16}{3}\right)\left(\frac{pc_1}{\varepsilon_r}\right)\left(\frac{h}{\lambda_0}\right)\left(\frac{W}{L}\right)\left(\frac{1}{e_r^{sw}}\right)\right] \quad (2.29)$$

Where the terms have been defined in the previous section on radiation efficiency. The result should be multiplied by 100 to get percent bandwidth. Note

that neglecting conductor and dielectric loss yields a bandwidth that is proportional to the substrate thickness h.

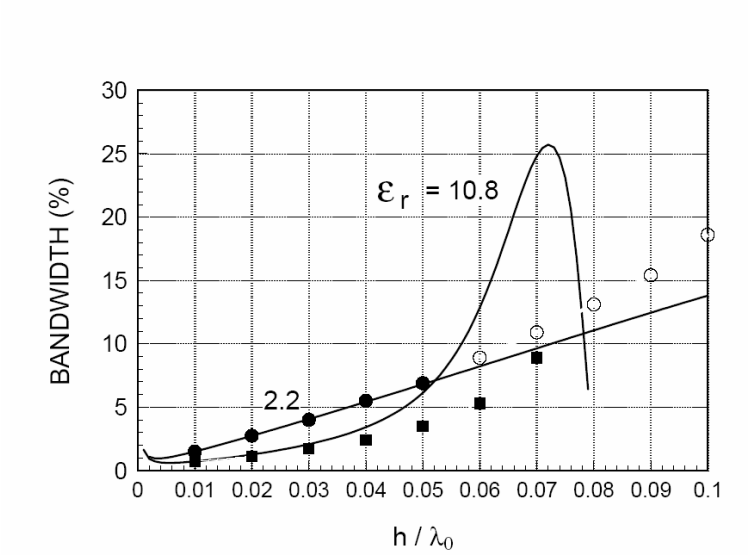

Fig. 2.6/ Calculated & Measured Bandwidth

Figure 2.6 shows calculated and measured bandwidth for the same patch in Figure 2.5. It is seen that bandwidth is improved by using a lower substrate permittivity, and by making the substrate thicker.

2.8 INPUT IMPEDANCE

A variety of approximate models have been proposed for the calculation of input impedance for a probe-fed patch. These include the transmission line method [9], the cavity model [10], and the spectral-domain method [11]. These models usually work well for thin substrates, typically giving reliable results for h / λ_0 < 0.02. Commercial simulation tools using FDTD, FEM, or MoM can be used to accurately predict the input impedance for any substrate thickness. The cavity model has the advantage of allowing for a simple physical CAD model of the patch to be developed, as shown in Figure 2.7.

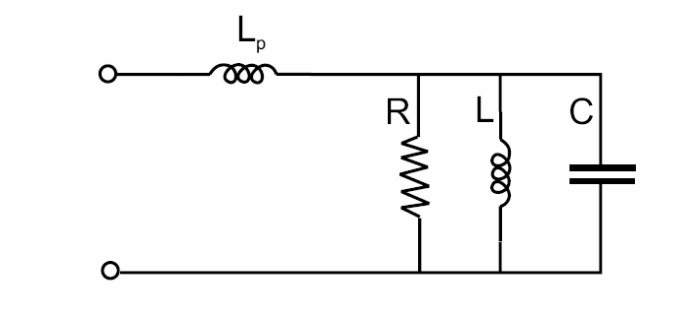

Fig. 2.7 / Equivalent Circuit of Patch Antenna

In this model the patch cavity is modelled as a parallel RLC circuit, while the probe inductance is modelled as a series inductor. The input impedance of this circuit is approximately described by

$$Z_{in} \approx jX_f + \frac{R}{1 + j2Q\left(f / f_0 - 1\right)} \tag{2.30}$$

where f_0 is the resonance frequency, R is the input resistance at the resonance of the RLC circuit (where the input resistance of the patch is maximum), $Q = Q_{\text{total}}$ is the quality factor of the patch cavity (20), and $X_f = \omega L_p$ is the feed (probe) reactance of the coaxial probe. A CAD formula for the input resistance R is

$$R = R_{edge} \cos^2\left(\frac{\pi x_0}{L}\right) \tag{2.31}$$

where the input resistance at the edge is

$$R_{edge} = \frac{\left(\frac{4}{\pi}\right)\left(\mu_r \eta_0\right)\left(\frac{L}{W}\right)\left(\frac{h}{\lambda_0}\right)}{\tan\delta_d + \left(\frac{R_s}{\pi \eta_0 \mu_r}\right)\left(\frac{1}{h/\lambda_0}\right) + \left(\frac{16}{3}\right)\left(\frac{pc_1}{\varepsilon_r}\right)\left(\frac{h}{\lambda_0}\right)\left(\frac{W}{L}\right)\left(\frac{1}{e_r^{sw}}\right)} \tag{2.32}$$

A CAD formula for the feed reactance due to the probe is

$$X_f = \frac{\eta_0}{2\pi}\mu_r\left(k_0 h\right)\left[-\gamma + \ln\left(\frac{2}{k_0 a\sqrt{\varepsilon_r \mu_r}}\right)\right] \tag{2.33}$$

where γ = 0.577216 is Euler's constant.

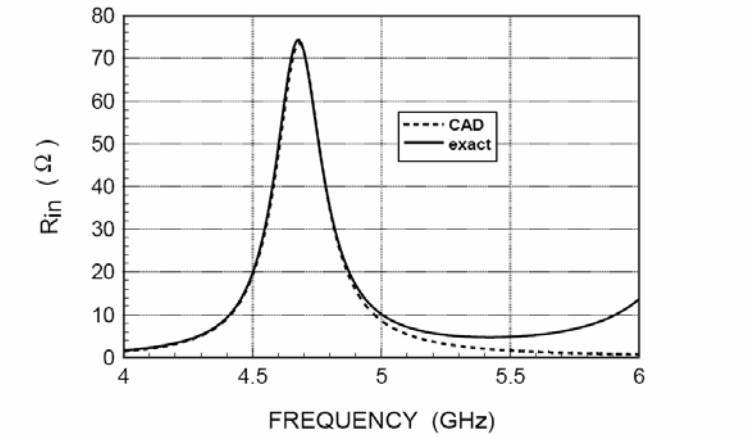

Fig. 2.8(a)

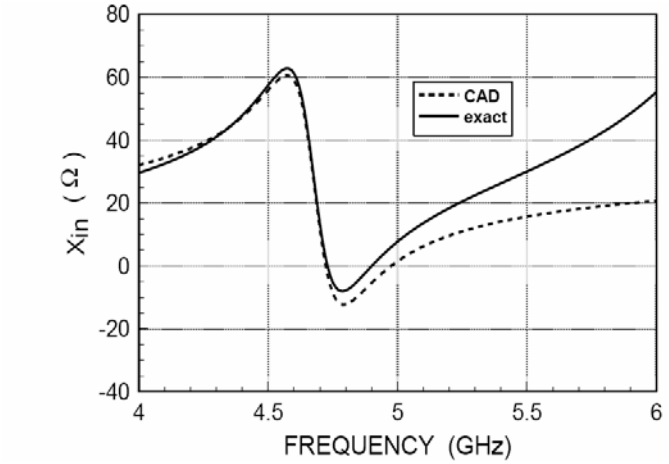

Fig. 2.8 (b)

Fig. 2.8 / Comparison of input Impedances

Figure 2.8 shows a comparison of the input impedance obtained from the simple CAD model (30) with that obtained by a more accurate cavity model analysis. At the resonance frequency, the substrate thickness is approximately 0.024 λ_0. Near the resonance frequency, the simple CAD model gives results that agree quite well with the cavity model.

2.9 IMPROVING PERFORMANCE

Much research has been devoted to improving the performance characteristics of the microstrip antenna. To improve bandwidth, the use of thick low-permittivity (e.g., foam) substrates can give significant improvement. To overcome the probe inductance associated with thicker substrates, the use of capacitive-coupled feeds such as the top-loaded probe [12] or the L-shaped probe [13] shown in Figure 2.9a and Figure 2.9b may be used. Alternatively, the aperture coupled fed shown in Figure 2.9c may be used, which also has the advantage of eliminating spurious probe radiation. To increase the bandwidth even further, a stacked patch arrangement may be used, in which a parasitic patch is stacked above the driven patch [8]. This may be done using either a probe feed or, to obtain even higher bandwidths, using an aperture-coupled feed (Figure 2.9c).

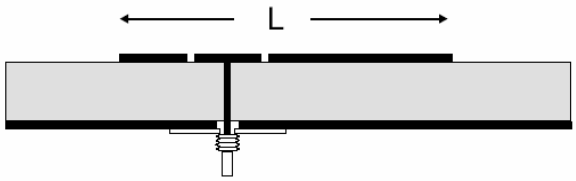

(a) Top Loading Probe Feeding

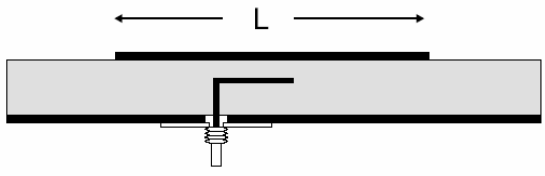

(b) L- Probe Feeding

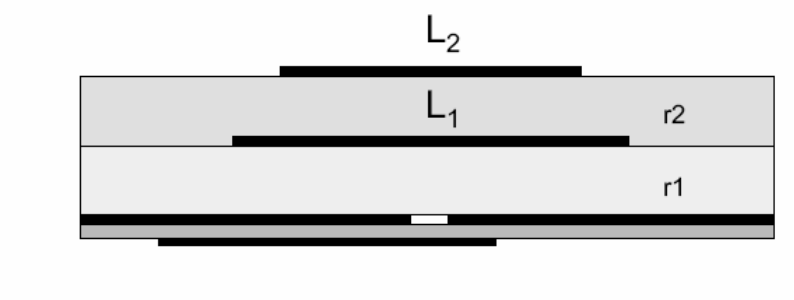

(c) Aperture Coupled Feeding

Fig. 2.9/ Feed Types

The bandwidth enhancement is largely due to the existence of a double resonance, and to some extent, to the fact that one of the radiators is further from the ground plane.

Bandwidths as large as one octave (2:1 frequency band) have been obtained with such an arrangement. By using a diplexer feed to split the feeding signal into two separate branches, and feeding two aperture-coupled stacked patches with different centre frequencies, bandwidths of 4:1 have been obtained [14]. Parasitic patches may also be placed on the same substrate as the driven patch, surrounding the driven patch. A pair of parasitic patches may be coupled to the radiating edges, the non-radiating edges, or all four edges [15]. This planar arrangement saves vertical height and allows for easier fabrication, allows the substrate area occupied by the antenna is larger, and there may be more variation of the radiation pattern across the frequency band since the current distribution on the different patches changes with frequency. Broad banding may also be achieved through the use of slots cut into the patch, as in the “U-slot” patch design [16]. This has the advantage of not requiring multiple layers or increasing the size of the patch as with parasitic elements.

Another variation of the microstrip antenna that has been introduced recently is the “reduced surface wave” microstrip antenna shown in Figure 2.10 [17].

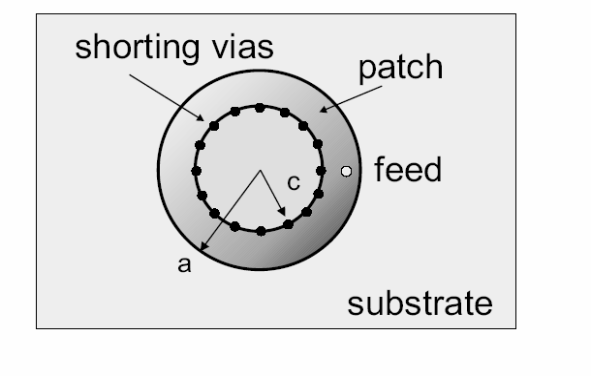

Fig. 2.10/ Reduced surface wave microstrip antenna

This design is a variation of a circular patch, with an inner ring of vias that creates a short-circuit inner boundary. By properly selecting the outer radius, the patch excites very little surface-wave field, and also only a small amount of lateral (horizontally propagating) radiation. The inner short-circuit boundary is used to adjust the dimensions of the patch cavity (between the inner and outer boundaries) to make the patch resonant. The reduced surface-wave and lateral radiation result in less edge diffraction from the edges of the supporting ground plane, giving smoother patterns in the front-side region and less radiation in the backside region. Also, there is less mutual coupling between pairs of such antennas, especially as the separation increases. The disadvantage of this antenna is that it is $\pi\eta\psi\sigma\iota\chi\alpha\lambda\lambda\psi\ \phi\alpha\iota\rho\lambda\psi\ \lambda\alpha\rho\gamma\varepsilon,\ \beta\varepsilon\iota\nu\gamma\ \alpha\beta\circ\upsilon\tau\ 0.60\lfloor_0$ in diameter, regardless of the substrate permittivity.

Chapter 3

Chapter 3 ACTIVE INTGRATED PATCH ANTENNA

3.1 INTRODUCTION

The number of mobile phones has burgeoned in recent years while satellite communication traffics including international telephone calls and Direct Broadcast Satellite Television (DBS-TV) have also proliferated significantly. Commercial cellular and PCS mobile communication [1] currently occupy the 800 MHz-2GHz spectral regions. With a view to achieving higher data rate and a wider range of service, military and commercial satellite communications [2], inclusive of voice, data and DBS-TV, operate in frequencies ranging from 4 – 30 GHz, and it may go up to 60 GHz and beyond. While the initial technological achievement in both mobile and satellite communications have been accelerated to render service with ample functionality, the current focus lies on lowering the cost of service while maintaining superior quality. One of the cardinal approaches for reducing system and operating cost is the conservation of system power resources and minimization of power wasted as heat. Out of the approximately 250W of power produce by the solar cell arrays on a typical satellite, more than 125W is dissipated as heat due to inefficient operation of the transmitter power amplifier [2].

The power amplifier (PAs) in a wireless transmitter amplifies the signal power before delivering it to the antenna for transmission. The transmitted power needs to be strong enough so that the signal received at the destination is clear and intense. For example, the power amplifier in a communication satellite has an output power level on the order of 40W. To propagate this amount of power to the antenna, the PA consumes an average about 75% of the total accessible

power [2]. If the PA operates at about 30% efficiency [2], then 70%-75% of the total power is converted to heat. Thus 52.5% of the total system power is dissipated as heat in the power amplifier. During an eclipse, the satellite is controlled by on board batteries whose lifetime is confined by the unnecessary waste of power due to conversion to heat. The life span of battery is also of relevance to the cellular phone. By using more efficient PAs in these transmissions, satellite solar cell arrays may possibly be made smaller. While batteries will last longer, prolonging the satellite lifetime as well. Cellular phone usage will be economical since batteries will last longer while cellular base station can curtail cost by drawing less electricity.

The heat produced due to inefficient power usage in the power amplifiers not only wastes valuable solar cell or battery power, but also causes thermal degradation of electronic devices. It requires bulky heat sinks to cool the transmitter. In addition to cutting down the cost, the benefits include increase in efficiency of power amplifier, heat dissipation reduction that moderates the heat-sink size of the system. This is very momentous in satellite communication; where thermal squander management is confronted due to the cacophonous environment of the space where the temperature varies from 4 ^{0}K to 100 ^{0}K approximately, when exposed to direct sun light. Less heat sinking also means small size and weight of the system, which directly metamorphose to further cost saving in satellite launching process. Some of the approaches being taken to ameliorate the power efficiency of transmitters include the use of high efficiency power amplifiers [3], the formulation of power efficient modulation techniques [4] and real time power control of the power amplifiers [5].

3.2 INTEGRATED ANTENNA CONCEPT

In wireless communications systems, transmit front-end consumes a large fraction of the total available power. In particular, the power amplifier preceding the antenna can consume more than 50% of the total average power. Therefore, increasing the power amplifier efficiency is essential to extend battery lifetime (e.g. on a satellite or in portable applications) and reduce power lost to heat that leads to thermal degradation of the electronics in the front end. Both these factors are important in reducing the total cost of the system. By integrating efficient power amplifiers in each unit cell of a transmit antenna array, a transmitter front-end may be optimized for efficient amplification and for combining the output of each unit cell in the low-loss medium of free space.

Active Integrated Antenna (AIA) has been a germinating area of research in recent years, as the microwave integrated circuit and monolithic microwave integrated circuit technologies became more mature allowing for high-level integration. From a microwave engineer's viewpoint, an AIA can be regarded as an active microwave circuit in which the output or input port is free space instead of a conventional 50-ohm interface. In addition to the original role of AIA as a radiating element, it renders certain circuit function like resonator, filter and duplexer as a radiating element. According to the antenna designer's point of view the AIA is an antenna that haunts signal in-built and wave processing capabilities such as mixing and amplification. A conventional AIA comprises of active devices such as Gunn diodes or three-dimensional devices to form an active circuit and planner antennas like dipoles, microstrip patches, bowties or slot antennas. The concept of active integrated antenna was investigated as

early as 1928 [6]. Radio broadcast receivers around 1MHz dealt with a small antenna with electron tube was familiar in those days. In 1960's & 1970's, the awareness for investigating active antenna grew due to the invention of high frequency transistors and some outstanding works reported in this area [7-16]. Various advantages of achieving the active devices in passive radiating elements are discussed in [17]. For example, these works comprise of increasing the effective length of short antenna and antenna bandwidth, decreasing the mutual coupling array elements and enhancing the noise factor. The vital propelling forces for the research on AIA's are the development of novel efficient quasi-optical power combiners during last 15 years [18-19]. The tangible purpose for the quasi-optical power combining is to combine the output power from an array of many solid-state devices in free space. It succeeds combiner loss limitations, which are prominent at millimetre wave frequencies [20-21]. Presently, manifold innovative designs on the AIA's concept have been offered and successfully demonstrated. AIA technology has been elaborated to a point where practical implementation for use in the latest microwave and millimetre wave system is achievable. Now days, it is implemented in a number of related fields such as power combining, beam steering and switching, retro directive arrays as well as high frequency power amplifier designs. In millimetre wave systems, AIA based designs are alluring because they support an effective solution to several fundamental problems at these frequencies, including higher transmission line loss, limited source power, reduced antenna efficiency and lack of high performance phase shifters.

3.2.1 ACTIVE ANTENNA DEFINITION

An antenna with some active processing elements before intercepting or producing electromagnetic wave is called an active antenna. The strenuousness that lies with this definition is that almost all antenna could be regarded as an active antenna as long as the active elements are relatively in closed vicinity to the antenna aperture; for instance, if the active elements are around the same substrate or say within a distance less than the real field distance. The following discussions on the definition are according to Itoh [22]; “For an antenna engineer an active integrated antenna is an antenna with a high degree of wave processing ability. For a Microwave engineer a more appropriate definition may be stated as: ‘active antenna is a microwave front end circuit in which the ports are not terminated in 50 ohm but are directly connected to free space’. It is no doubt that this definition absolutely depicts the capability of an active antenna but still it is not conclusive since there is no clear test for a high degree wave processing capability. The pivotal principle of this definition is whether the active element actually has an impact on the interception of the radiation of the electromagnetic waves, if negative then the active element is not actually part of a post interception (receive case), or pre interception (transmit case) processing block. Therefore an active fully integrated antenna can be defined as: “An antenna whose radiation properties are intimately associated with an active element or elements behaviour’.”

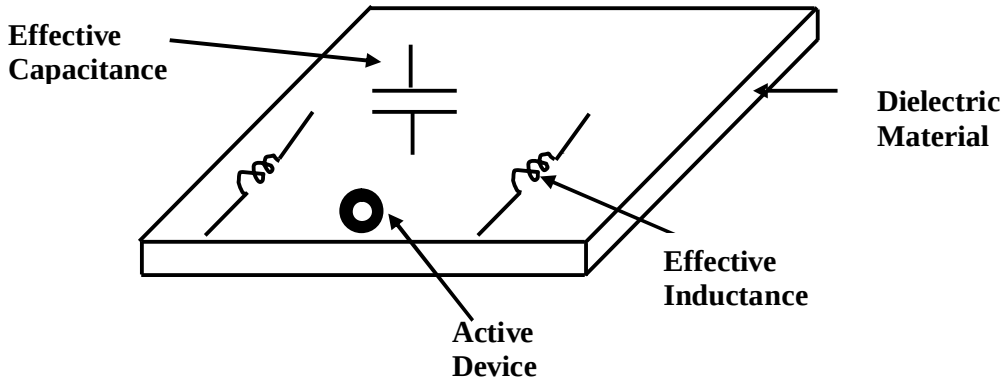

Fig.3.1/Integrated Antenna structure

Simple addition of an amplifier to the output of an antenna does not qualify it as an active antenna since the amplifiers behaviour is independent of the passive behaviour. As a diode and its D.C. biasing [23] would impact the radiating behaviour of the antenna, so in the same way addition of a Varactor diode to the passive structure would be considered to be an active antenna (Fig. 3.1).

3.2.2 FULLY AND QUASI INTEGRATED ACTIVE ANTENNAS

It is tangible that some antennas currently classified as active antennas, may not fall into the above category; therefore these antennas are called partially integrated or quasi-integrated active antennas. Antenna having active components can be classified either as a fully integrated or quasi-integrated active antenna. The component that exists in active antenna requires an external power source. If it comes under the above category then it is a fully integrated active antenna, otherwise it is a quasi-integrated antenna. The different symbolic diagrams explaining these concepts are shown below in fig.3.2.

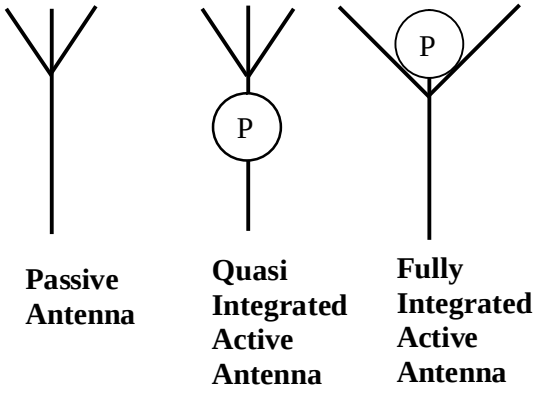

Fig 3.2/Symbolic Representation of Antennas

Two of the symbolic representations of the antennas shown above are active antennas. Therefore, a processing block 'P' with a circle represents them. The processing block contains either linear or non-linear functions and depends upon D.C. biasing. Hence the fully integrated antenna includes such a processing block in the radiation mechanism. Consequently the D.C. biasing values of a fully integrated antenna will influence the radiation properties. Due to D.C. bias of active antenna, the active properties like a noise have some correlation to the radiation properties.

On implementing a passive antenna, an intercepted wave results in a received signal; whereas a transmitted signal results in producing an electromagnetic wave. As per above discussion, it has direct correlation with active integrated antenna. In an active antenna a signal or electromagnetic wave may not have a direct correlation. A receive active antenna may give a signal output without intercepting an electromagnetic wave. Any signal out put contains no information due to lack of electromagnetic wave. Hence, Quasi-integrated

active antenna, fully integrated active antenna (i.e. whether partially or fully integrated) still has a direct correlation with the transfer of information. This does not adhere to a 'signal' in case of passive antenna.

3.2.3 ACTIVE INTEGRATED ANTENNA APPROACH

The selection of antenna is of unique importance in the active integrated approach. Planar-type antennas such as the patch or slot are considered good for minimizing inter connects, as they are suitable for direct integration with microstrip or coplanar waveguide (CPW). Antenna characteristics, only at the system operating frequency, make the point of consideration for an antenna designer. When the use of antenna comes for harmonic tuning, antenna characteristics over a broad frequency span must be considered. These characteristics are categorized into two parts. First one satisfies input impedance at operating frequency and higher harmonics must be chosen to maximize amplifier performance. While second characteristics states that radiation properties of the antenna is chosen for optimal wireless performance. In an antenna design the input impedance of the antenna is a vital point. It states that the input impendence at the fundamental frequency must be close to the optimum output impedance of the amplifier maximum power added efficiency (PAE) or P_{out}. Besides, the antenna should present a reactive termination at undesired higher harmonics. The later constraint is contrary to many planar antennas. For consideration, resonant higher modes of the rectangular patch antenna approximately occur at multiples of the fundamental resonance. If not modified, this antenna is not opted for harmonic tuning. The radiation properties of the antenna are very important for optimal wireless performance. The antenna

need to have sufficient gain and radiation pattern the chosen application along with the low cross-polarization level at the fundamental frequency is indispensable.

3.2.4 AMPLIFYING ACTIVE INTEGRATED ANTENNA

The maximum power-consuming component in transmitter designs are power amplifiers, therefore high efficiency power amplifiers are of enormous important for highly compact & light weight transmitters in wireless communications. A little increment in PAE is very vital, if it can be designed without measure degradation in linearity. In the near past, the AIA concept has been extended into the push-pull power amplifier design, where the power of two anti-phase driven class-B power amplifiers are directly combined through a dual feed planar antenna. In the traditional microwave frequency push-pull power amplifier, the two FET devices are combined through a broad band 180-hybrid or balun. The loss incorporated with the output hybrid restricts the practical efficiency of this type of power amplifiers, microwave & millimetre wave frequencies. The next chapter discusses this configuration.

In the AIA active devices are directly integrated with the antenna, permitting the antenna to serve as power combiner and harmonically tuned load. In addition to its original function as a radiating element it minimizes circuit size and insertion loss.

3.2.5 HARMONIC RADIATION REDUCTION

Harmonic radiation is another significant issue in wireless systems. Harmonic radiations are caused when the power amplifier generates consequential harmonics which may radiate through the antenna resulting

degraded system performance. One striking example where this effect can be considerable problem is co-site interference, which may occur when a number of antennas operating at different frequencies are mounted in close juxtaposition. Equipping additional filters to clear up the resulting EMI problem is not only exorbitant but decreases the transmitter efficiency there by degrading the receiver noise figure. The harmonic tuning techniques bestowed here not only improve the amplifier efficiency but also reduce unwanted harmonic radiation. As derived from the fundamental, the harmonic frequency may have a different radiation pattern, on account of which the harmonic radiated power has to be gauged in all directions.

3.3 INTEGRATED ANTENNA CONCEPT

In 1893 Hertz [24] initiated the concept of end-loaded transmitter and resonant square-loop antenna receiver. In this antenna there is no need of matching networks between the circuit and antenna terminals in case of transmitter as well as receiver. There after, Frost described an amplifying antenna in June 1960 [25]. Investigators of Ohio State University, USA demonstrated both diode and transistor-integrated antenna [26-27]. Boehnker, Copland and Robertson described a mixer-integrated antenna using a tunnel diode and a spiral antenna. This antenna is called "*Antennafier*".

3.3.1 DIODE- INTEGRATED ACTIVE MICROSTRIP ANTENNA

These active integrated antennas have wide applications in Microwave and Millimetre wave devices. Kwok and Weller [28] shared the use of BARITT diode for Doppler-sensing applications in 1979. Armstrong et al. [29]

demonstrated an active BARITT–integrated Microstrip patch antenna Doppler sensor in 1980. The Microstrip patch antenna behaved as a Self-Oscillating Mixer (SOM), with BARITT-diode integration.

Bhartia and Bahl introduced the Varactor-integrated Microstrip patch antenna in 1982 [30]. In 1984, the first monolithic Gunn-integrated end-fire antenna was developed by Wang and Schwarz [31]. In 1984 and 1985, Thomas et al [32-33] reported Gunn-integrated rectangular Microstrip patch antenna operating at X-band frequencies.

In 1986, Michael Dydyk [34] proposed an IMPATT integrated circular Microstrip patch. In 1987, Young and Stephan [35] used the Gunn-integrated active Microstrip patch antenna as distributed oscillators. In 1988, Hammer and Chang [36, 37] also investigated Gunn-integrated Microstrip antenna for spatial power combining. Navarro, Shu and Chang were integrated a different type of antenna called a notch or tapered slot antenna with a Gunn diode in 1990 [38, 39]. The stepped notch antenna design was modified and improved with addition of a Varactor by Navarro et al [40] in 1991.

Ekstom et al. [41] demonstrated a bismuth bolometer detector integrated end-fire notch antenna at 348 GHz in 1992. Similarly, in 1993, Acharya et al. [42] showed a detector integrated end-fire notch antenna at 802Ghz. York and Compton [43] used a dual Gunn-integrated antenna to provide more power and lower the cross polarization level. Stiller et al. [44] developed an active V-band monolithic IMPATT integrated radiating oscillator in 1996.

3.3.2 TRANSISTOR INTEGRATED ACTIVE MICROSTRIP ANTENNA

Although diodes have shown higher operating frequencies and higher output power levels, transistors are low-priced and provide higher Dc to RF conversion efficiency at lower operating voltages. Smaller operating currents translate heat-sinking requirements. Further, transistors perform a variety of function using a single technology allowing flexibility in a multiple function active antenna design.

In 1971, Ramsdale and Maclean [45] used Bipolar Junction Transistors (BJTs) and dipoles for transmitting applications. They demonstrated large height reductions in 1974[46] and later in 1975 [47] using integrated aerials.

The Microstrip patch antenna was first integrated with a FET by Chang, Hummer and Gopal Krishnan [48] in 1988. In 1989, Guttich [49] demonstrated one of the most complete Hybrid integrated antennas. A notch antenna and coupled Slot lines were integrated with a FET and mixer diodes to create a complete RF front–end. York et al [50] introduced a compact FET- integrated Microstrip patch antenna in 1990. In the same year, Birkeland and Itoh [51] introduced another approach to edge couple FETs to Microstrip patches. According to their theory, two and four FETs were integrated with a single patch antenna.

Birkeland & Itoh proposed another approach in 1991 [52]. It uses a directional Microstrip coupler to develop two port FET oscillators. Hall & Haskins in 1992 [53] and in 1994 [54] demonstrated an edge-fed dual FET integrated Microstrip patch antenna oscillator. In this year, Wu et al [55] introduced a push-pull FET-integrated active antenna design.

In 1993, Wu and Chang [56] developed a CPW-fed FET integrated slot-CPW antenna amplifier configuration. In 1994, a folded slot antenna configuration was introduced by Tsai et al [57].

Deal, Qian and Itoh [58] investigated new integrated antenna power amplifier architecture in 1998. In this topology, a multi-fed patch antenna is used as the load of a class-B push-pull amplifier. The same authors reported another paper on Integrated-Antenna Push-Pull Power Amplifiers [59]. In this approach, the antenna serves as an out-of-phase power combiner and tuned load for higher harmonics. In 2002, Hall, Gardner and Ma reported a paper on Active Integrated Antennas [60]. In this paper, they described various types of integrated antennas together with possible ways of exploiting the technology. They used two FET based oscillators along with a patch antenna to form 30 GHz push-pull patch oscillators.

3.4 OSCILLATOR TYPE ACTIVE INTEGRATED ANTENNA

Integrating an active solid-state device directly with an antenna forms an integrated antenna oscillator. The active solid-state device could be a diode such as Gunn, IMPATT, BRITT, etc, or a transistor such as MESFET, high electron mobility transistor (HEMT), hetero junction bipolar transistor (HBT). In the traditional approach, the antenna and oscillator are two separate components interconnected by a transmission line. The deliverance is given to optimize the performance of the oscillator and antenna independently because there is an apparent distinction between the circuit components and the radiating structures. In the integrated antenna oscillator there is no conspicuous discrimination or boundary between the oscillator and antenna. The active device lies within the

volume normally coupled with the radiating structure. The antenna succours as a load and radiator for the active device. The AIA oscillator has the convenience of smaller size, lower cost and lower loss, as compared to the conventional approach. The general integrated antenna oscillator circuit is shown in fig. 3.3. The transistor consisting of three terminals is a two port network which offers to the feed input impedance that follows with one port termination on the other side. The active device impedance is a function of frequency, d.c. bias current, R.F. current, and temperature. Early integrated antenna had come into limelight in 1960s.

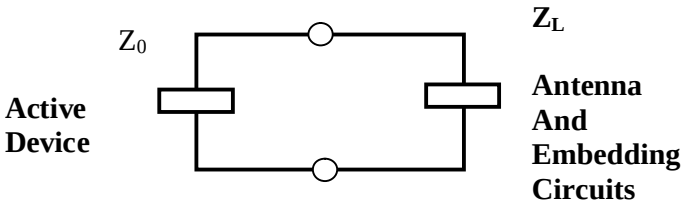

Fig.3.3/General Integrated Antenna Oscillator circuit

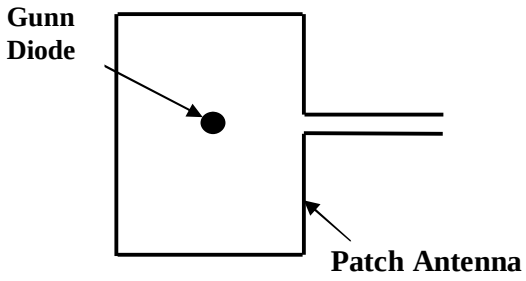

Fig.3.4/Integrated Gunn-patch antenna Oscillator

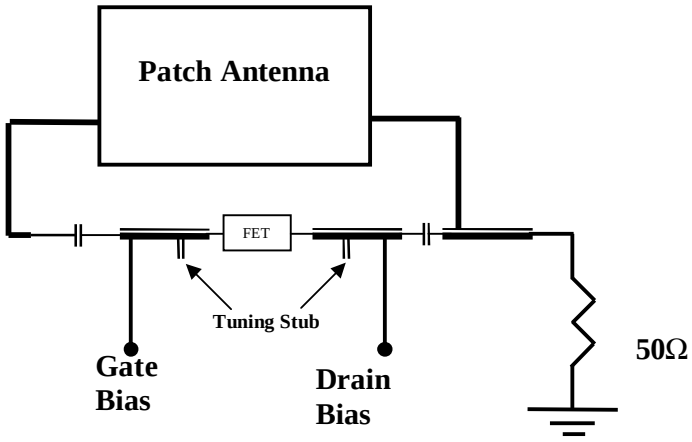

Fig.3.5/ Integrated Antenna Oscillator using FET

The perception observed was of very little use till mid 1980s. When integrated antennas became approbation for compact mobile systems and spatial power combining, it was sought to solve power deficiencies of solid-state devices. Thomas et al [61-62] reported Gunn integrated rectangular Microstrip patch antenna operating at X-band frequencies. The active Microstrip Patch was a compact inexpensive microwave source, which could be used for Doppler sensing or spatial power combining applications. The design comprises of a Gunn diode and a rectangular Microstrip patch antenna. The antenna succours as a resonator and load for the radiating oscillator. Fig 3.4 & 3.5 show the configuration of the active antenna oscillator. The Gunn diode was mounted, between the patch and the ground plane, offset along the patch to locate it at the 10Ω - feed point. For better phase noise, the integrated Gunn patch antenna Oscillator can be injected locked to a stable source using an external source or mutual coupling [63-65].

3.5 FREQUENCY CONVERSION TYPE ACTIVE INTEGRATED ANTENNA

In 1977 [66], invention of a quasi-optical mixer at 100-120 GHz to replace the waveguide mixer initiated work on frequency conversion type AIA [67 –74]. Mostly the work focused on the quasi-optical mixer, baring some exceptions [77, 79] where quasi-optical multipliers were also dealt with. Recent interests in intelligent highway systems and non-contact ID's require intensive work on quasi-optical transponders using self-oscillating mixers or sub-harmonically pumped mixers to realize necessary simple and low-cost components.

A quasi-optical mixer, which can functions as a receiver front end, integrates a mixer to a receiving antenna. The integration of the local oscillator (LO) can be on the same substrate, or can be supplied by an external source through free space. A self-oscillating mixer can eliminate the need of a separate LO, utilizing the nonlinear property of oscillating device for frequency conversion [69]. However, realization of LO with sufficient power level to drive the mixer at millimetre-wave frequencies is difficult. A sub-harmonically pumped mixer can be a solution by using an LO frequency at one-half the value required for a conventional mixer [68]. Its practical application is demonstrated on a non-contact identification transponder. It receives a 6 GHz interrogation signal as the harmonically pumped LO power. Then it uses a frequency of around 12 GHz for a modulated ID code to provide the required response. Transmission and reception employ a broadband bow-tie antenna is used for receiving as well as transmitting.

3.6 OTHER FORMS OF ACTIVE INTEGRATED ANTENNA

Previous sections have described a number of AIA configurations and have suggested befitting application areas. To comprehend several systems requirement can be cited in order to conclude that such technology is applicable to communications and sensors in a wider sense. For transmitting elements, stability, purity and capability of frequency tuning and modulation are essential. Sensitivity and selectivity are important for receive elements. Finally, the ability to duplex both transmit and receive functions is requisite for many systems.

3.6.1 Transmitting Elements

Stand-alone antenna oscillators have inherently low stability. The combination of a single active device oscillator with an antenna generally has a bandwidth of a few percent resulting in external quality factor less than a few 10s. While this may be admissible in short-range sensor systems such as intruder alarms; it is too low for most multi-channel communications applications. In addition, long-term stability must be possessed and tuning made more accurate. Patch oscillator control using a PLL [79] has been shown to reduce phase noise to certain acceptable levels; for example the Digital Enhanced Cordless Telephone (DECT) standard finds them useful. A phase noise of 70 dBc/Hz at 10 kHz has been consummated at an operating frequency of around 1.8 GHz. It is reckoned that, using chip-based PLLs, a compact single-substrate transmitter could be made with overall size1.5 times the patch-antenna size.

PLL techniques become uphill at very high frequencies and an alternative technique using a coupled cavity beneath the antenna oscillator has been displayed [80]. Using scale models at 4 GHz of millimetre-wave oscillators, a

phase noise of 78 dBc/Hz at 10-kHz offset was gained for both a patch and a slot oscillator. Measurements of copper-plated cavities micro-machined in silicon at 34 GHz suggested that better phase noise than the above could be obtained at millimetre wavelengths. Simulations, using the Van der Pol method, demonstrated that the use of a coupled cavity escalated the oscillator start up time by about a factor of three. The use of a single long cavity beneath two oscillators improved mutual locking so that if they had slightly different free-running frequencies, due to manufacturing differences, there was an increased chance of the two locking together. Out-of-band radiation must be restrained in most practical systems and careful oscillator design is needed. Circular sector patches [81] and shorted quarter-wavelength patches [82] have been shown to give a reduction of over 10 dB in radiation at harmonic frequencies. Analysis is also available [83] to guide design methods. When locked oscillators are used to provide either frequency or phase modulation, then the finite locking time places a limit on the capacity of the communications link. This effect is accelerated when locked oscillator arrays are, modulated through the locking signal applied to a single element only for simplicity. Van der Pol analysis [84] has put forth that the data rate is inversely proportional to the array length and for a seven-element linear array is of the order of 10 Mb/s.

3.6.2 Receiving Elements

Direct down-conversion receive elements have been extensively reported [85]. If increased sensitivity and selectivity is required, then super heterodyne techniques must be used. However, if a single-substrate configuration is used, then substantial radiation from the Local Oscillator (LO) will result. For a 0-dBm

LO power, an adequate isotropic radiated power of 25 dBm had been measured, with results confirmed by theory [86]. To counter the undesirable radiation from equipment for the DECT, shielding can be used, but this reduces the degree of integration and will result in increased cost and size.

3.6.3 Duplex Elements

Various forms of duplex elements have been demonstrated. If the oscillator active device is also used as a self-oscillating mixer, then simple Doppler radar elements can be made. A time-division communications function can be executed by switching the oscillator between transmit and LO frequency. Polarization duplexing, with an oscillating active device connected to one side of a square patch and a low-noise amplifier attached to an orthogonal side, as shown in Fig.3.6, allows synchronous transmit and receive operation [87]. If one pair of element is rotated about 180^0, it increases the isolation in a two-element array, which is measured at 45 dB. This isolation would consent to a pair of 8.8 element arrays to form duplex link with a range of approximately 100 m. Concurrent transmit–receive operation on the same frequency and polarization has been demonstrated by the integration of an active circulator in the form of a ring with three embedded amplifiers surrounding a quarter-wavelength patch [88]. Isolation of 25 dB was accomplished over a relatively narrow bandwidth.

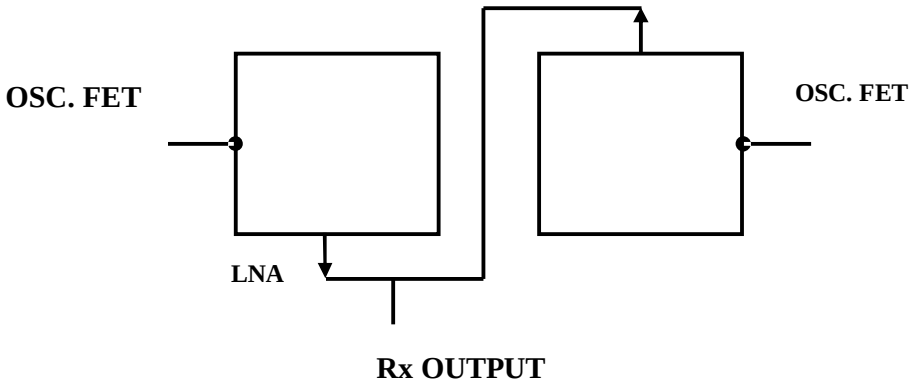

Fig.3.6/Simultaneous Transmit-Receive Active Antenna

3.7 CONCLUSION

The AIA was a paradigm shift in small and conformal antenna research. It is an interdisciplinary topic, and hence throws various challenges to the antenna and RF research communities alike. This chapter has outlined various areas in which research continues to be carried out. It is contemplated that this technology with possible modification & supplements will find in many uses in future wireless communication systems.

Chapter 4

Chapter 4 DUAL-FED ACTIVE INTEGRATED ANTENNA

4.1 INTRODUCTION

Due to spectrum congestion at lower frequencies and the spurt in the wireless communication, it is essential to look for miniaturized systems with higher bandwidth, and high efficiency of frequency reuse. The frequency range suitable for systems of such characteristics are the microwave, millimeter-wave and beyond. Once, the frequency range is identified, it is essential to realize systems for that range. One of the major subsystems in such communication systems is the (transmitting or receiving or transceiver) front end, which can consume majority of power. Thus a successful design must put innovative efforts to realize compact and high efficiency front-ends.

At University of California, Los Angeles (UCLA), the group of Prof. T. Itoh has proposed an integrated-antenna push-pull power amplifier as a compact and high efficiency RF transmitter. In this configuration, a 180-degree hybrid splits the input power and feeds them (which are in anti-phase) to two FETs. The outputs from the FETs are given to a dual-fed Microstrip patch or slot antenna in such a manner that the fundamental mode is excited 180 degree out of phase by each feed. This chapter describes the principle of such dual-fed antenna and proposes a modification to the input circuit.

4.2 PRINCIPLE

Dual-feed antennas [1-6] can be described as a three-port structure, where ports 1 and 2 are the antenna feeds, and port 3 is an invisible radiation port shown in Fig 4.1(a). Three conditions must exist if the two-feed antenna is to be used as an efficient power combiner in a tuned push-pull PA. First, the antenna must radiate efficiently with acceptable patterns. Second, the input impedance of the antenna should be suitable for harmonic tuning. Finally, negligible power should flow from feed port to feed port when push-pull excitation is applied, which will directly limit the power-combining efficiency.

Two structures that satisfy these conditions are the Microstrip patch and slot antennas. The patch antenna has Microstrip feeds placed at opposite radiating edges to excite the proper radiation mode. For such structures, used with push-pull excitation, each feed will excite identical radiation modes with identical phase in the antenna. Therefore, the radiated power will combine in free space. Additionally, the radiated fields will be essentially that of the single-feed patch or slot antenna. Therefore, each of these structures satisfies the first condition. Each of these structures can also be used for harmonic tuning. Finally, the feed-feed coupling of each of these structures is ideally zero when push-pull excitation is applied. For the rectangular patch antenna, the mode coupling between feeds 1 and 2 will be the Microstrip mode. With push-pull excitation (odd mode) applied at each feed, the voltage at the center of the patch must be zero. Therefore, a virtual short circuit exists at the center of the patch and no net power will be guided between feeds 1

and 2. This creates a standing wave in the cavity that exactly corresponds to the desired radiation mode of the fundamental resonance. Therefore, any propagating energy will be directly transformed into the radiation mode. Since no power will flow between the two feed ports, only antenna losses will limit the power-combining efficiency. In the case of small antenna losses, the combining efficiency will, therefore, approach 100%.

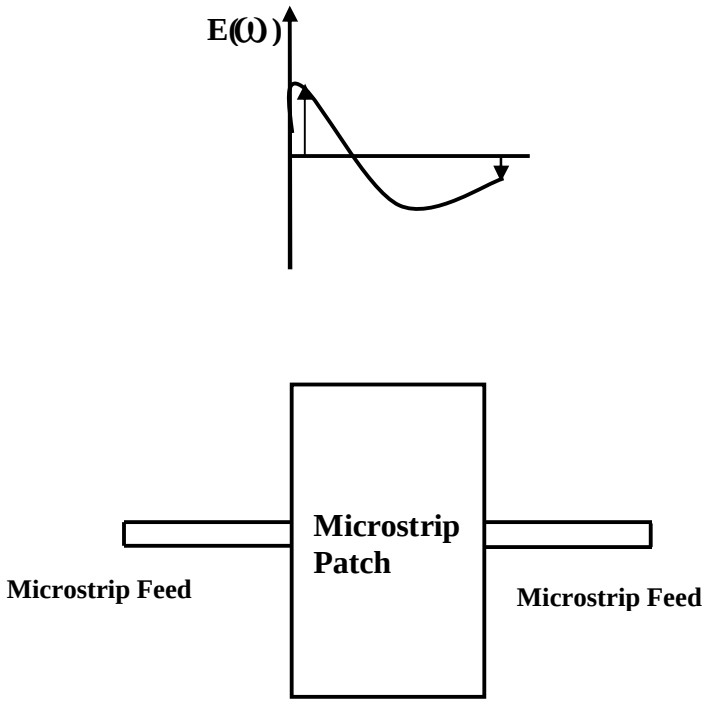

(a) Dual- fed Microstrip Antenna

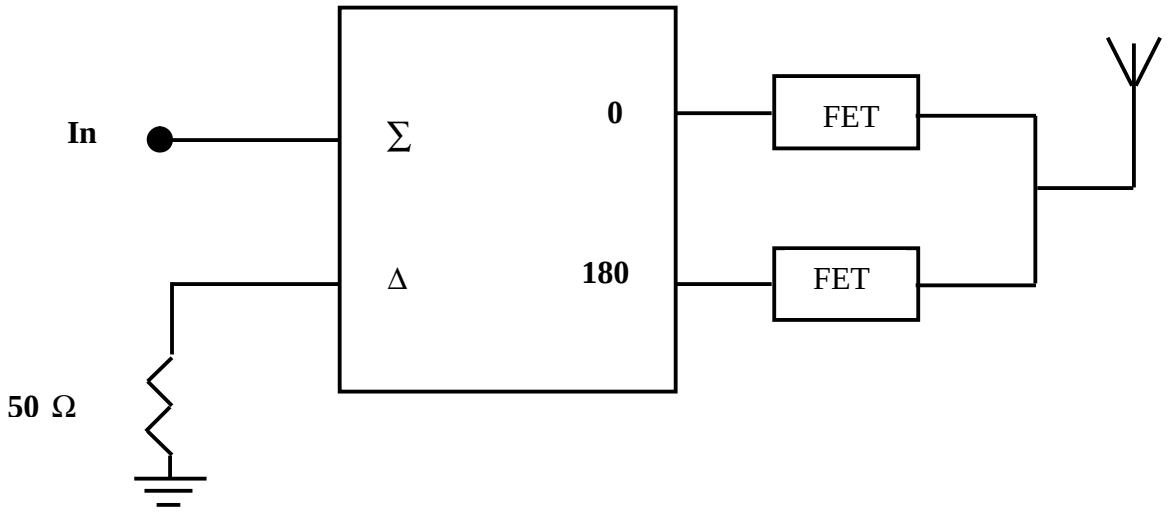

(b) Schematic of a Push-pull AIA Front-End

Fig. 4.1 / Push-Pull AIA

4.3 SPLITTING AMPLIFIER

Basically, a 0° splitter is a passive device which accepts an input signal and delivers multiple output signals with specific phase and amplitude characteristics. The output signals theoretically possess the following characteristics:

1. Equal amplitude.

2. 0° phase relationship between any two output signals.

3. High isolation between each output signal.

Table 4.1: Insertion Loss:

Number of Out puts	Theoretical Insertion Loss (dB)
2	3.0
3	4.8
4	6.0
5	7.0
6	7.8
8	9.0
10	10.0
12	10.8
16	12.0
24	13.8
48	16.8

4.3.1 Basic Splitter

Since the 0° power splitter is a reciprocal passive device it may be used as a power combiner simply by applying each signal singularly into each of the splitter output ports. The vector sum of the signals will appear as a single output at the splitter input port. The power combiner will exhibit an insertion loss that varies depending upon the phase and amplitude relationship of the signals being combined. For example, in a 2 way 0° power splitter/combiner, (Fig.4.2) if the two input signals are equal in amplitude and are in-phase then the insertion loss is zero.

However, if the signals are 180° out-of-phase the insertion loss is infinite. And, if the two signals are at different frequencies, the insertion loss will be equal the theoretical insertion loss shown above. The power combiner will also exhibit isolation between the input ports. The amount of isolation will depend upon the impedance termination at the combiner output or sum port. For example, in the 2 way 0° power splitter/combiner of Fig.4.2 if port S is open then the isolation between ports A and B would be 6dB. And, if port S is terminated by matched impedance (for maximum power transfer) then the isolation between ports A and B would be infinite.

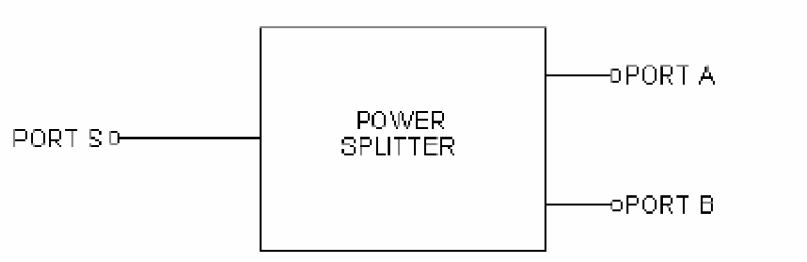

Fig.4.2/ When used as a 0° power splitter

The following signal processing functions can be accomplished by power splitter/combiners:

1. Add or subtract signals vectorically.

2. Obtain multi in-phase output signals proportional to the level of a common input signal.

3. Split an input signal into multi-outputs.

4. Combine signals from different sources to obtain a single port output.

5. Provide a capability to obtain RF logic arrangements.

4.3.2 Analysis of a basic power splitter

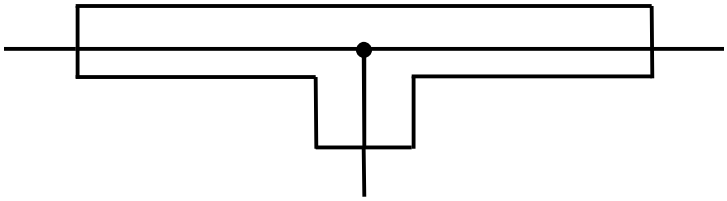

Fig. 4.3(a) / Basic 2 way 0° power splitter, simple "T"

The most basic form of a power splitter is a simple "T" connection, which has one input and two outputs (Fig.4.3 (a)). If the "T" is mechanically symmetrical, a signal applied to the input will be divided into two output signals, equal in amplitude and phase. The arrangement is simple and it works, with limitations.

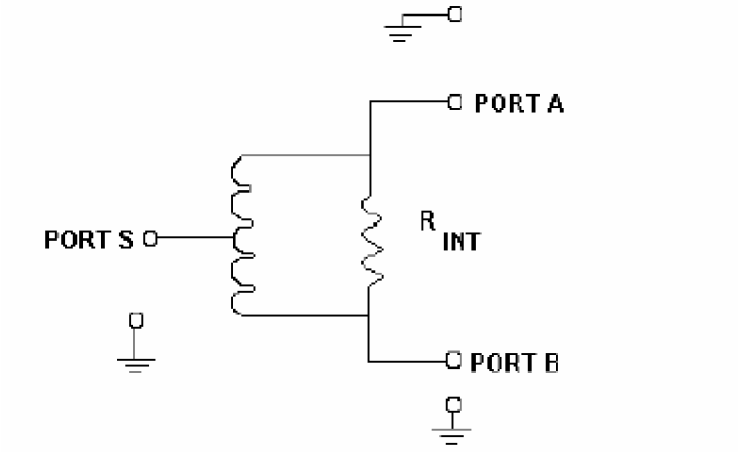

Fig. 4.3(b)/ In two-way splitter/combiner

Fig. 4.3/ Power Splitters

The two obvious limitations are impedance mismatch and poor isolation. In a 50-ohm system, each output would be connected to 50-ohm impedance, thus offering 25-ohm impedance to the input port. Thus, the impedance looking into the common or input port would present a mismatch in a 50-ohm system. To correct this mismatch, a 25 to 50-ohm matching transformer would be necessary for the simple "T".

The second serious limitation of a simple "T" is the poor isolation. Suppose, for example, two antennas are feeding a receiver input using a simple "T" as a combiner. If one antenna appears as a short at its resonant frequency, it would load down the other antenna and, in effect, wipe out the receiver input. However, a properly designed power combiner would provide high isolation between inputs so that the antenna "short condition" at one input would have little influence on the other input and would cause approximately a 3:1 VSWR mismatch at the output port, considering the receiver input. In a simple "T" circuit power combiner the isolation between input ports will depend upon the impedance termination at the output port. If the output port is open then the input ports would have zero isolation between them. And, if the output port were terminated by matched impedance the isolation would be 3dB.

Improving upon the simple "T" circuit, consider the basic lumped element power splitter/combiner circuit of Fig. 4.3(b). The transformer has an equal number of turns from the center tap to each end. Therefore, as an auto transformer (2 to 1 turn’s ratio) the impedance across the output ends is 4 times larger than the

impedance across the center tap to one end**.** As a power combiner, an input signal applied to port A will cause a current to flow through the transformer and experience a 180° phase shift by the time it arrives at port B. Similarly, a current will also flow through the resistor, R_{int} and will not experience a phase shift by the time it arrives at port B. When R_{int} equals the impedance across the transformer ends then, then the currents appearing at port B will be equal in amplitude but opposite in phase and cancel. The net result is that no voltage appears at port B from the input signal applied at port A. Thus, there is theoretically infinite isolation between the ports.

4.4. PUSH-PULL AMPLIFIER

There are various advantages of a push–pull PA over single ended amplifiers. They include the potential for broadband performance [7] and twice the output power of a single-ended amplifier. Thus, for a given output power, it becomes possible to use two lower cost devices. The conventional push–pull PA architecture splits the input power and feeds them in anti-phase to the two FETs through an 180-degree hybrid. The Fourier analysis of the device drain current waveform can be expressed as

$$i_{d1} = i_{dpeak}\left(\frac{1}{\pi}+\frac{1}{2}\sin\omega_0 t-\frac{2}{\pi}\sum_{n=2,4,\ldots}^{\infty}\frac{1}{n^2-1}\cos n\omega_0 t\right) \tag{4.1}$$

$$i_{d2} = i_{dpeak}\left(\frac{1}{\pi}-\frac{1}{2}\sin\omega_0 t-\frac{2}{\pi}\sum_{n=2,4,\ldots}^{\infty}\frac{1}{n^2-1}\cos n\omega_0 t\right) \tag{4.2}$$

In these expressions, i_{dpeak} is the magnitude of the drain peak current and ω_0 is the operating frequency. Equations (4.1) and (4.2) show presence of in-phase higher harmonic components along with anti-phase fundamental terms in the output. It is common for microwave-frequency push–pull PA to combine two FET devices using a broadband 180-degree hybrid or a balun. At microwave and millimeter-wave frequencies, the loss, due to the output stage hybrid in such typical structures, directly limits the practical efficiency of this class of amplifier [8]. Moreover, in designing a highly efficient PA, the load impedance is most important. It must provide a reactive termination at higher harmonics to reflect the power back to the FET with the proper phase [5].

The AIA approach aims at integrating active devices with the antenna (Fig.4.4). As a result the antenna can serve as a power combiner and a harmonically tuned load, besides acting as a radiating element. It results in minimization of circuit size and insertion loss. Fig.4.4 shows the schematic of such a circuit. As in a conventional push–pull PA, a ring hybrid at the input stage splits the input power and feeds the two FETs with two anti-phase waveforms. At the output stage, the balanced waveforms will provide the proper anti-phase excitation of the antenna. Thus the need for a 180-degree hybrid or balun will be eliminated, and a high level of integration with the push–pull PA will be achieved simultaneously.

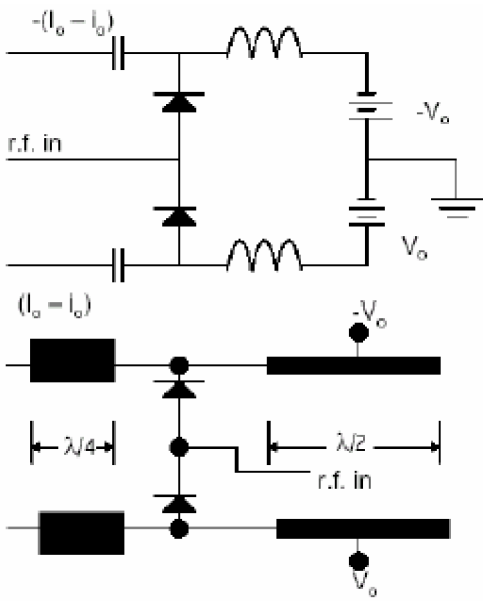

Fig: 4.4/ Schematic of Diode Splitter;
(a) Splitter Configuration; (b) Schematic for Realization

4.5. THE PROPOSED ARCHITECTURE

In the conventional push–pull PA architecture, the input power is split and fed in anti-phase to the two FETs through a 180-degree hybrid (Fig.4.1). In this work [9-11], a pair of diodes dc biased in series but functioning as a parallel pair in the rf circuit (Fig.4.4) replace the hybrid. Each diode is biased at Io, Vo as the Quiescent point and experiences the same rf current “io”. The polarity of the rf current is the same as the dc bias current in one diode but opposite in the other diode. Thus, the rf current pushes one diode to a high current state, (Io – io), while it pulls the other diode to a lower current state –(Io – io). In this Push-pull circuit the overall impedance of the device is the arithmetic sum of each individual diode. For two

identical diodes connected in push-pull, the overall impedance and the power handling capability should be doubled. For the overall device impedance level equal to that of a single diode, individual diodes in the push-pull circuit can have twice the junction area, and, thus raise the overall device power handling capability by a factor of four. Here we assume that there is no serious current crowding effect occurring when the junction area is doubled.

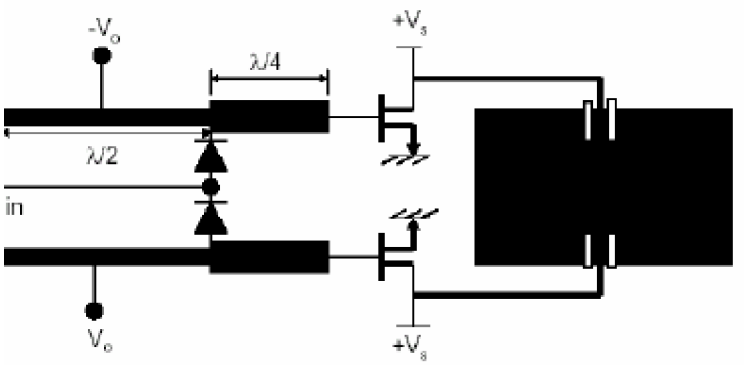

Fig: 4.5/ Schematic of Push-pull Antenna Circuit

Fig. 4.4(b) shows a circuit realization of the splitter configuration. Half-wavelength open circuited stubs are for bias isolations. The quarter-wavelength open circuited stubs provide the rf path while maintaining dc isolation. Here, each diode can be individually biased. Due to this individual bias controllability it is possible to make minor adjustments in matching diode characteristics as well as operating points. When the individual biasing is not essential, the two diodes can also be biased together by a common dc source.

In this paper, the AIA concept is applied to design a compact and high-efficiency push–pull PA using a Microstrip antenna. Fig.4.5 shows the schematic of this circuit. A pair, of IMPATT diodes, is used at the input stage to split the input power and feed the two FETs with two anti-phase waveforms. At the output stage, the balanced waveforms provide the proper anti-phase excitation of the antenna, thereby eliminating the need for a 180-degree hybrid or balun, while simultaneously achieving a high level of integration with the push–pull PA.

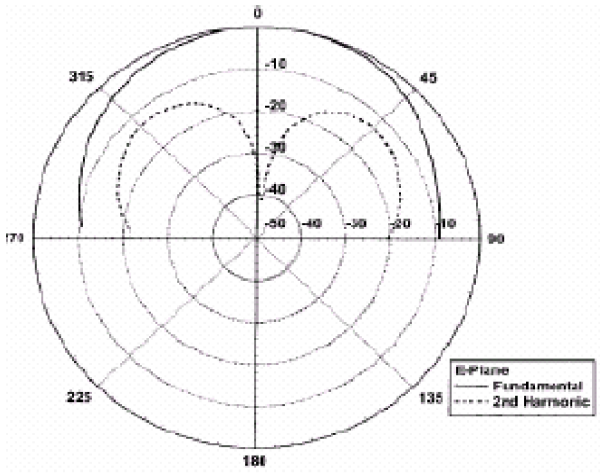

Fig. 4.6/ Simulated Radiation Patterns of Push-pull AIA

4.6. DISCUSSIONS AND RESULT

As mentioned earlier the output, of the diode circuit, contains even harmonics. The FET amplifiers have a finite bandwidth, i.e. they are band-pass circuits. Thus the harmonics in their pass-band will be amplified and those outside will be attenuated. This effectively reduces the harmonic content at the output of the FET amplifiers. Similarly, the patch antenna, being a high Q device, has a narrow bandwidth. Thus it will reject the harmonics outside its bandwidth. Thus using this

circuit we are able to reduce the harmonic content substantially. The remaining harmonics cancel out each other during the addition, since they are in phase and added in opposite directions.

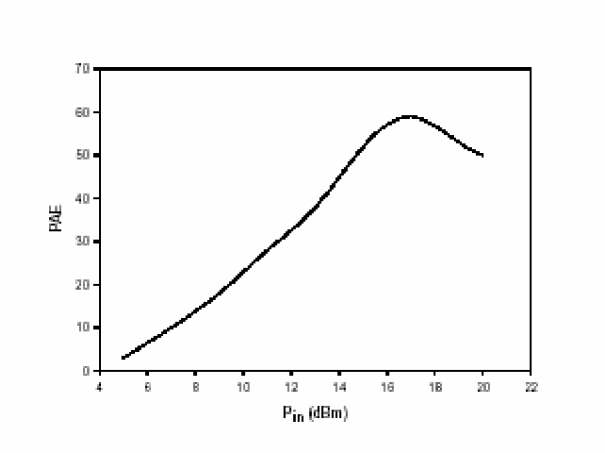

Fig.4.7 / Simulated PAE of Push-pull AIA

Fig 4.6 shows the simulated E-plane pattern for the fundamental and 2nd harmonic. The higher harmonics have very small amounts of power and are not considered here. It shows that second harmonic cancellation is not perfect. Integration of the total radiated power of the fundamental and second harmonics estimates the 2nd harmonic suppression. From this, it is found that the total power in the second harmonic is about 20 dB down from the fundamental.

In AIA system, the knowledge of the amplifier PAE is essential. Simulated PAE is shown in fig. 4.7. Maximum PAE is approximately 55%. It indicates that the circuit will work properly, and the output power from the two devices will be combined effectively.

4.7. ANTENNA INTEGRATION AS SMART LOAD

As Shown in Fig.4.1, Dual- feed antenna is used in the schematic circuit. It can be elucidated as a three-port structure, where ports 1 and 2 are the antenna feeds and port 3 is an invisible radiation port. Three conditions must exist if the two-feed antenna is to be used as an efficient power combiner in a tuned push-pull PA. First, the antenna must radiate efficiently with acceptable patterns. Second the input impedance of the antenna should be acceptable for harmonic tuning. Finally, negligible power should flow from feed port to feed port when push-pull excitation is applied, which will directly limit the power-combining efficiency. With two distinct examples, it can be shown that all the conditions can be met so that the power–combining efficiency will approach 100%. In case of patch antenna the mode coupling between feeds 1 and 2 will be the Microstrip mode. With push-pull excitation (odd mode) applied at each feed, the voltage at the center of the patch must be zero. Therefore, an imperative short circuit exists at the center of the patch and no net power will be guided between feeds 1 and 2. This begets a standing wave in the cavity that exactly corresponds to the desired radiation mode of the fundamental resonance. Therefore, any propagating energy will be directly transformed into the radiation mode. Since no power will flow between the two feed ports, losses of antenna will check the power-combining efficiency. In the case of small antenna losses, the combining efficiency will, therefore, approach 100%. Since the patch antenna combines phase as well as power, which acts as a load to the circuit, is called a smart load.

A supplementary comment due to the narrow bandwidth of the patch is that the overall system bandwidth is regulated according to the antenna bandwidth.

4.8. CONCLUSION

This chapter discussed architecture for an integrated antenna push-pull amplifier. Power splitting is accomplished through a pair of diodes. This structure eliminates the necessity of bulky hybrids, at the input and output, and their associated losses. PAE simulation indicates high efficiency operation of this novel push-pull PA. The following chapter discusses some of the short comings of such AIA and suggests balanced amplifier as an alternative to the push pull amplifier.

Chapter 5

Chapter 5 BALANCED AMPLIFYING ANTENNA

5.1 INTRODUCTION

As discussed in the previous chapter, a solid-state device is integrated with conformal antenna to form an active integrated antenna. For oscillator type active antennas, instability is introduced and maintained through proper circuit design. In contrast to this, stability is the primary criterion in the circuit design of amplifying type active integrated antennas. The purpose here is to enhance the signal for transmission or during reception, right on the site of transmission or reception. Thus in effect the realized gain of the patch is enhanced due to the amplification. High gain is desirable over a broad band for transmission applications; while good noise performance with reasonable gain flatness is desirable for reception.

Most high power amplifying antennas contain two independent devices without any internal transversal connection between them. Invariably these devices are connected in the push-pull [1] configuration. However they can also be combined in a variety of configurations created by external components such as 180-degree splitters/combiner (baluns [2]), 3 dB quadrature couplers (like branch line or Lange couplers), in phase couplers (like Wilkinson couplers), etc. In microwave circuits the balanced [3] configuration also finds wide application. Usually the push-pull configuration is used for relatively narrow band commercial applications from UHF to S-band. Due to its popularity with the circuit designers, it has been implemented in active integrated antenna. The goal of this chapter is to compare the push-pull configuration with the balanced one and then design a balanced amplifying antenna. The next section summarises the push-pull amplifier.

5.2 PUSH-PULL CONFIGURATION

The microwave push-pull configuration has two independent devices each admitting an individual signal of half the total power. Its key elements are an input 0-180-degree power splitter driving two identical devices in antiphase and a 0-180-degree output power combiner adding the output power of the two devices in the load. This type of splitter and combiner are known as baluns (BALanced UNbalanced). They transform [4] a balanced system that is symmetrical with respect to ground to an unbalanced system with one side grounded. Figure 5.1 shows a schematic block diagram of the push pull configuration.

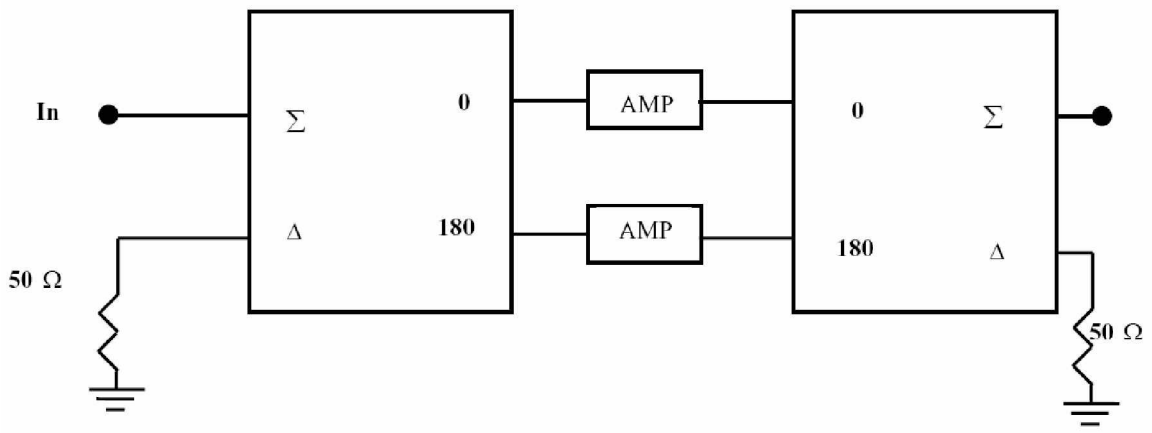

Figure 5.1/ Schematic of a Push-Pull Configuration

Such configuration is easier to match, since it gives 4 times higher impedance [5] in comparison to single ended configuration with same output power. The virtual ground [5] in such configuration can be utilized for more compact and simpler matching structures. Inherently it cancels even products and harmonic contents such as F2 – F1, 2F1, 2F2, F1+F2 etc. However, the baluns can't eliminate the input & output powers reflected by the devices. Hence, the input and

output external match is poor. Theoretical isolation between the input and output, with conventional baluns, is 6dB only. This can some times cause instability.

5.3 BALANCED CONFIGURATION

The balanced amplifier employs two quadrature hybrids. Reflections of the input signals due to poor matching are channelled back to a matched load where they get absorbed. Same phenomenon occurs at the output port also. Therefore, theoretically, both at input and output ports one will see matched loads. A schematic of this configuration is depicted at figure 5.2.

The real advantages of an ideal balanced configuration include good isolation & hence improved stability; good input & output external matching; cancellation in the load of products and harmonics like 2F1+F2, 2F2+F1, 3F1, 3F2, … and attenuation by 3dB of products like F1 ± F2, 2F1, 2F2, …. The disadvantages incorporate matched load to dissipate power in the decoupled port; no virtual ground & hence less compact structural realization.

5.4 BALANCED AMPLIFYING ANTENNA

Normally, active integrated antenna amplifier design still follows the procedure of microwave transistor amplifiers. The only difference being that the radiating patch acts the load in transmitting case and as source impedance for the receiving antenna. If Z_s is the complex source impedance and Z_l is the input impedance of the patch antenna, then the transducer power gain G_T is defined as the ratio of power delivered to the load Z_l to the power available from the source [7]. The expression for G_T in terms of Γ_s and Γ_l is

$$G_T = \frac{1-|\Gamma_s|^2}{|1-\Gamma_{in}\Gamma_s|^2}|S_{21}|^2 \frac{1-|\Gamma_l|^2}{|1-S_{22}\Gamma_l|^2} \quad (5.1)$$

$$G_T = \frac{1-|\Gamma_s|^2}{|1-S_{11}\Gamma_s|^2}|S_{21}|^2 \frac{1-|\Gamma_l|^2}{|1-\Gamma_o\Gamma_l|^2} \quad (5.2)$$

In the above equations,

$$\Gamma_{in} = S_{11} + \frac{S_{12}S_{21}\Gamma_l}{1-S_{22}\Gamma_l} \quad (5.3)$$

$$\Gamma_o = S_{22} + \frac{S_{12}S_{21}\Gamma_s}{1-S_{11}\Gamma_s} \quad (5.4)$$

For unconditional stability of the transistor, the necessary and sufficient condition is expressed by the following two inequality, in terms of Δ (= $S_{11}S_{22}$-$S_{21}S_{12}$).

$$K = \frac{1-|S_{11}|^2-|S_{22}|^2+|\Delta|^2}{2|S_{12}S_{21}|} > 1 \quad (5.5)$$

$$|\Delta|^2 < 1 \quad (5.6)$$

The following subsection gives sample design of a balanced amplifier.

5.4.1 AMPLIFIER DESIGN

The single tone performance of both push-pull and balanced configurations should be alike. The balanced amplifier has clear edge over the push-pull counterpart in terms of the output impedance matching. It is also more stable due to good isolation between its input and output sides. These characteristics have

inspired us to consider a balanced configuration for the active antenna instead of the push pull configuration.

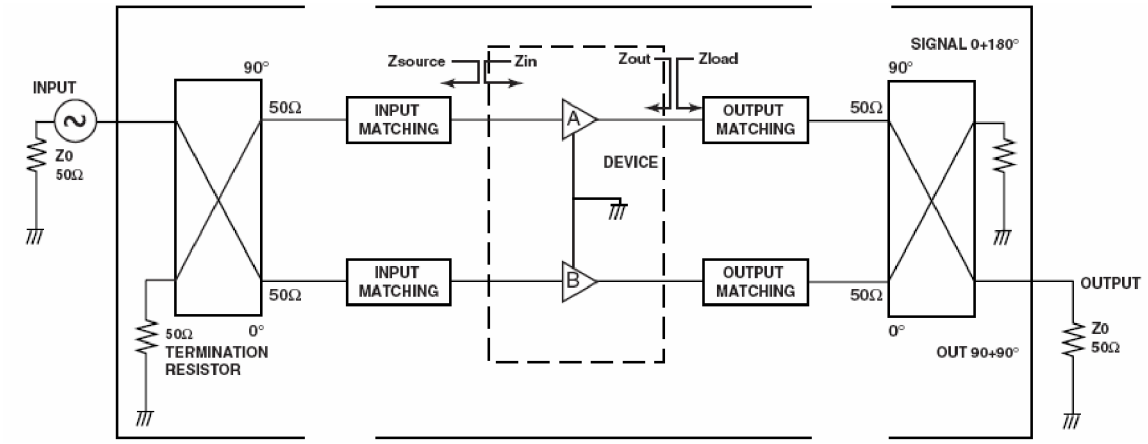

Figure 5.2/ Schematic of Balanced Amplifier

The simplest design considers a balanced amplifier with a 50 ohm load. This amplifier is simulated using Microwave Office [6]. The design parameters are shown in Table 5.1. In this range, the AT31011 [9] exhibits good stability. Figure 5.3 shows the input & output stability, NF and gain circles under different bias conditions. The schematic of the design follows in figure 5.4.

The biasing condition of t310113c offers better noise figure and gain along with comparable stabilities. Hence, this was selected. First a single ended amplifier was designed. Using the optimization feature of the Microwave Office, the amplifier was designed for optimized gain and noise figure. Then the balanced amplifier was implemented using the additional components given in Table 5.2 and microstrip lines for tuning (single stub) on a substrate for which specifications are given in Table 5.3.

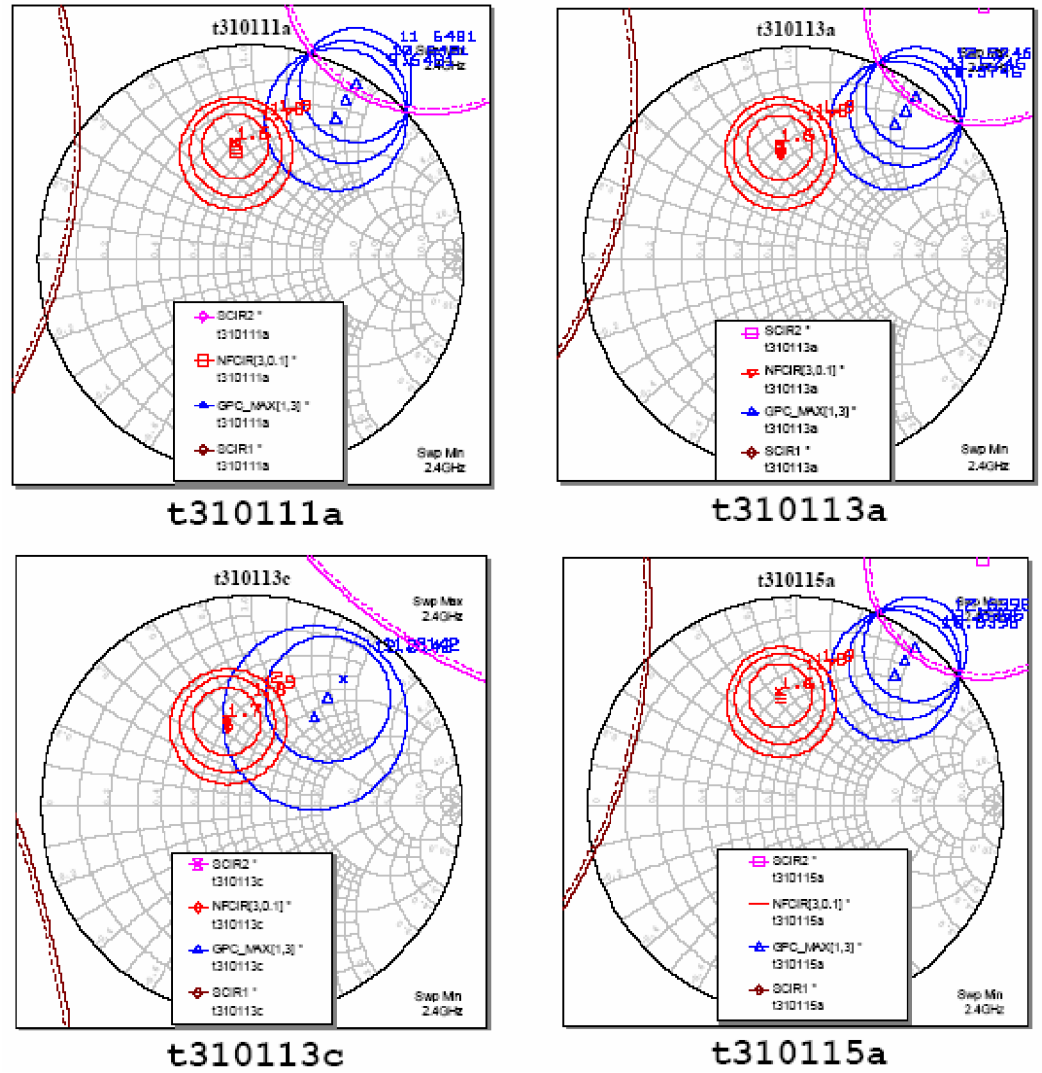

Figure 5.3/ Input/Output Stability, Gain Circles & Noise for various bias

Table 5.1: Design Parameters

Operating Frequency	Gain	Noise Figure	Bandwidth*	Bias Point (t310113c)
2.4 GHz	>10dB	<2dB	200 MHz	V_{CE}=2.7V I_C = 5mA

*For gain variation within 1 dB

Table 5.2: Other Components of the Balance Amplifier

Component	Type	Frequency	Power	Impedance
1A1306-3	Surface mount hybrid coupler	1.9 – 2.7 GHz	60W	
RFP-050060-15X50-2	Terminator	0 – 6 GHz	4W	50 Ohms

Table 5.3: Substrate Parameters

ε_r	tanδ	Substrate Thickness	Metallization
2.94	0.0025	60 mil	1.4 mil Copper

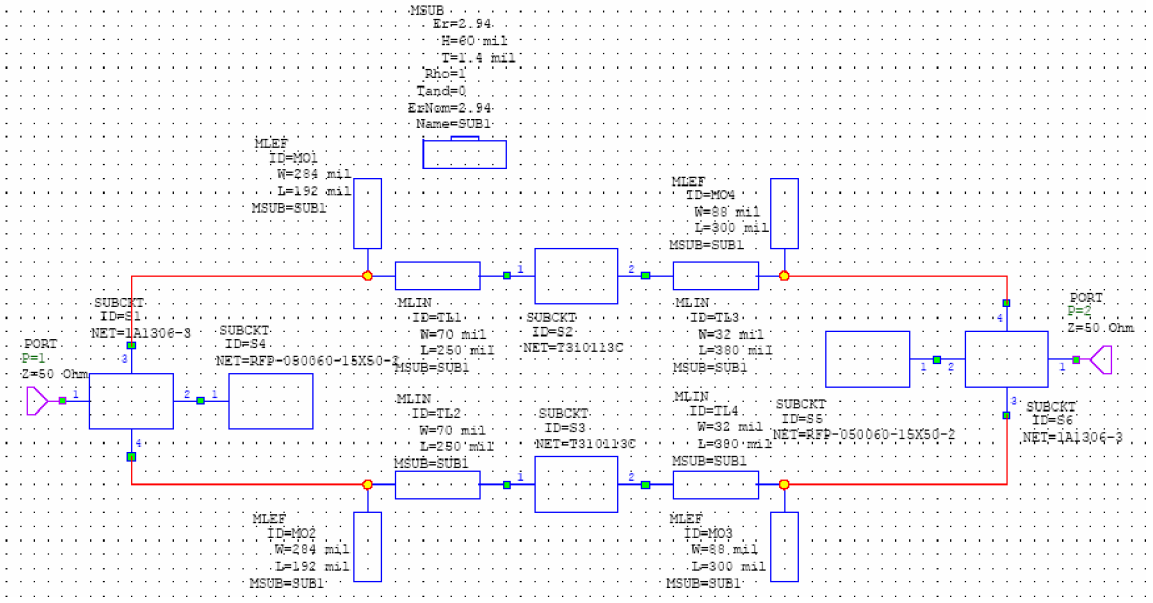

Figure 5.4/ Design Schematic of Balanced Amplifier

From figure 5.5 for the VSWR, the matching at the input and output ports over the desired frequency band is observed to be excellent. The performance of the amplifier is observed in figure 5.6 for the noise figure and the gain. Both these observations indicate a satisfactory design.

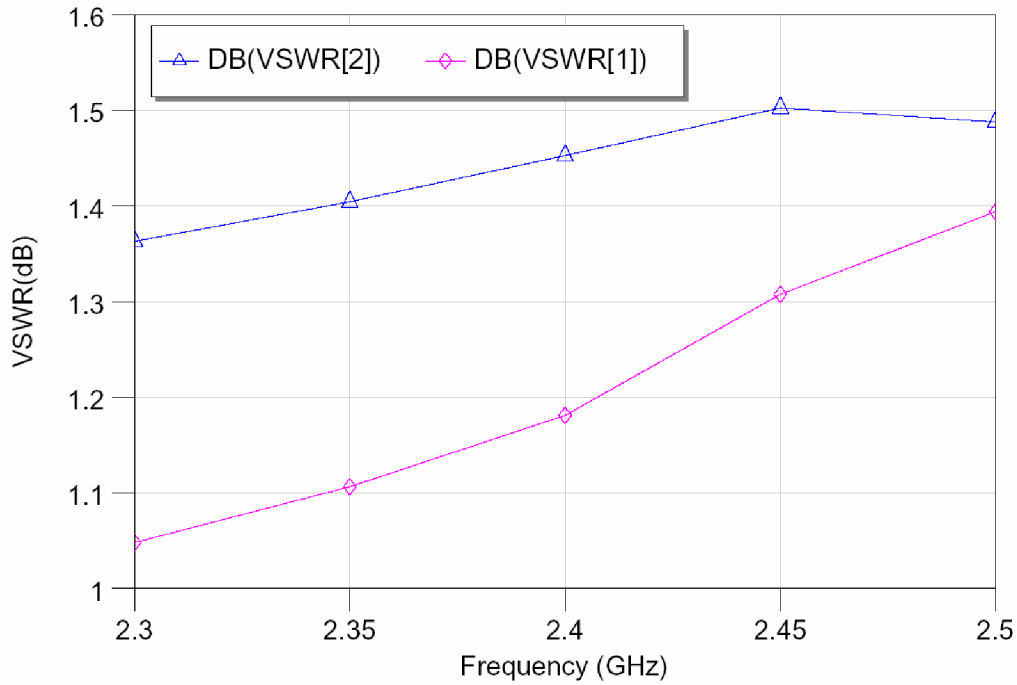

Figure 5.5/ VSWR at the input (#1) and output (#2) ports.

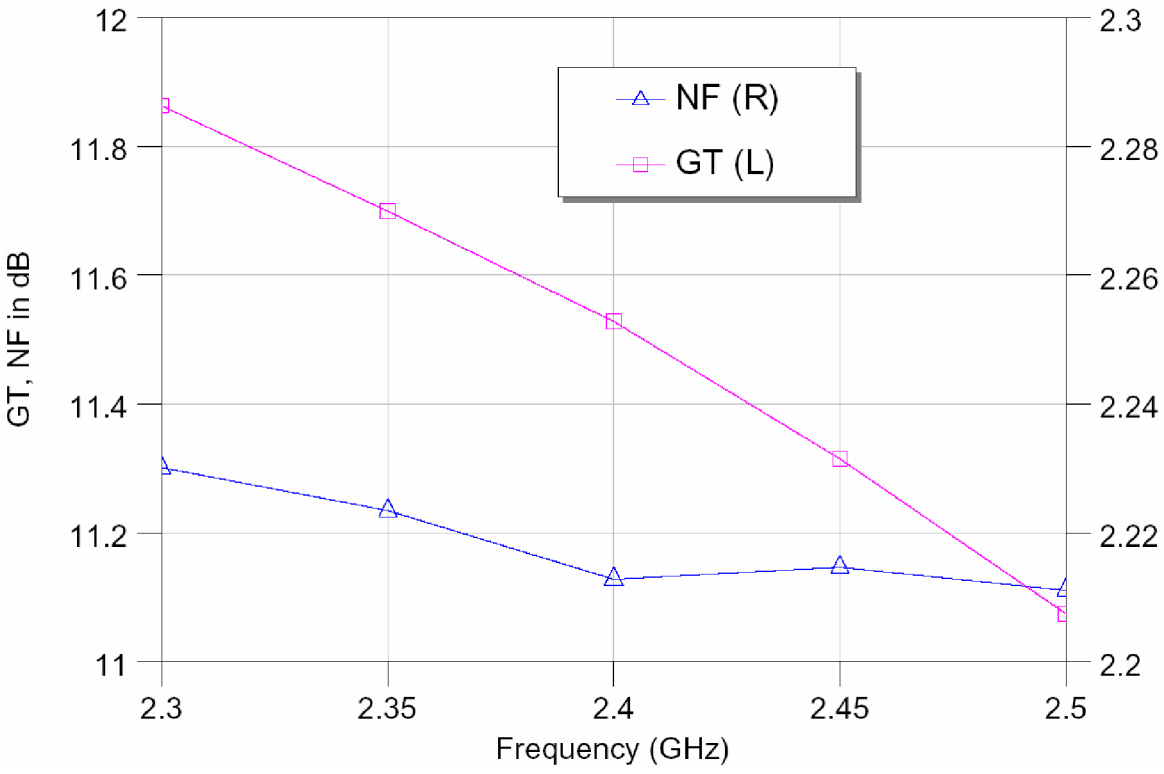

Figure 5.6/ Response of Balanced Amplifier

5.4.2 SINGLE FEED ACTIVE ANTENNA

The next step is replacement of the 50-ohm load at the output by a patch antenna. A rectangular patch antenna was designed to resonate at 2.4 GHz on the above mentioned substrate for ease of integration. The length and width of the antenna were found to be 1753.1 mil and 1409.5 mil. It is inset fed with a 50 ohm microstrip line through a distance of 459.4086 mil from the centre of the radiating edge to obtain 50 ohm input impedance at the design frequency of 2.4 GHz. Figure 5.7 shows this antenna. The results of this preliminary design are shown below in figures 5.8 for the S-Parameters and figure 5.9 for the noise figure and gain. The antenna radiation pattern is shown in figure 5.10.

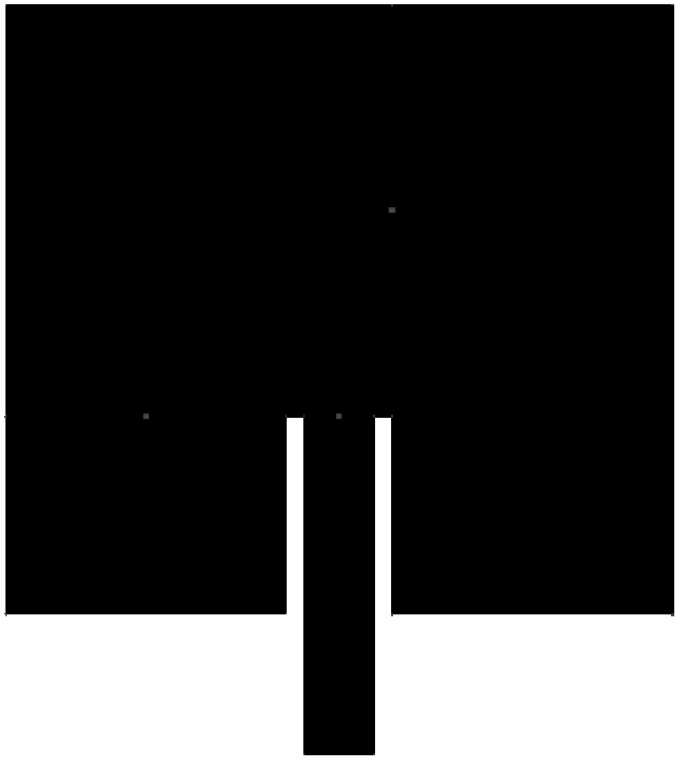

Figure 5.7/ Inset Fed Patch Antenna (1753.1 mil X 1409.5 mil; inset depth 459.4086 mil)

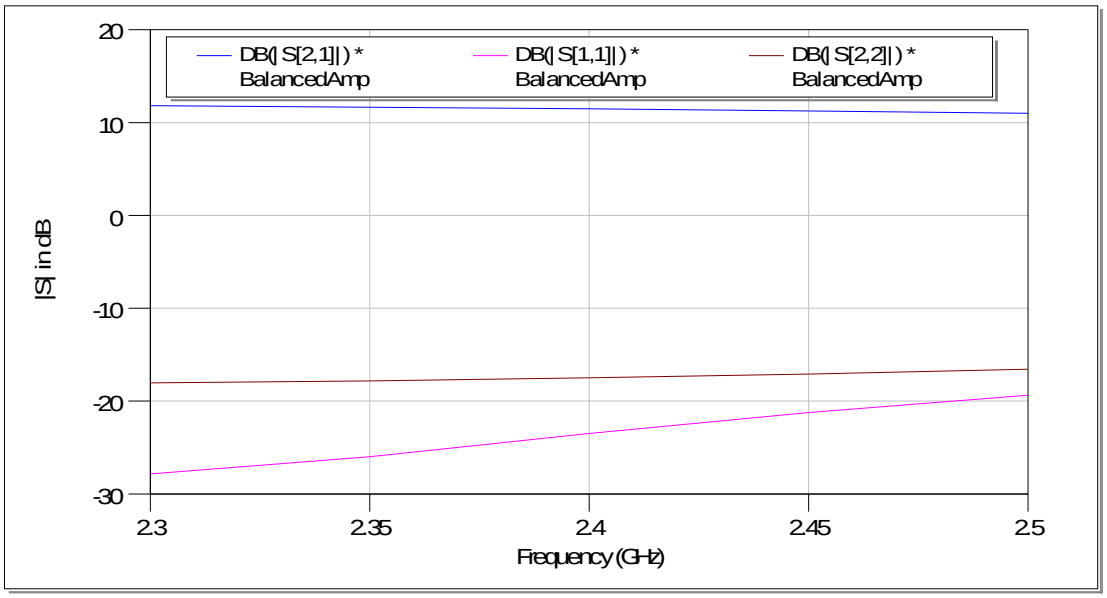

Figure 5.8/ S-Parameter for Balanced Amplifying Rectangular Patch Antenna

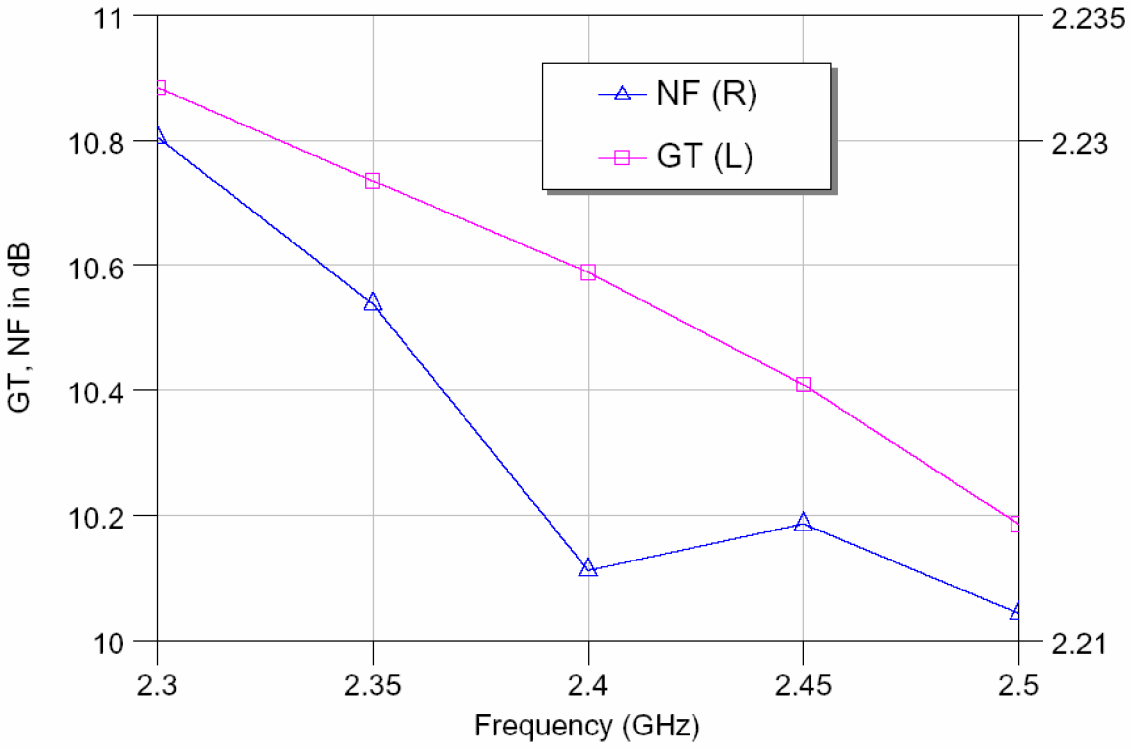

Figure 5.9/ NF and Gain of Balanced Amplifying Rectangular Patch Antenna

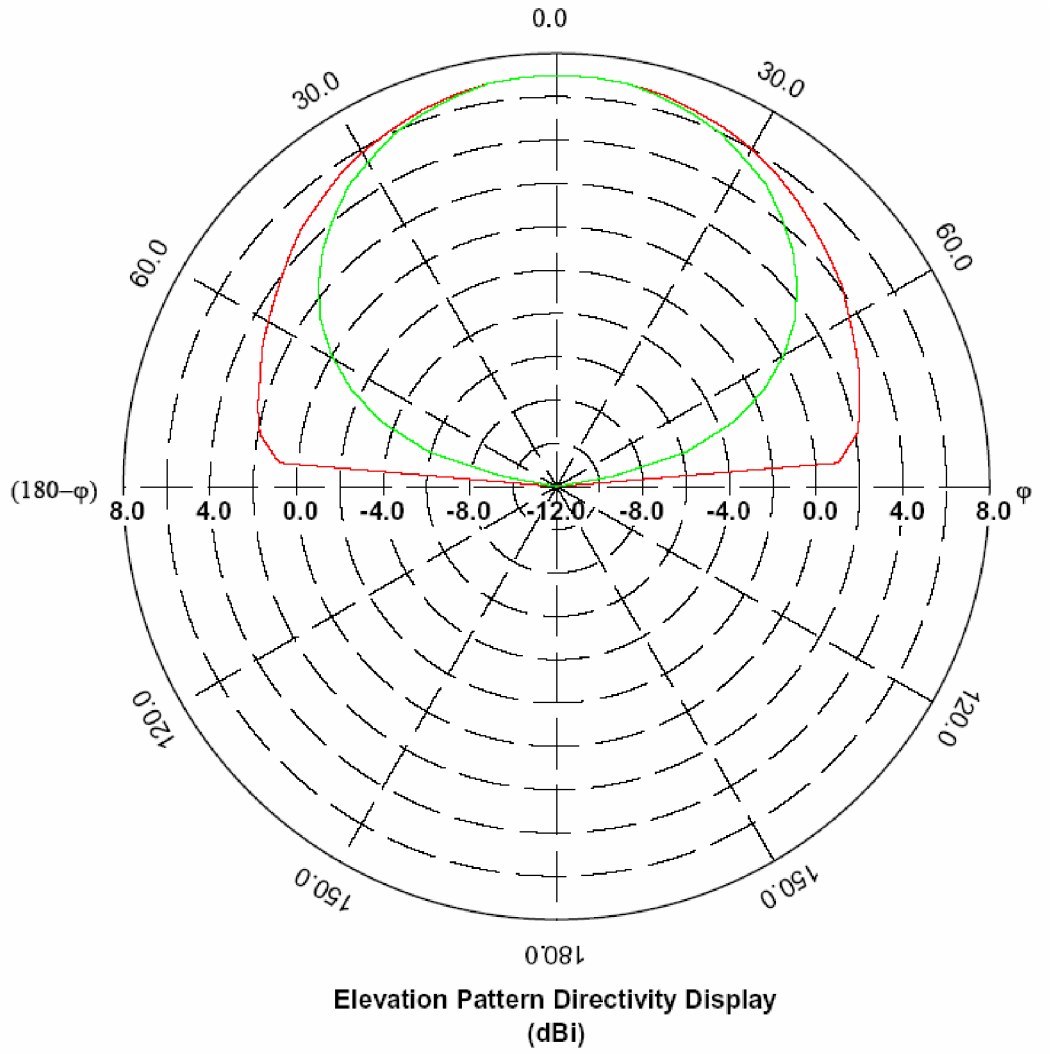

Fig. 5.10/ Radiation pattern of mono-fed Balanced Amplifying Antenna (Red line E_θ and green line E_ϕ)

The isolation between the two sides of the amplifier is observed in figure 5.8. It is also seen that the antenna is properly matched (S22 around -22dB) at the desired frequency of 2.4 GHz. The noise factor is slightly more than 2.21dB, where as the gain is more than 10dB. The radiation pattern at 2.4 GHz is undistorted,

which suggests that the antenna is radiating in its dominant mode and the radiation is not contaminated by harmonic interferences.

5.4.3 DUAL FEED ACTIVE ANTENNA

The inherent disadvantage with the balanced amplifier is the use of the matching load on the return path. This section examines the possibility of elimination of this load from the output port, using dual feed concept. It will also discusses the results obtained using this concept.

As is well known, the output from the two amplifiers differs by 90 degree in phase. We propose to use the rectangular patch antenna with orthogonal inset feeds at two different points, as shown in figure 5.11. The feeding microstrip lines at these places differ by quarter-wave length. Thus the feed will inherently introduce a phase difference of 90 degree. This throws a challenge in antenna design, because of the mutual impedance of between the feed lines. Due to the existing mutual impedance, electrical isolation of the feed lines becomes a daunting task. The following procedure is adopted for this design.

First the amplifier is designed for a 50 ohm termination. Then the antenna is simulated. The starting point assumes no mutual coupling between the feeding lines. So to guess the feed points we calculate the position where the self impedance shall be 50 ohms. Then a simulation is done and S-Parameters are found out. Then by trial and error method, the feed positions were continuously changed. The next step is the use of the antenna as an integral part of the balanced amplifier. For this the antenna is assumed to be a three port device, with two input ports (to be

connected to the amplifier output) and an imaginary output port matched to free space. Then S-parameters for a three-port circuit are generated, using the S-parameter information of the input ports and the imaginary output port. This S-parameter file is then used for simulation in the Microwave Office. This is used as a three port sub-circuit. The two input ports are connected to the amplifier and the output port is terminated on a 376.6 ohm port. Figure 5.12 (a) and 5.12(b) show the S-parameters at these three ports and between them respectively.

Fig. 5.11/ Orthogonally Dual Fed Patch Antenna

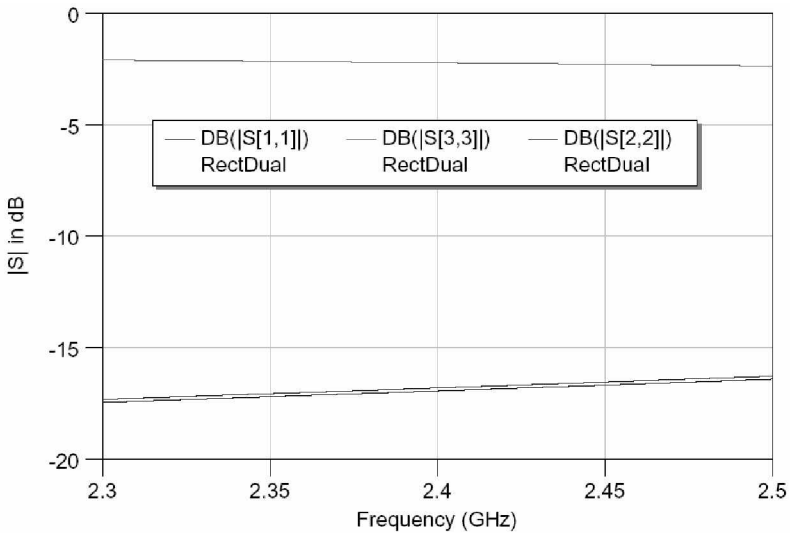

Fig. 5.12(a)/ S-Parameters of the Equivalent Three Port for Antenna at each port

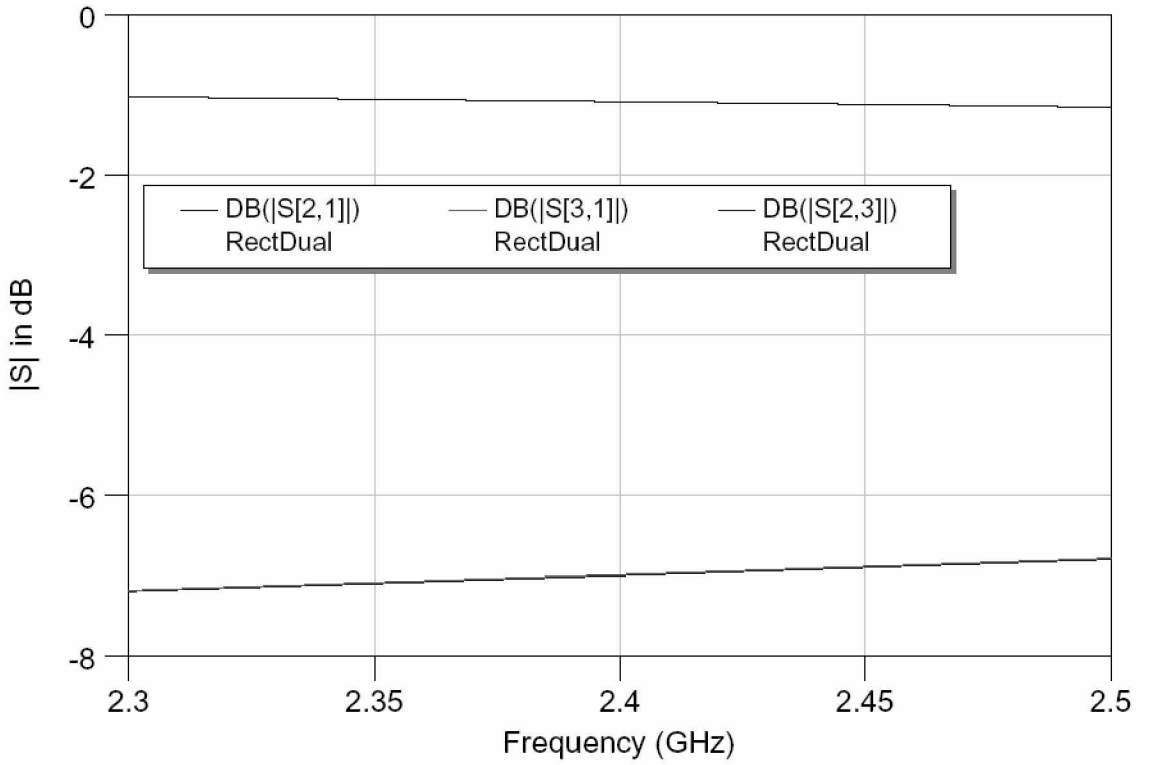

Fig. 5.12(b)/ Equivalent Three S-Parameters of Port for Antenna between ports

The simulation schematic is shown in the figure 5.13 below. The results of the simulation for the gain and noise figure between the port 1 and port 2 are shown in figure 5.14. The radiation pattern of the dual fed antenna is shown in figure 5.15. It is observed that the patterns of the mono-fed and dual fed antennas are identical. It suggests the same mode is being excited in both the cases and harmonics are not interfering. The reason for this can be that the antenna due to its symmetry has two distinct locations for excitation of the desired mode. By design optimization, these locations are being used for feeding. The 90 degree phase shift between the outputs from the two ends of the balanced amplifier is being cancelled out due to use of additional quarter-wave length on one of the feeding lines of the antenna.

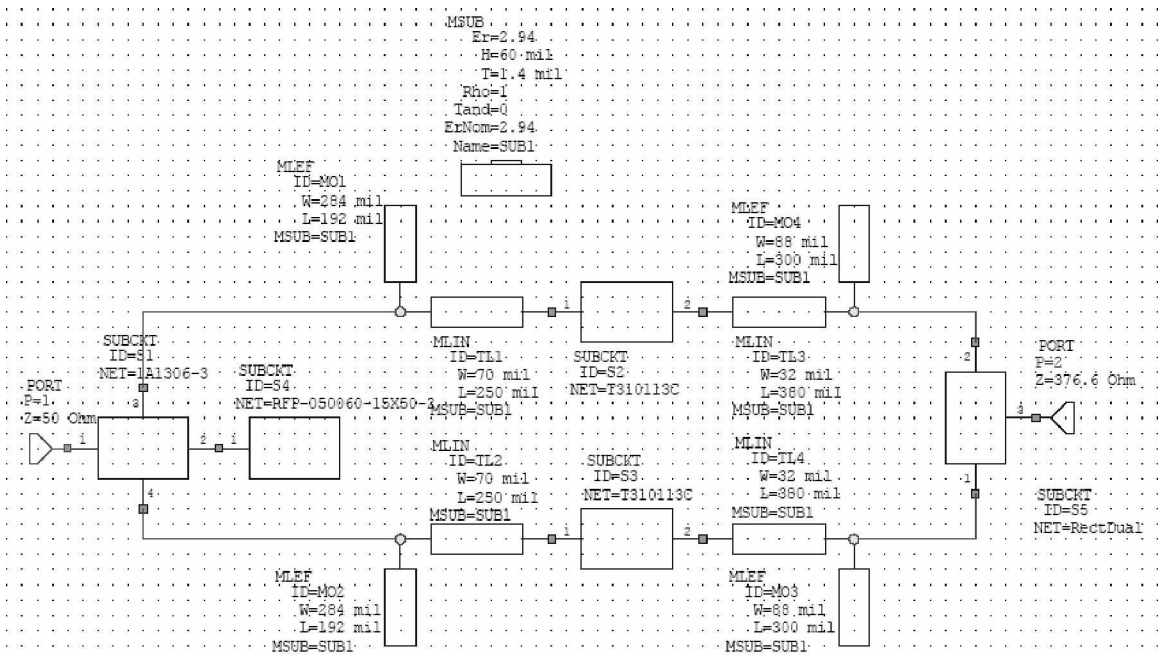

Fig. 5.13/ Simulation Schematics of the Dual Fed Balanced Amplifying Antenna

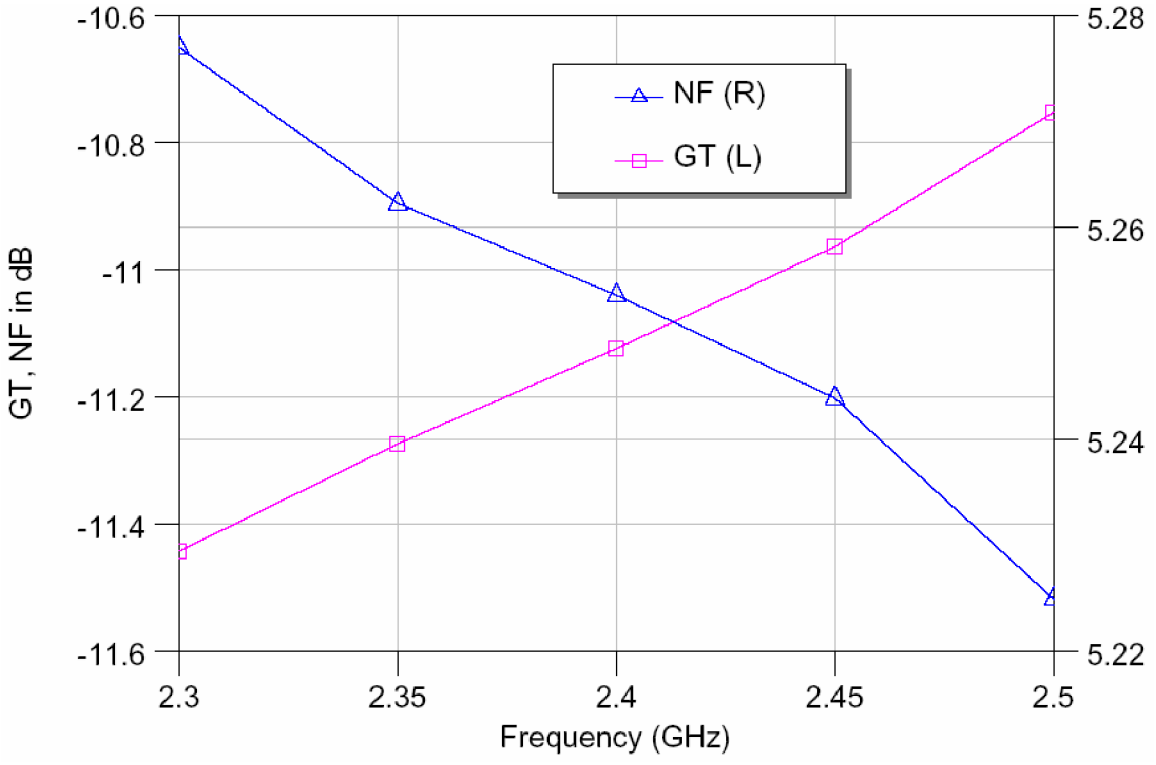

Fig. 5.14/ Gain and Noise Figure of the Dual Fed Balanced Amplifying Antenna

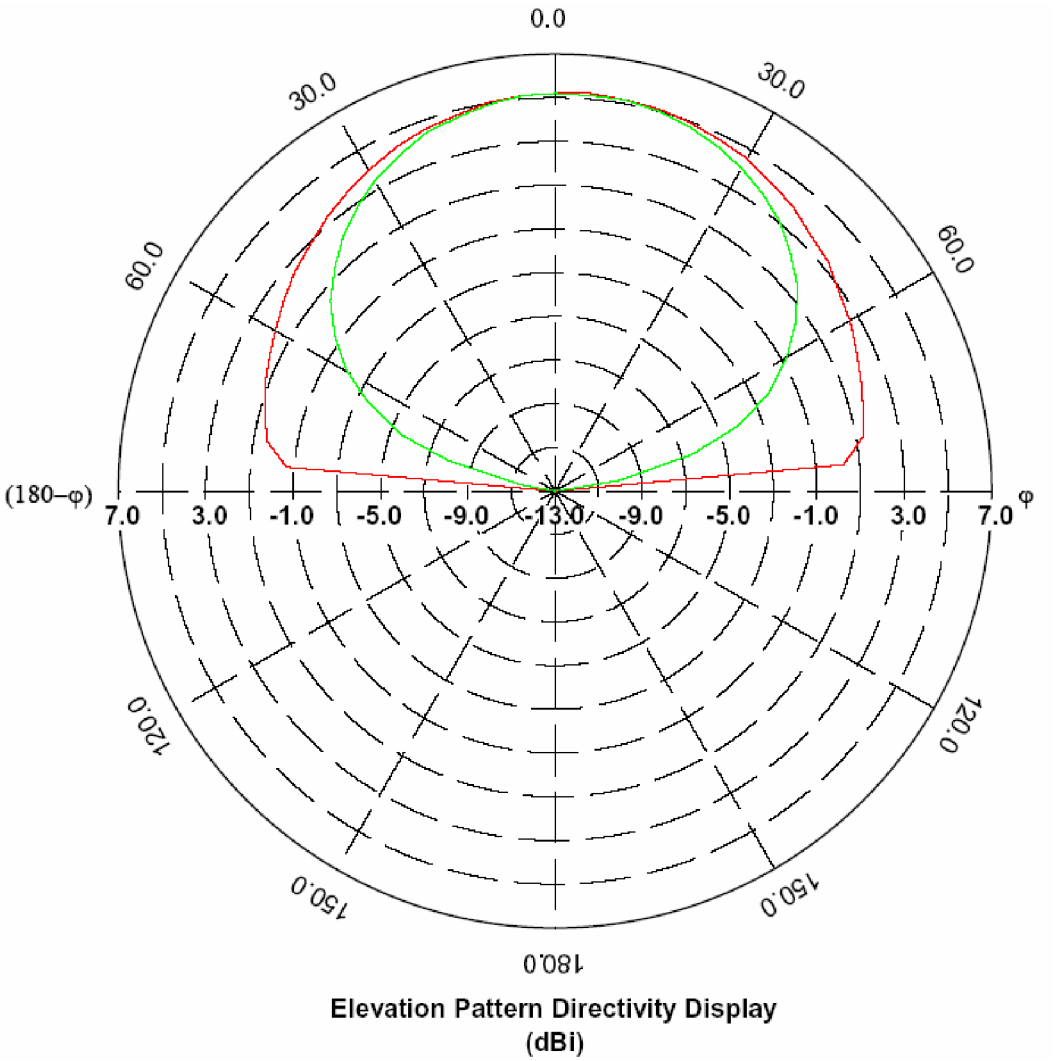

Fig. 5.15/ Radiation pattern of dual-fed Balanced Amplifying Antenna (Red line E_θ and green line E_ϕ)

5.5 Conclusion

This chapter considered both push-pull and balanced amplifiers and compared their characteristics. It was found that both have relative merits and demerits. Considering the merits of the balanced amplifier, we tried to test that configuration for amplifying antenna, which has been found to be successful.

For implementing the balanced amplifying antenna, first a balanced amplifier was designed. Its characteristics were observed for noise factor and gain. Then an inset fed rectangular antenna was used to replace the 50 Ohm matched termination in the output port of the hybrid coupler. Again the noise and gain characteristics were observed.

At the end, the hybrid was replaced by a dual fed patch antenna. First the dual fed patch antenna was designed and optimized to minimize the coupling between the two ports. Then the antenna ports were connected to the out put ports of each amplifying device. The antenna in this case behaves like a hybrid terminator, connected to free space via a virtual 376.6 Ohms port. For termination in the free space, a port of impedance 376.6 Ohms was used to terminate the system. The noise factor and gain were then measured.

In all the cases it was observed that it is not possible to obtain minimum noise figure and maximum gain simultaneously.

Chapter 6

Chapter 6 BALANCED AMPLIFYING ANTENNA FOR CIRCULAR POLARIZATION

6.1 INTRODUTION

The previous chapter started with two important amplifying techniques for use in active integrated antenna. Their relative advantages and disadvantages were discussed. Also, it was noted that the push-pull configuration has wide applications in the active integrated antenna. The balanced amplifying antenna was then suggested as an alternative to the push pull antenna due to its better isolation between the input and output ends as well as superior matching properties.

In this chapter, we consider another important application for which the balanced amplifying antenna is naturally more suitable than the push-pull amplifying antenna. The polarization is an important aspect of the antenna technology. There are many practical situations, which require circularly polarized antenna. The outputs of the balanced amplifier are 90 degree apart in phase and hence it can be a suitable candidate for active circularly polarized antenna. This concept is used in this chapter; which starts with circularly polarized antenna.

6.2 CIRCULARLY POLARIZED ANTENNA

The inherently antenna radiates elliptically polarized waves; linear polarization being a particular case of it. The elliptical polarization is characterized by three quantities: axial ration, tilt angle and the sense of rotation [1, 2]. For linear polarization, the axial ration is zero or infinite while the tilt angle gives its orientation. Circular polarization is obtained for unit axial ratio, where the tilt angle losses its

meaning. Thus the quality of circularly polarized wave is determined by the axial ratio [3].

Antennas can give circular polarization if two orthogonal components with equal amplitude but in phase quadrature are radiated. A patch antenna capable of supporting two orthogonal modes in phase quadrature simultaneously or an array of linearly polarized patches with proper orientation and phasing is capable of producing circular polarization. This chapter considers both these structures simulated using Microwave Office and IE3D. The next section considers a single element circularly polarized patch antenna.

6.3 DUAL ORTHOGONAL FED ACTIVE CP PATCH ANTENNA

We consider a square antenna with dual inset feeds on orthogonal sides of the patch. Unlike in conventional passive square antenna with dual orthogonal feeds, the feed structure does not introduce the 90-degree phase shift here. The reason for this lies in the amplifying system, which produces outputs, which are 90 degree out of phase. The schematic of the dual fed patch antenna is shown in figure 6.1. The physical parameters of the antenna for the design frequency of 2.4 GHz are given in Table 6.1.

Fig. 6.1/ Dual fed Square Patch Antenna

Table 6.1: Physical parameters of the dual fed patch antenna

Patch Size	Feed length	Feed width	Feed gap	ε_r	tanδ	Substrate Thickness	Metallization
1.416X10^3 mil	507.1609 mil	75.473 mil	39.37 mil	2.94	0.0025	60 mil	1.4 mil Copper

The S-parameter of the feeding port #1 and the polar radiation pattern of the antenna are shown in figures 6.2 and 6.3 respectively.

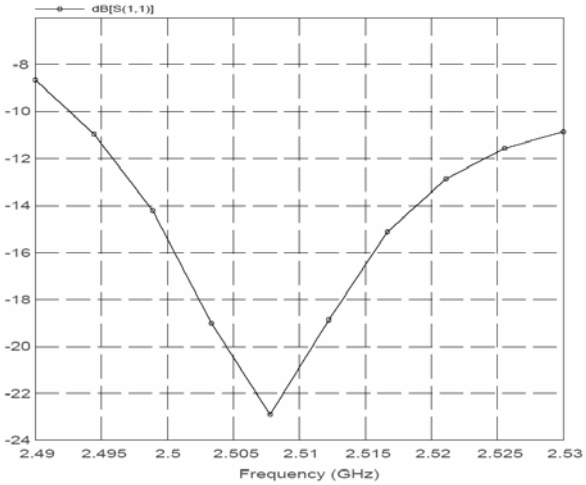

Fig. 6.2/ S-Parameter of dual Fed square patch antenna

Fig. 6.3/ Elevation Pattern Directivity (dBi) [Outer E-Theta; Inner E-Phi]

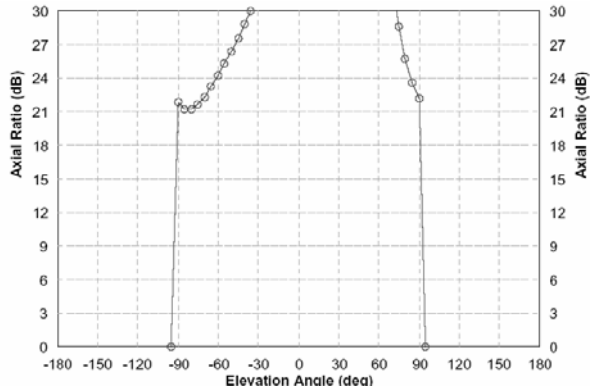

Fig. 6.4(a)/ Axial Ratio of dual fed patch (Phi = 0 plane, 2.4 GHz)

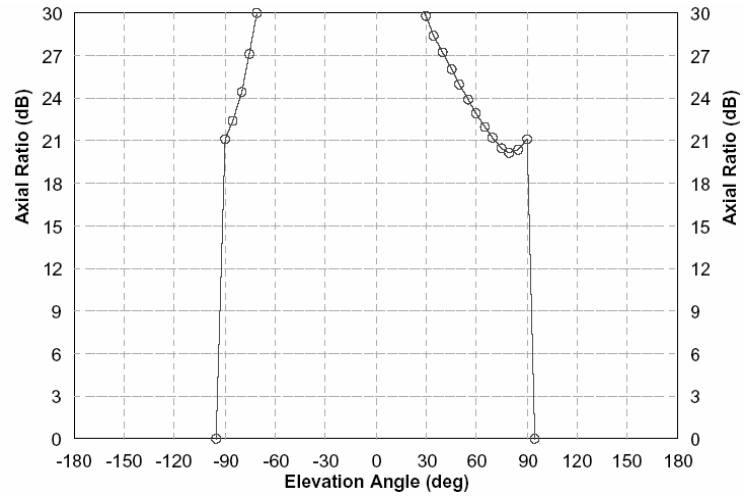

Fig. 6.4(b)/ Axial Ratio of dual fed patch (Phi = 90 plane, 2.4 GHz)

It is to be noted that the design frequency for the antenna was 2.4 GHz. However, the antenna was optimized to minimize the coupling between the feeding ports, subsequently found to resonate at 2.507 GHz. This is evident in figure 6.3, which is for the port 1. The plot for the port two is exactly the same, and hence is not shown here, because on the plot they will be indistinguishable. Figure 6.4 (a) & (b) depict the axial ratio at the design resonant frequency (i.e. 2.507 GHz) of the dual fed patch antenna. It is to be noted that both the feed are at the same phase

and hence no orthogonal feed. This is the reason for high axial ratio, which means the antenna does not radiate circular polarization wave, although all its four edges are radiating simultaneously.

The S-parameters of this two-port antenna were stored in a separate file. Then a power combiner was simulated. The S-parameter of the two input ports and the output port were set so that the input impedances at these ports are 50 ohms, 50 ohms and 376.6 ohms respectively. Once this power combiner was designed, its S-parameters were compared with those of the antenna S-parameters at 2.507 GHz for the two input ports. Then the S-parameters of the combiner were scaled to these S-parameters at 2.507GHz frequency. The same procedure was followed for other frequencies in the 2.49 – 2.53 GHz band. Thus the power combiner with the scaled S-parameters can be assumed to simulate the antenna. This is due to the assumption that this antenna has two input ports and one imaginary fictitious output port of impedance 376.6 ohms, through which it radiates to free space.

This power combiner is then used with the balanced amplifier at the output port. The schematic of this simulation is shown in figure 6.5 below. The design of the balanced amplifier used here is the same as given earlier in chapter 5 earlier. The simulated result for the noise figure and the gain of the amplifier are shown in figures 6.6. It is observed that the total gain of the system at 2.5 GHz is 5.21 dB. The noise figure at the same frequency is -11.3 dB. It suggests that the noise figure is within the design value of 2dB. In other words the system is working as LNA in this case. The reason for this can be good isolation between the feeding ports to the

antenna. This system will be immune to the spectral impurity, since the antenna being high Q component posses a narrowband to support any harmonic meaningfully. The problem of spectral purity can arise if a broadband antenna is used instead.

The polar radiation pattern of the antenna for both LHCP and RHCP is shown in figure 6.7. Figure 6.8 depicts the axial ratio in the given band for the dual fed CP patch antenna. It is to be noted that there exists a phase difference of 90 degree between the two feed, inherently due to the balanced amplifying stage preceding the patch. This is the reason for lower axial ratio, which means the antenna is radiating circular polarization wave due to simultaneous radiation from its four edges with proper phasing.

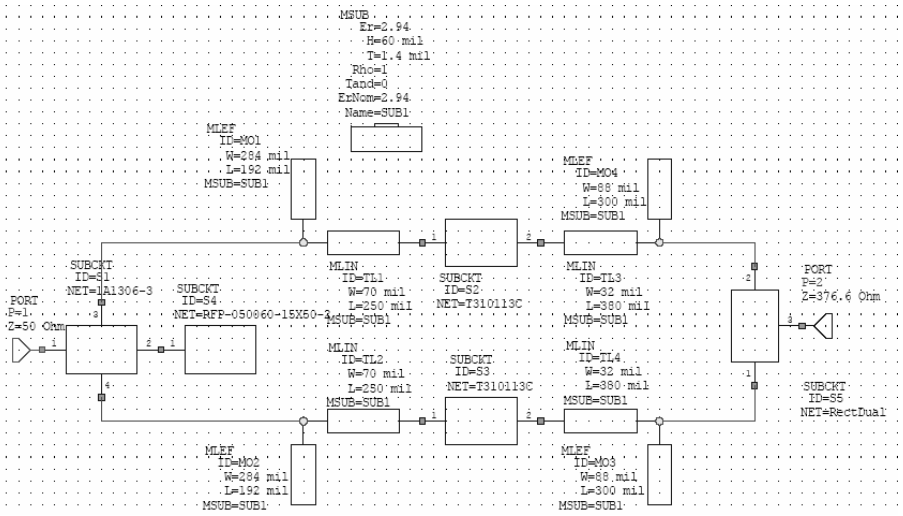

Fig. 6.5/ Schematic of the Balanced Amplifying CP Antenna Simulation

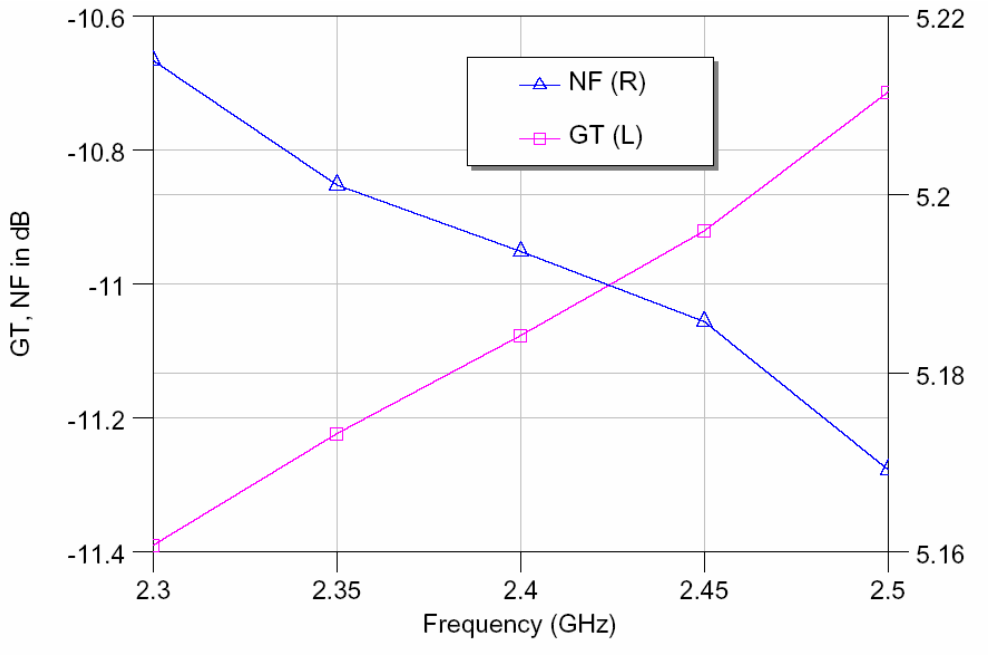

Fig. 6.6/ NF and GT of the Balanced Amplifying CP Antenna

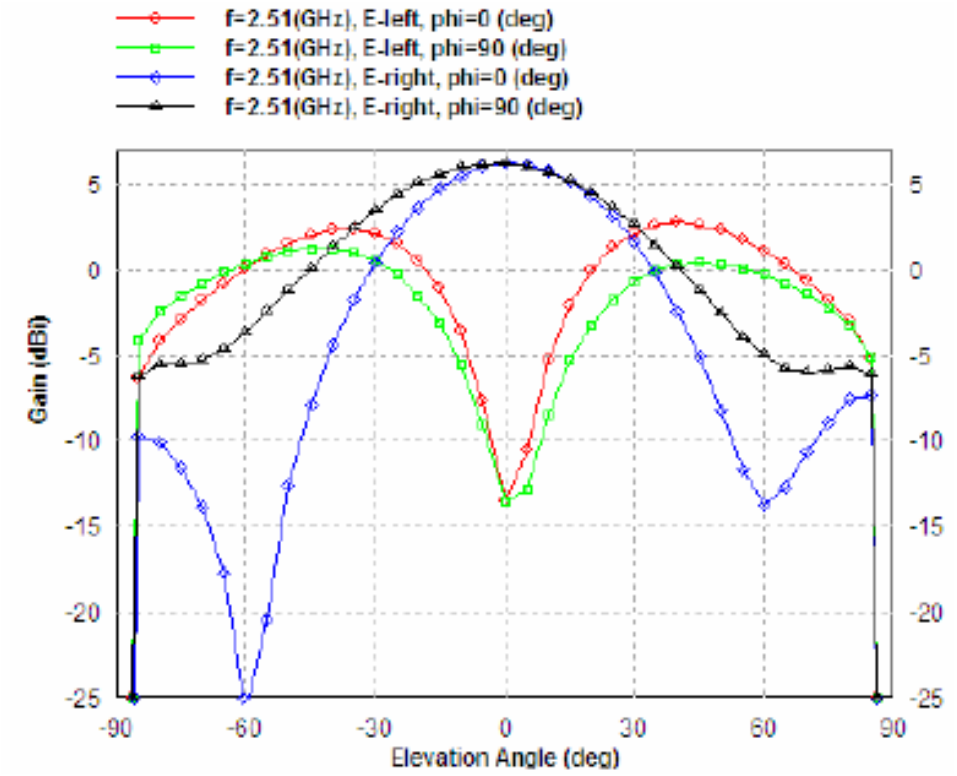

Fig. 6.7/ Radiation pattern of the CP antenna

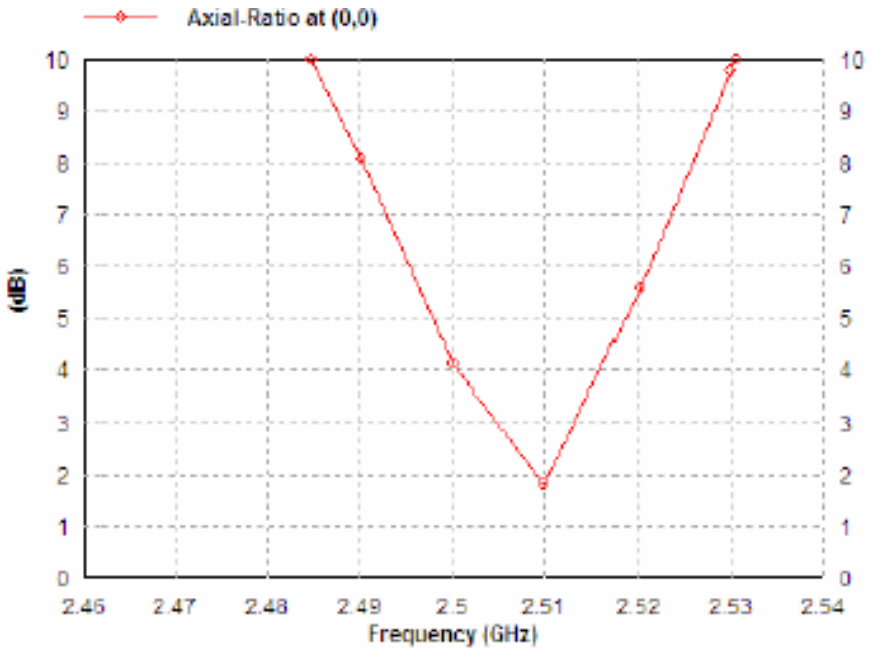

Fig. 6.8/ Variation of AR with frequency for dual fed CP antenna

Figure 6.9 shows the efficiency variation with the frequency. It is observed here that the antenna efficiency is around 87% at 2.49GHz, which drops down beyond this frequency. However the radiation efficiency remains almost constant at 90%.

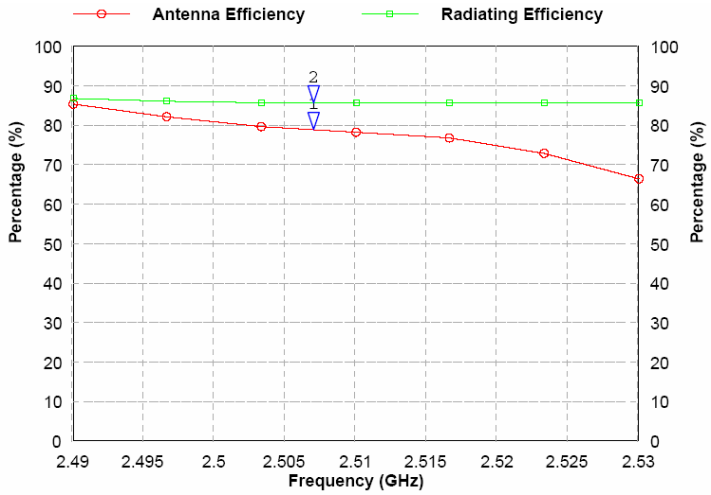

Fig. 6.9/ Efficiency of the Dual Fed CP Antenna

Figure 6.10 shows the gain of the stand-alone dual fed antenna for circular polarization. It is observed that it is maintained at around 6 dBi throughout the designated band.

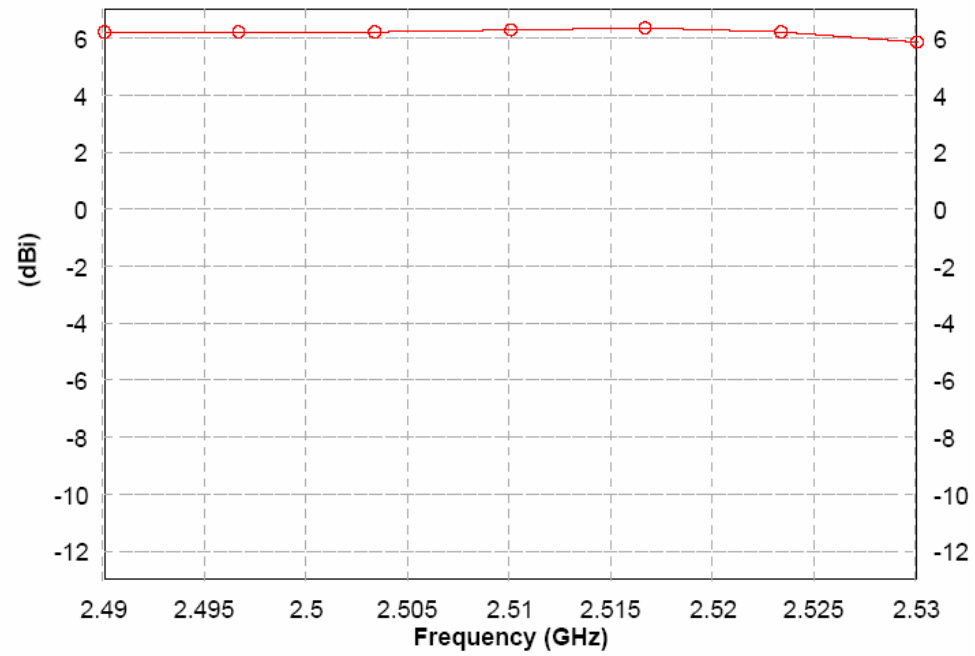

Fig. 6.10/ Gain of the dual fed CP antenna

6.4 SEQUENTIALLY FED ACTIVE CP ARRAY ANTENNA

In this section we consider a planner arrangement of the patch antenna elements to form an array. Each element in the array is linearly polarised. The phase of the feeding in the array increases progressively from 0 degree to 270 degree. In other words the elements are uniformly distributed in each of the phase quadrant by such a feeding arrangement. Thus the phase quadrature part is taken care off. This leaves us with the problem of orthogonal radiating elements. To achieve this we will consider only four elements, arranged at the four corners of a square domain. The manner of arrangement is such that each antenna sees its

adjacent ones to be radiating from an edge orthogonal to its edge of radiation. To achieve this, each antenna is rotated by 90 degree sequentially. The schematic of the arrangement is shown in figure 6.11.

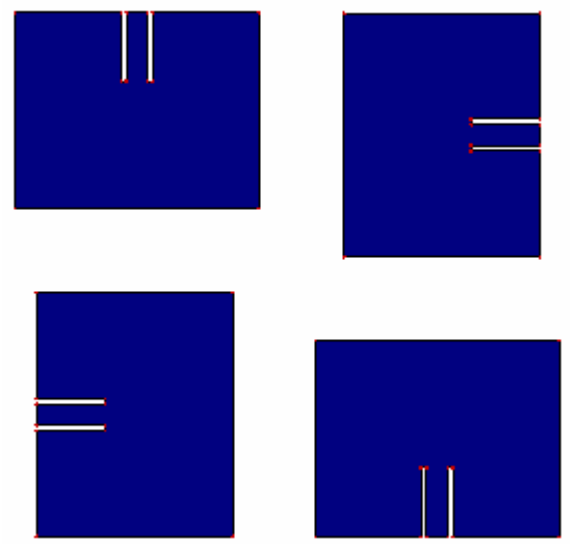

Fig. 6.11/ Sequentially Rotated Array for CP

The physical parameters for this array are shown in the table 6.2. The substrate parameters are the same as those of the square patch discussed in the above section.

Table 6.2: Physical Dimension of Array

Patch Width	Patch Length	Inset feed depth	Gap between adjacent edges
1753.1 mil	1409.5 mil	459.4086 mil	602.346 mil

This array is first tested for its performance. The design frequency for this array was 2.4GHz. However, the arrangement was optimized to maximize the antenna efficiency. The variation of efficiency with frequency is depicted in figure 6.12. It is observed that the frequency for highest gain is 2.36GHz.

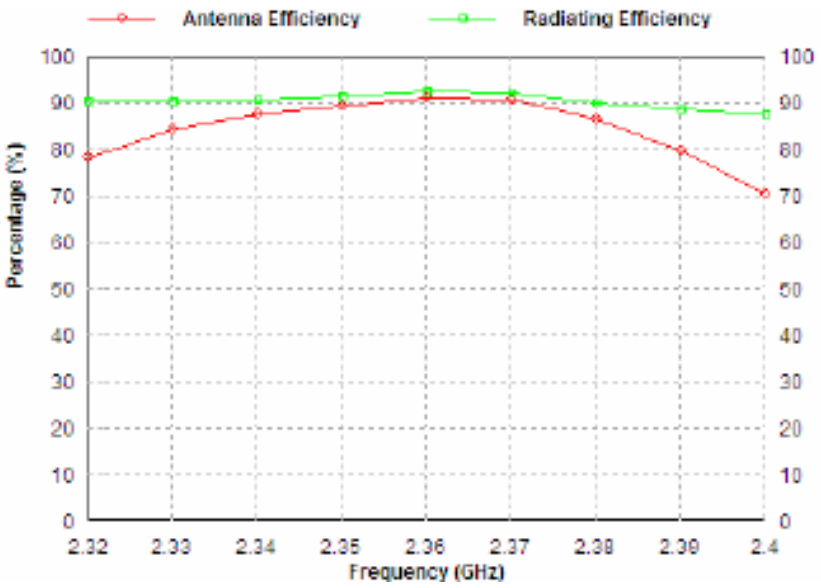

Fig. 6.12/ Variation of efficiency with frequency for sequentially rotated array

The elevation gain patterns for both RHCP & LHCP are shown in figure 6.13. Figure 6.14 shows the variation of axial ratio and figure 6.15 shows the variation of gain with frequency. It is observed that the gain remains almost constant at 8dBi over the frequency band; whereas good axial ratio (AR = 2.4) is obtained for 2.37 GHz.

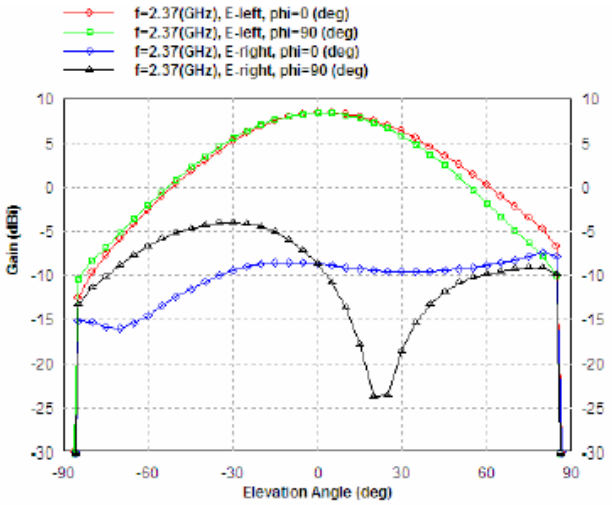

Fig. 6.13/ RHCP & LHCP pattern for the sequentially fed array

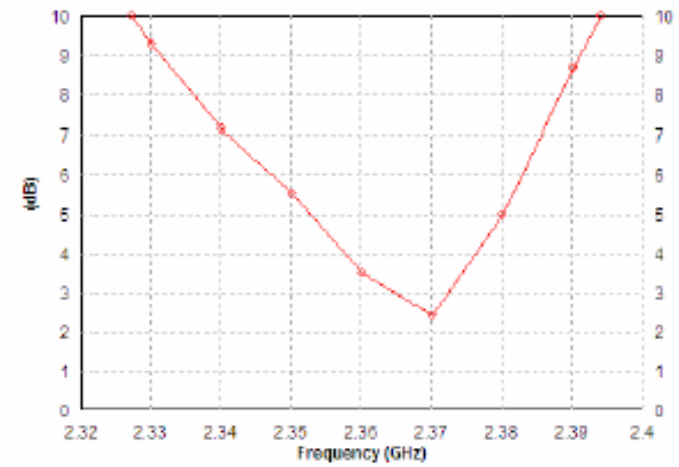

Fig.6.14/ Axial Ratio variation with frequency

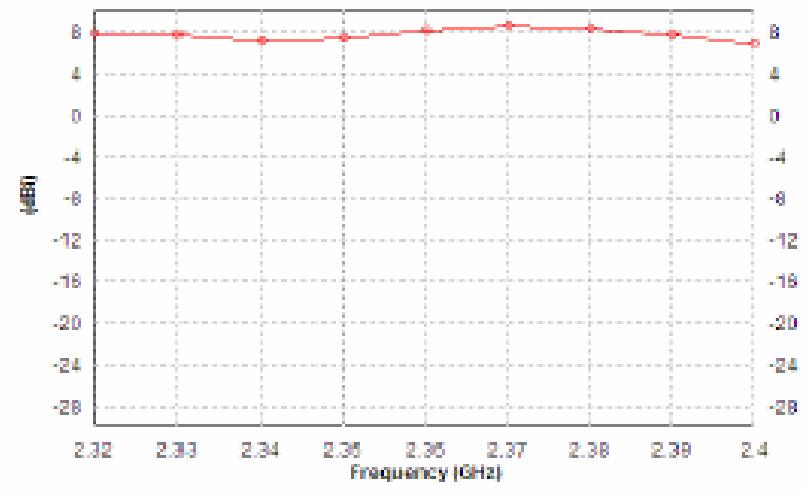

Fig.6.15/ Gain ~ Frequency Characterization

As per the above discussion, the elements of the array are to be sequentially fed with progressive phase shifts. On the other hand the balance amplifier has two output terminals. It means it is necessary to generate two more terminals, in such a manner that 0^0 – 90^0 – 180^0 – 270^0 degree phase shift across the terminals can be realized. Additional amplification is necessary to compensate for non-radiating losses like conductor loss, dielectric loss, etc. This can be done by combination of

hybrids. First a 0^0 – 180^0 hybrid is taken. Each of its output is then connected to 0^0 - 90^0 hybrids. Then from the 0^0 end 0^0 – 90^0 phases will be obtained. Similarly from the 180^0 end 180^0 – 270^0 phases will be obtained. A pair of balanced amplifier is used at each of the ends, i.e. 0^0 – 90^0 phase-ends and 180^0 – 270^0 phase-ends. The outputs from the balanced amplifiers are then accordingly connected to the antennas. The schematic of microwave simulation is shown in figure 6.16.

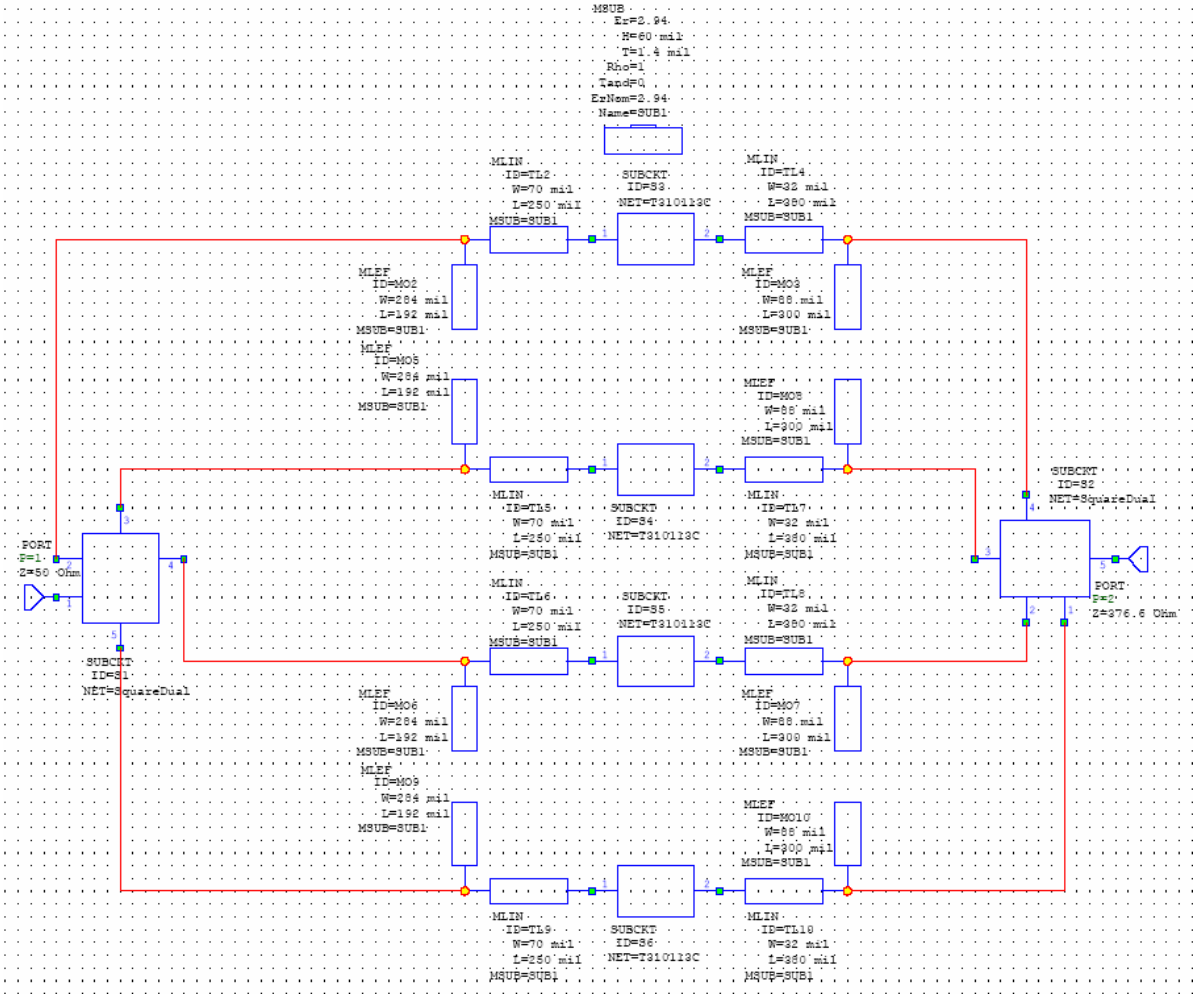

Fig. 6.16/ Amplifying Sequential fed CP antenna Schematic

The details of phase splitter connected to the port #1 are shown in figure 6.17. It contains a 180^0 and two 90^0 hybrids as discussed earlier. The equivalent sub-circuit for the antenna array models the four antennas as lossless coupled transmission lines gap coupled to another transmission line of characteristics impedance 376.6 ohms. The transmission lines representing the antenna are designed in such a manner that their input impedances are equal to the input impedance of the corresponding antennas. The design is similar to that of the power combiner explained earlier.

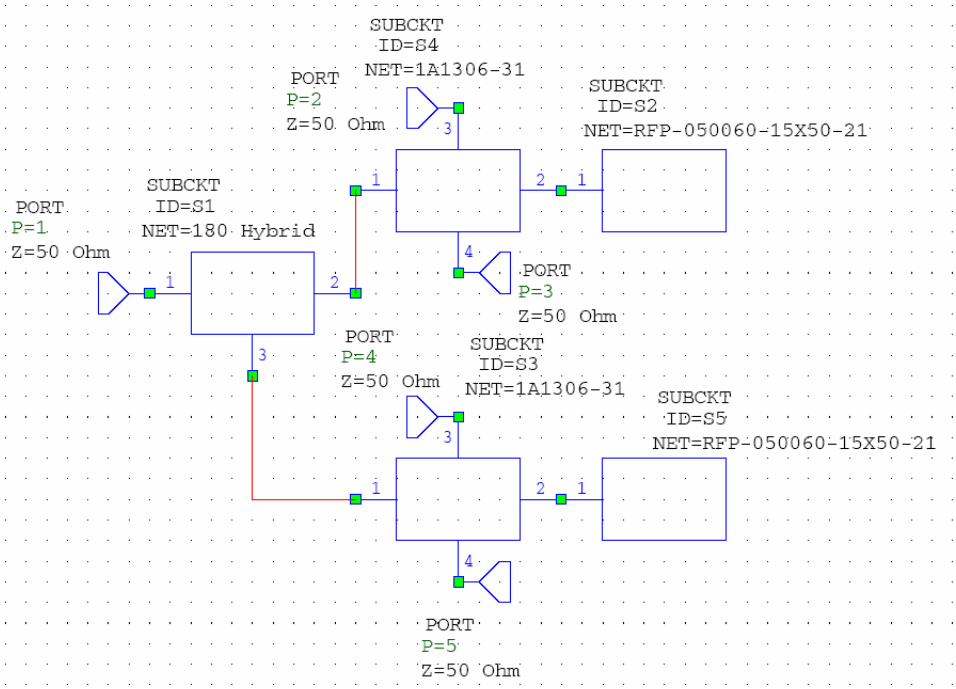

Fig. 6.17/ Sub-circuit of Phase Splitter

The gain and noise figure of the balanced amplifying sequentially fed circular polarized antenna is shown in figure 6.18. It can be noticed that compared to the dual feed case; the noise figure is considerably reduced here to be less than -19 dB.

This is within acceptable design limit. The gain is also between 6.3 to 6.5 dB. The reason for this can be the use of a pair of balanced amplifier.

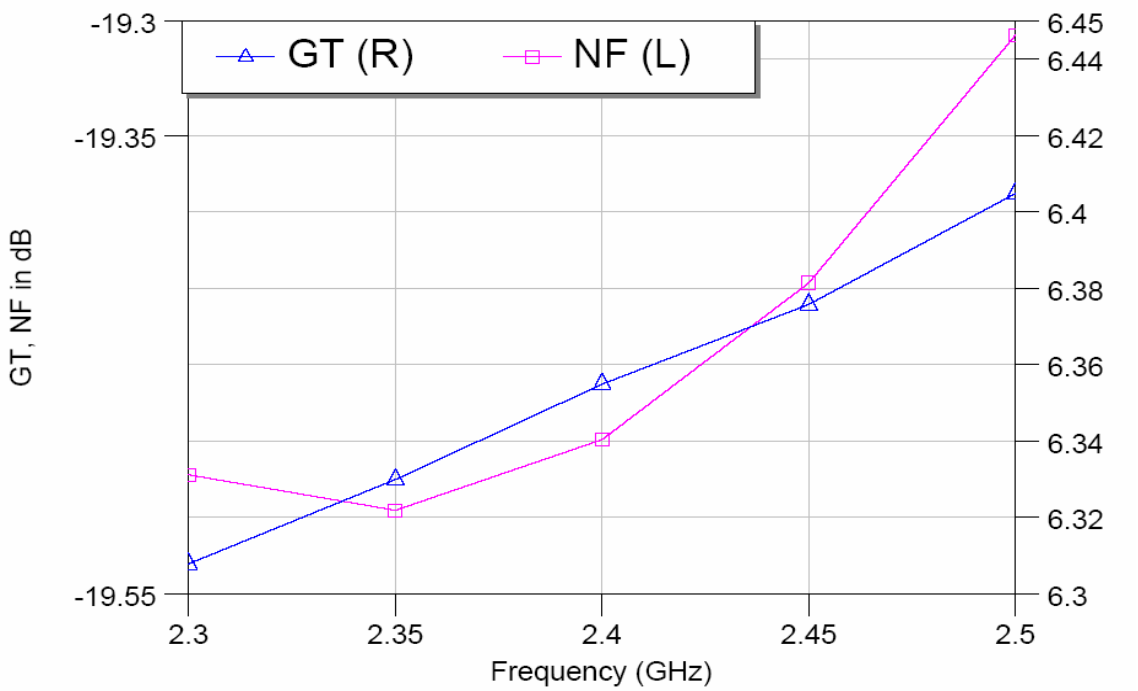

Fig. 6.18/ NF & GT of Sequential Fed Balanced Amplifying CP Antenna

6.5 CONCLUSION

This chapter exploited the use of balanced amplifier for design of active circularly polarized antenna. Two different configurations were considered. It was observed that sequentially fed array gives better performance than the dual fed antenna, as far as the noise figure and gain are concerned. However as stand alone circularly polarized antenna their performances do not vary very much. The design complexities in both the cases are involved. Neither there is any closed form formulae nor is a defined procedure to follow for keeping the mutual coupling between the ports to minimum. This is to be achieved by trial and error and hence is the most difficult part in the whole design process.

Chapter 7

Chapter 7 CONCLUSION AND FUTURE SCOPE

7.1 INTRODUCTION

This treatise embodies the results and the procedure of the endeavour of the author towards contribution to incremental knowledge on amplifying type active integrated antenna. It contains seven chapters, including this as the last chapter. This chapter describes in details the technical difficulties encountered during carrying out of this work; and hence suggest open areas related to this work. Before proceeding further, it summarizes the work carried out in relation to this thesis.

7.2 SUMMARY OF THE WORK DONE

The introduction chapter described the motivating factor for carrying out this work. In that process, it outlined the present and future communication systems requirements. Accordingly, the outline of the study was worked out, with brief description of what is to be expected in each of the chapter following the chapter one.

The second chapter reviewed the microstrip antenna technology. In particular it focused on the rectangular microstrip antenna. The working principle and CAD formulations were presented along with available results in the literature.

The active integrated antenna is an objective shift in the antenna research. This was the focus of the third chapter. It dwelt upon various types of definitions for the active integrated antenna for their appropriateness. Then it classified the AIA in to various categories. It also discussed various types of AIA excluding the amplifying type active integrated antenna.

It is evident from the available literature that the amplifying active integrated antenna has not been investigated much due to various reasons, except for the case of spatial power combining arrays. The fourth chapter took up this area and presented some of the recent developments. It also suggested an improved design [1 – 3] for the push-pull type active integrated antenna, using diode amplifiers as the first stage in place of passive splitters.

The focus on amplifying antenna is mostly on use of power amplifier. The push-pull amplifying circuit is very popular in this area, and hence most of the research is directed in this area. The fifth chapter compared the push-pull configuration with the balanced configuration, and suggested the use of the later for AIA. Thus the Balanced Amplifying Antenna concept [4] has been incorporated into this chapter.

The sixth chapter dealt with an area, which has got least attention. It dealt with circularly polarized active integrated antennas. It reasoned out the natural suitability of the balanced amplifier for this type of antenna. It suggested two types of balanced amplifying CP antennas: the dual fed antenna [5] and the sequentially fed [6] balanced amplifying antenna.

7.3 FUTURE SCOPE

The investigation has been limited mostly to theoretical study due to lack of experimental facilities. Detailed experimental studies can be taken up at a later stage to find out a design procedure for balanced amplifying antennas.

The UWB technology is gaining attention now a day. It requires broadband antennas. Suitable modification in the design technology to design UBW antennas will be another challenging job.

Exploiting the suitability of metamaterials based active integrated antenna can be another interesting area. Similarly realization of adaptive and smart antennas in active antenna configuration can be investigated in future.

The list of opportunities is endless if there is scope and perseverance.

REFERENCES

CHAPTER 1

[1] Lawrence Harte, Steve Prokup, and Richard Levine, Cellular and PCS: The Big Picture, McGraw-Hill, New York, 1997.

[2] Garry D. Gordon and Walter L. Morgan, “Principles of Communications Satellites”, Wiley, NY, 1993.

[3] G. Hanington, P.F. Chen, P.M Asbeck, and L.E. Larson, “High-efficiency power amplifier using dynamic power-supply voltage for CDMA applications," IEEE Trans. Microwave Theory Tech., vol. 47, no. 8, pp. 1471, Aug. 1999.

[4] Kykkotis, C., Hall, P. S., and Ghafouri-Shiraz, H., “Performance of active antenna oscillator arrays under modulation for communication systems” IEE Proc. Microwaves, Antennas and Propagation, vol. 145, no 4, Aug 1998, pp313-320.

[5] William R. Deal, Vesna Radisic , Y. Qian and T. Itoh, “Integrated-Antenna Push-Pull Power Amplifiers,” IEEE Trans. MTT, Vol.47,No.8 , Aug. 1999.

CHAPTER 2

[1] R. Garg, P. Bhartia, I. Bahl, and A. Ittipiboon, Microstrip Antenna Design Handbook, Artech House, 2000.

[2] K. F. Lee, Ed., Advances in Microstrip and Printed Antennas, John Wiley, 1997.

[3] D. M. Pozar and D. H. Schaubert, Microstrip Antennas: The Analysis and Design of Microstrip Antennas and Arrays, IEEE Press, 1995.

[4] F. E. Gardiol, “Broadband Patch Antennas,” Artech House.

[5] D. R. Jackson and J. T. Williams, “A comparison of CAD models for radiation from rectangular microstrip patches,” Intl. Journal of Microwave and Millimeter-Wave Computer Aided Design, Vol. 1, No. 2, pp. 236-248, April 1991.

[6] D. R. Jackson, S. A. Long, J. T. Williams, and V. B. Davis, “Computer-aided design of rectangular microstrip antennas”, ch. 5 of Advances in Microstrip and Printed Antennas, K. F. Lee, Editor, John Wiley, 1997.

[7] D. M. Pozar, “A reciprocity method of analysis for printed slot and slot-coupled microstrip antennas,” IEEE Trans. Antennas and Propagation, vol. AP-34, pp. 1439-1446, Dec. 1986.

[8] J.-F. Zürcher and F. E. Gardiol, Broadband Patch Antennas, Artech House, 1995.

[9] H. Pues and A Van de Capelle, “Accurate transmission-line model for the rectangular microstrip antenna,” Proc. IEE, vol. 131, pt. H, no. 6, pp. 334-340, Dec. 1984.

[10] W. F. Richards, Y. T. Lo, and D. D. Harrison, “An improved theory of microstrip antennas with applications,” IEEE Trans. Antennas and Propagation, vol. AP-29, pp, 38-46, Jan. 1981.

[11] D. M. Pozar, “Input impedance and mutual coupling of rectangular microstrip antennas,” IEEE Trans. Antennas and Propagation, vol. AP-30, pp. 1191-1196, Nov. 1982.

[12] C. J. Prior and P. S. Hall, “Microstrip disk antenna with short-circuited annular ring,” Electronics Letters, Vol. 21, pp. 719-721, 1985.

[13] Y.-X. Guo, C-L. Mak, K-M Luk, and K.-F. Lee, “Analysis and design of L-probe proximity fed patch antennas,” IEEE Trans. Antennas and Propagation, Vol. AP-49, pp. 145-149, Feb. 2001.

[14] K. Ghorbani and R. B. Waterhouse, “Ultrabroadband printed (UBP) antenna,” IEEE Trans. Antennas and Propagation, vol. AP-50, pp. 1697-1705, Dec. 2002.

[15] G. Kumar and K. C. Gupta, “Nonradiating edges and four edges gap coupled multiple resonator broadband microstrip antennas,” IEEE Trans. Antennas and Propagation, vol. AP-33, pp. 173-178, Feb. 1985.

[16] S. Weigand, G. H. Huff, K. H. Pan, and J. T. Bernhard, “Analysis and design of broad-band single-layer rectangular U-slot microstrip patch antennas,” IEEE Trans. Antennas and Propagation, vol. 51, pp. 457-468, March 2003.

[17] D. R. Jackson, J. T. Williams, A. K. Bhattacharyya, R. Smith, S. J. Buchheit, and S. A. Long, “Microstrip patch designs that do not excite surface waves,” IEEE Trans. Antennas and Propagation, vol. 41, pp. 1026-1037, Aug. 1993.

CHAPTER 3

[1] Lawrence Harte, Steve Prokup, and Richard Levine, Cellular and PCS: The Big Picture, McGraw-Hill, New York, 1997.

[2] Garry D. Gordon and Walter L. Morgan, “Principles of Communications Satellites”, Wiley, NY, 1993.

[3] Thomas B. Mader, Quasi-Optical Class-E Power Amplifiers, Ph.D. thesis, Univ. of Colorado, Boulder, CO, 1995.

[4] Kamilo Feher, Digital Communications: Satellite/Earth Station Engineering, Noble, Atlanta, 1997.

[5] G. Hanington, P.F. Chen, P.M Asbeck, and L.E. Larson, “High-efficiency power amplifier using dynamic power-supply voltage for CDMA applications," IEEE Trans. Microwave Theory Tech., vol. 47, no. 8, pp. 1471, Aug. 1999.

[6] H.A. Wheeler, “Small antennas,” *IEEE Trans. Antennas Propagat*., vol. AP-23, pp.462-469, July 1975.

[7] J.R. Copeland, W. J. Roberston, and R. G. Verstraete, “Antennafier arrays,” *IEEE Trans. Antennas Propagat*., vol. AP-12, pp.227-233, Mar. 1964.

[8] H.H. Meinke, “Active antennas,” *Nachrichtentech*. Z., vol. 19, pp.697-705, Dec. 1966.

[9] A. P. Anderson, W. S. Davies, M. M. Dawoud, and D. E Galanakis, “Notes on transistor-fed active-array antennas,” *IEEE Trans. Antennas Propagat*., vol. AP-19, pp.537-539, July 1971.

[10] M. M. Dawoud and A. P. Anderson, “Calculations showing the reduction in the frequency dependence of a two-element array antenna fed by microwave transistors,” *IEEE Trans. Antennas Propagat*., vol. AP-20, pp.497-499, July 1972.

[11] _____, “The performance of transistor fed monopoles in active antennas,” *IEEE Trans. Antennas Propagat*., vol. AP-21, pp.371-374, may 1973.

[12] M. I. Kontorovich and N.M. Lyapunova, “Active antennas,” *RadioEng. Electron. Phys*. Vol. 19, pp.126-127, 1974.

[13] T. S. M. Maclean and P. A. Ramsdale, “Short active aerials for transmission,” *Int. J. Electron*., vol. 36, pp.261-269, Feb. 1974.

[14] M. M. Dawoud and A. P. Anderson, “Experimental verification ofthe reduced frequency dependence of active receiving arrays,” *IEEE Trans. Antennas Propagat*., vol. AP-22, pp.342-344, Mar.1974.

[15] P. K. Rangole and S. S. Midha, “Short antenna with active inductance,” *Electron. Lett.,* vol. 10, pp. 462-463, Oct. 1974.

[16] J.P. Daniel and C. Terret, “Mutual coupling between antennas optimization of transistor parameters in active antenna design”, *IEEE Trans. Antennas Propagat*. vol. AP-23, pp.513-316, July1975.

[17] B. Grob, Basic Electronics, 6th ed. New York: McGraw-Hill, 1959, ch. 8.

[18] J. Lin and T. Itoh, “Active integrated antennas,” *IEEE Trans. Microwave Theory Tech*., vol. MTT-42, pp. 2186-2194, Dec. 1994.

[19] R. A. York and Z. B. Popovic, Eds., “*Active and Quasi-Optical Arrays for solid-State Power Combining”,* New York: Wiley, 1997.

[20] L. Wandinger and V. Nalbandian, “Millimeter-wave power combining using quasi-optical techniques,” *IEEE Trans. Microwave Theory Tech.*, vol. MTT-31, pp. 189-193, Feb. 1983.

[21] J. W. Mink, “Quasi-optical power combing of solid-state millimeter-wave sources,” *IEEE Trans. Microwave Theory Tech.*, volMTT-34, pp. 273-279, Feb. 1986.

[22] Tasu Itoh ‘Active Integrated Antenna for Wireless Applications’ Asia Pacific Conference 3A01-4 1997 pp. 309-312.

[23] T. Omiston, “ PhD Synopsis”.

[24] R. Hertz, Electric Waves, Macmillan, New York 1893.

[25] A. D. Frost, “Parametric Amplifier Antenna”, Proc. IRE, Vol.48, p.1163, 1960.

[26] C. H. Boehnker, J. R. Copeland, and W. J. Robertson, “Antennaverters and Antennafiers-Unified Antenna and Receiver Circuitry Design,” in Tenth Annual Symposium on the USAF Antenna Research and Development Program, 1960.

[27] J. R. Copeland and W. J. Robertson, “Design of Antennaverters and Antennafiers,” Electronics, pp.68 71, 1961.

[28] S. P. Kwok and K. P. Weller, “Low Cost X-band MIC BARITT Doppler Sensor,” IEEE Trans. Microwave Theory Tech., Vol.27, No.10, pp.844-847, 1979.

[29] B. M. Armstrong, R. Brown, F. Rix, and J. A. C. Stewart, “Use of Microstrip Impedance-Measurement Technique in the Design of a BARITT Duplex Doppler Sensor,” IEEE Trans. Microwave theory Tech., Vol. MTT-28, No.12, pp.1437 1442,1980.

[30] P. Bhartia and I. J. Bhal, “Frequency Agile Microstrip Antennas,” Microwave J., Vol.25, No. 10, pp.67-70, 1982.

[31] N. Wang and S. E. Schwarz, “Monolithically Integrated Gunn Oscillator at 35 GHz,” Electron. Lett., Vol.20,No.14,pp.603-604, 1984.

[32] G. Morris, H. J. Thomas, and D. L. Fudge, “Active Patch Antennas,” in Military Microwave Conference, pp.245-249, London, England,1984.

[33] H. J. Thomas, D. L. Fudge, and G. Morris, “Gunn Source Integrated Microstrip Patch,” Microwaves RF, Vol.24, No.2, pp. 87-90, 1985.

[34] M. Dydyk, “Planar Radial Resonator Oscillator,” IEEE MTT-S Int. Microwave Symp. Dig., pp.167-168, 1986.

[35] S. L. Young, and K. D. Stephan, “Radiation Coupling of Inter-Injection-Locked Oscillator,” SPIE, Millimeter Wave Technology IV and Radio Frequency Power Sources, Vol. 791, pp. 69-76, 1987.

[36] K. A. Hummer and K. Chang, “Spatial Power Combining Using Active Microstrip Antennas,” Microwave Opt. Tech. Lett., Vol.1, No.1, pp. 8-9, 1988.

[37] K. A. Hummer and K. Chang, “Microstrip Active Antennas and Arrays,” IEEE MTS-S Int. Microwave Symp. Dig.-pp. 963-966, 1988.

[38] J. A. Navarro, Y. H. Shu, and K. Chang, “Active End fire antenna Elements and Power combiners Using Notch Antennas,” IEEE MTT-S Int. Microwave Symp. Dig. pp. 793-796, 1990.

[39] J. A. Navarro, K. A. Hummer, and K. Chang, “Active Integrated Antenna Elements,” Microwave J., Vol.35, pp.115-126, 1991.

[40] J. A. Navarro, Y. H. Shu, and K. Chang, “Wideband Integrated Varactor-Tunable active notch Antennas and Power combiners,” IEEE MTT-S Int. Microwave Symp. Dig. pp. 1257-1260, 1991.

[41] H. Ekstrom, S. Gearhart, P. R. Acharya , G. M. Rebeiz, E. L. Kollberg, and S. Jacobsson, “348 GHz End-fire Slotline Antennas on Thin Dielectric Membranes,” IEEE Microwave Guided Wave Lett., Vol.2, No.2, pp.357-358, 1992.

[42] P. R. Acharya, H. Ekstrom , S. S. Gearhart , S. Jacobsson, J. F. Johansson, E. L. Kollberg, and G. M. Rebeiz , “Taperd Slotline Antennas at 802 GHz ,” IEEE Trans. Microwave Theory Tech., Vol. 41, NO.10 ,pp.1715-1719, 1993.

[43] R. A. York and R. C. Compton, “Dual- Device Active Patch Antenna with Improved Radiation Characteristics,” Electron Lett., Vol. 28, No. 11, pp.1019-1021, 1992.

[44] A. Stiller, K. M. Strohm et al, “A radiating Monolithic Integrated Planar Oscillator at 55 GhZ”, IEEE Microwave Guided Wave Lett. Vol.6, No.2,pp-100-102, 1996.

[45] P. A. Ramsdale and T. S. M. MacLean, “Active Loop-Dipole Aerials,” proceedings of the IEE, Vol. 118, No.12, pp.1698-1710, 1971.

[46] T. S. M. Maclean and P. A. Ramsdale, “Short Active Aerials for Transmission,” Int. J. Electron., Vol. 36, No. 2, pp. 261-269,1974.

[47] T. S. M. Maclean and G. Morris, “Short Range Active Transmitting Antenna with Very Large Height Reduction,” IEEE Trans. Antennas propagat., Vol. 23, No.3,pp.286-287,1975.

[48] K. Chang, K. A. Hummer, and G. Gopala krishnan, “Active Radiating Element Using FET source Integrated with Microstrip Patch Antenna,” Electron. Lett. Vol.21, pp.1347-1348, 1988.

[49] U. Guttich, “Planar Integrated 20 GHz Receiver in Slot line and Coplanar Wave-guide Technique,” Microwave and Optical Technology Letters, Vol.2, No.11, pp.404-406, 1989.

[50] R. A. York, R. D. Martinez and R. C. Compoton, “Active Patch antenna element for array applications”, Electron Lett., pp. 494-495, vol. 26, No.7, 1990.

[51] J. Birkel and T. Itoh, “Spatial Power Combining Using Push-Pull FET Oscillators with Microstrip Patch Resonators,” IEEE MTT-S Int. Microwaves Symp. Dig., pp. 1217-1220, 1990J.

[52] Birkeland and T. Itoh, “Two-port FET Oscillators with Applications to Active Arrays,” IEEE Microwave Guided wave Lett. Vol. 1, No. 5, pp. 112-113, 1991.

[53] P. S. Hall and P.M. Haskins, “Microstrip Active Patch array with Beam scanning,” Electron Lett. Vol. 28, No. 22, pp. 2056- 2057, 1992.

[54] P. S. Hall, I. L. Morrow, P.M. Haskins and J. S. Dahele, “Phase Control in Injection-Locked Microstrip Antennas,” IEEE MTT-S Int. Microwave Symp. Dig., pp. 1227-1230, 1994.

[55] X. D. Wu and K. Chang, “Compact Wideband Integrated Active Slot Dipole Antenna Amplifier,” Microwave Opt. Tech. Lett. Vol. 6. No. 15, pp. 856-857, 1993.

[56] X. D. Wu and K. Chang, “Compact Wideband Integrated Active Slot Dipole Antenna Amplifier,” Electron Lett. Vol. 29, No. 5, pp. 496-497, 1993.

[57] H. S. Tsai, M. J. W. Rodwell and R. A. York, “Planar Amplifier Array with Improved Bandwidth using Folded- Slots,” IEEE Microwave Guided Wave Lett., vol. 4, No. 4, pp. 112-114, 1994.

[58] William R. Deal, Vesna Radisic , Y. Qian and T. Itoh, “Novel Push-Pull Integrated Antenna Transmitter Front-End,” IEEE Microwave and Guided Wave Lett., Vol. 8, No. 11,Nov. 1998.

[59] William R. Deal, Vesna Radisic , Y. Qian and T. Itoh, “Integrated-Antenna Push-Pull Power Amplifiers,” IEEE Trans. MTT, Vol.47,No.8 , Aug. 1999.

[60] P.S. Hall, P. Gardner and G. Ma “Local oscillator radiation from active integrated antennas”, Electronics Letters, 9th Dec 1999, vol 35, No 25, pp2163-2164

[61] G. Morris, H.J. Thomas and D.L. Fudge, “Active Patch Antennas,”*1984 Military Microwave Conference*, London, England, pp. 245-249, October 1984.
[62] H.J. Thomas, D.L. Fudge and G. Morris, “Gunn Source Integrated with Microstrip Patch,” *Microwave & RF*, Vol. 24, No. 2, pp. 87-90, 1985.
[63] K.D. Stephan and S.L. Young, “Mode stability of Radiation-Coupled Inter-injection-Locked Oscillators for Integrated Phased Arrays,” *IEEE Tans. On Microwave Theory and Techniques*, Vol.36, No. 5, pp. 921-924, May 1988.
[64] K.A. Hummer and K. Chang, “Spatial Power Combining Using Active Microstrip Antennas,” *Microwave Opt. Tech. Lett.*, Vol. 1,No. 1, pp. 8-9, 1988.
[65] K.A. Hummer and K. Chang, “Microstrip Active Antennas and Arrays,” *IEEE MTT-S Int. Microwave Symp. Dig.*, (New York), pp.963-966, May 1988.
[66] A. R. Ken, P. H. Siegel and R. J. Mattauch, “A simple quasi-optical mixer for 100-120 GHz,” *IEEE-MTTS Int. Microwave Symp. Dig.,* 1977,pp. 96-98.
[67] K. D. Stephen, N. Camilleri, and T. Itoh, “A quasi-optical polarization-duplexed balanced mixer for millimetre-wave applications,” IEEE Trans. Microwave Theory Tech., vol. MTT-31, pp. 164-170, Feb. 1983.
[68] K. D. Stephen and T. Itoh, “A planar quasi-optical sub-harmonically pumped mixer characterized by isotropic conversion loss,” IEEE Trans. Microwave Theory Tech., vol. MTT-32, pp. 97-102, Jan. 1984.
[69] V. D. Hwang and T. Itoh, “Quasi-optical HEMT and MESFET self-oscillating mixers,’’ IEEE Trans. Microwave Theory & Tech., vol. MTT-36, pp. 1701-1705, Dec. 1988.
[70] J. Zmuidzinas and H. G. LeDuc, “Quasi-optical slot antenna SIS mixers,” IEEE Trans. Microwave Theory Tech., vol. 40, pp. 1797-1804, Sept. 1992.
[71] P. A. Stimson, R. J. Dengler, H. G. LeDuc, S. R. Cypher, and P. H. Siegel, “A planar quasi-optical SIS receiver,” IEEE Trans. Microwave Theory Tech., vol. 41, pp. 609-615, April 1993.
[72] S. V. Robertson, N. L. Dib, G. Yang, and L. P. B. Katehi, “A folded slot antenna for planar quasi-optical mixer applications,” in 1993 IEEE AP-S Inr. Symp. Dig., vol. 2, pp. 600-603, June 1993.
[73] K. Cha, S. Kawasaki, and T. Itoh, “Transponder using self-oscillating mixer and active antenna,” to be appeared in the 1904 IEEE MTT-S Inr. Microwave Symp., San Diego, CA, May 23-27, 1994.

[74] C. W. Pohanz and T. Itoh, “A microwave non-contact identification transponder using suhharmonic interrogation,” to be appeared in the *1994* IEEE MTT-S Inr. Microwave Symp., San Diego, CA, May 23-27, 1994.

[75] N. Camilleri and T. Itoh, “A quasi-optical multiplying slot array,“ *IEEE Trans. Microwave Theory Tech.,* vol. MTT-33. pp. 1189-1 195, Nov.1985. *Applied Microwave.* vol. *5,* no. 1, pp. 88,91-94,96.99--100. 102, Winter 1993.

[76] S. Nam, T. Uwano, and T. Itoh, “Microstrip-fed planar frequency multiplying space combiner,” *IEEE Trans. Microwwe Theory Tech..* vol. M’IT-35, pp. 1271-1276, Dec. 1987.

[77] Andrews, J.W. and Hall, P.S, “Oscillator stability and phase noise reduction in phase lock active Microstrip patch antenna” Electron. Letts, 30th April 1998, vol 34, no 9, pp 833-835.

[78] Zheng, M, Gardner, P, Hall, P S, Hao, Y, Chen, Q and Fusco, V F, “Cavity control of active integrated antenna oscillators”, IEE Proc., Microwaves, Antennas and Propagation, accepted for publication.

[79] Buesnal, G. R., Cryan, M. J. and Hall, P.S., “Harmonic control in active integrated patch oscillators”, Electron. Letts., vol 34, no 3, 5 February 1998, pp228-229.

[80] V. Radisic, Y. Qian, and T. Itoh, “Class-F power amplifier integrated with circular sector Microstrip antenna,” *IEEE MTT-S Int. Microwave Symp. Dig*., Dever, CO, June 1997, pp. 687-690.

[81] Cryan, M. J. and Hall, P. S., “Analysis of harmonic radiation from an integrated active antenna”, Electron. Letts, Nov 1997.

[82] Kykkotis, C., Hall, P. S., and Ghafouri-Shiraz, H., “Performance of active antenna oscillator arrays under modulation for communication systems” IEE Proc. Microwaves, Antennas and Propagation, vol 145, no 4, Aug 1998, pp313-320.

[83] Ma, G., Hall, P. S. and Gardner, P. and Hajian, M, “Direct conversion active antennas for modulation and demodulation”, Microwave and Opt tech Letts, vol 28, no 2, Jan 20, 2001, pp89-93

[84] Ma, G., Hall, P.S. and Gardner, P., “Local oscillator radiation from active integrated antennas”, Electronics Letters, 9th Dec 1999, vol 35, No 25, pp2163-2164.

[85] Cryan, M J, Hall, P S Tsang, K S H and Sha, J “Integrated active antenna with full duplex operation”, IEEE Trans, MTT-45, no 10, Oct 1997, pp1742-1748.

[86] Kalialakis, C, Cryan, M J, Hall, P S and Gardner, P, “Analysis and design of integrated active circulator antennas”, IEEE Trans, MTT, vol 48, no 6, June 2000, pp 1017-1023.

CHAPTER 4

[1] V. Radisic, S. T. Chew, Y. Qian, and T. Itoh, “High efficiency power amplifier integrated with antenna,” *IEEE Microwave Guided Wave Lett.,* vol. 7, pp. 39–41, Feb. 1997.

[2] V. Radisic, Y. Qian, and T. Itoh, “Class F power amplifier integrated with circular sector Microstrip antenna,” in *IEEE MTT-S Int. Microwave Dig.,* Denver, CO, June 1997, pp. 687–690.

[3] W. R. Deal, V. Radisic, Y. Qian, and T. Itoh, “Novel push–pull integrated antenna transmitter front-end,” *IEEE Microwave Guided Wave Lett.*, vol. 8, pp. 405–407, Nov. 1998.

[4] W. R. Deal, V. Radisic, Y. Qian, and T. Itoh, “A high efficiency slot antenna push–pull power amplifier,” in *IEEE MTT-S Int. Microwave Symp. Dig.*, Anaheim, CA, 1999, pp. 659–662.

[5] W. R. Deal, V. Radisic, Y. Qian, and T. Itoh, “Integrated antenna push–pull power amplifiers,” *IEEE Trans. Microwave Theory and Tech.*, vol.

47, pp. 1418–1425, Aug. 1999.

[6] C. Y. Hang, W. R. Deal, Y. Qian, and T. Itoh, “Push–pull power amplifier integrated with Microstrip leaky-wave antenna,” *Electron. Lett.*, vol. 35, pp. 1891–1892, Oct. 1999.

[7] P. C. Hsu, C. Nguyen, and M. Kintis, “Uniplanar broad-band push–pull

FET amplifiers," *IEEE Trans. Microwave Theory Tech.*, vol. 45, Dec. 1997.

[8] J. L. B. Walker, *High-Power GaAs FET Amplifier*. Norwood, MA: Artech House, 1993.

[9] S. K. Behera, D. R. Poddar and R. K. Mishra, "Novel Push-Pull Integrated Antenna For Wireless Front-End", in Proceedings of **International Conference on Communication, Devices and Intelligent system, Jadavpur University, India** Jan. 9-10, 2004. pp. 217-219.

[10] S. K. Behera, R. K. Mishra and D. R. Poddar, "A Novel Design for Active antenna", 5th Indian Conference on **Microwave, Antenna, Propagation and Remote Sensing-In CMARS-2005.**

[11] S. K. Behera, D. R. Poddar and R. K. Mishra, "Dual Active Integrated Antenna", **International Conference on Computer & Devices for Communication (CODEC-2006),** University of Calcutta.

CHAPTER 5

[1] K. Inoue, K. Ebihara, H. Haematsu, T. Garashi, H.Takahashi and J. Fukaya, "A 240 W Push-Pull GaAs Power FET for W-CDMA Base Stations", 2000 IEEE MTT-S Digest, pp. 1719-1722.

[2] R. Basset, "Three Balun Designs for Push-Pull Amplifier", Microwave July 1980, pp. 47-53.

[3] S. Song and R. Basset, "S-Band Amplifier Modelled for Wireless Data", Microwave & RF, November 2000, pp. 53-160.

[4] S. Cripps, RF Power Amplifiers for Wireless Communications, Artech House Boston London, pp. 294-302.

[5] L. Max, "Balanced Transistors: A New Option for RF Design", Microwaves, June 1977, pp. 40-46.

[6] “AWR Design Environment”, Applied Wave Research Inc.

[7] G. Gonzales, *Microwave Transistor Amplifiers: Analysis and Design,* 2nd ed., Prentice Hall, Upper Saddle River, NJ, 1997.

[8] “Low Current, High Performance NPN Silicon Bipolar Transistor”, Agilent (HP) Technical Data 5965 – 8919E.

ONLINE RESOURCES

[1] http://www.educatorscorner.com/experiments/pdfs/exp98/exp98tech.pdf

[2] http://literature.agilent.com/litweb/pdf/5967-5486E.pdf

CHAPTER 6

[1] C. A. Balanis, “Antenna Theory, Analysis and Design,” John Wiley & Sons, New York, 1997.

[2] W. L. Stutzman, G. A. Thiel, “Antenna Theory and Design,” John Wiley & Sons, New York, 1981.

[3] P. S. Hall, J. S. Dahel, “Dual and Circularly polarized microstrip antennas,” in Advances in Microstrip and Printed Antennas, K. F. Lee, W. Chen (Eds.), John Wiley & Sons, New York, 1997.

[4] R. L. Bauer, J. J. Schuss, “Axial Ratio of Balanced and Unbalanced Fed Circularly Polarized Patch Radiator Arrays,” IEEE AP-S Int. Symp. Ant. Propag., 1987, pp. 286 – 289.

[5] P. S. Hall, J. S. Dahel, J. R. James, “Design Principles of Sequentially Fed, Wide Bandwidth, Circularly Polarized Antennas,” IEE Proc., Pt.H, Vol. 136, 1989, pp. 381 – 389.

[6] P. S. Hall, “Applications of Sequentially Feeding to Wide Bandwidth, Circularly Polarized Antennas,” IEE Proc., Pt.H, Vol. 136, 1989, pp. 390 – 398.

Chapter 7

1. S. K. Behera, D. R. Poddar and R. K. Mishra, “Novel Push-Pull Integrated Antenna for Wireless Front-End” **International Conference on Communications, Devices and Intelligent Systems (CODIS-2004),** pp. 217-219,8-10 January 2004.Jadavpur University, Kolkata.
2. S. K. Behera, R. K. Mishra and D. R. Poddar, “A Novel Design for Active antenna”, 5th Indian Conference on **Microwave, Antenna, Propagation and Remote Sensing-In CMARS-2005.**
3. S. K. Behera, D. R. Poddar and R. K. Mishra, “Dual Active Integrated Antenna”, **International Conference on Computer & Devices for Communication (CODEC-2006),** University of Calcutta.
4. S. K. Behera, D. R. Poddar and R. K. Mishra, “Balanced Amplifying Active Patch Antenna”, IETE Journal of Research (Communicated).
5. S. K. Behera, D. R. Poddar and R. K. Mishra, “2.4 GHz Balanced Amplifying Active Antenna for Circular Polarization”, Microwave and Optical Wave Letters (Communicated).
6. S. K. Behera, D. R. Poddar and R. K. Mishra, “ Sequentially Fed Balanced Amplifying Antenna for Circular Polarization” IEEE Trans. on Antennas & Propagation (Communicated).